The Evolutionary Genetics and Developmental Basis of Eyespot Morphology in Butterfly Wings

Antónia A. T. F. Monteiro

Thesis presented for the degree of Doctor of Philosophy

University of Edinburgh

October 1996

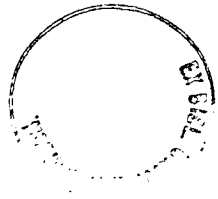

I declare that I have performed all of the work in this thesis and have written all the chapters with the exception of the mathematical appendices and a couple of paragraphs in chapter 5, written by Prof. Hans Metz of Leiden University and the computer diffusion program, in the same chapter, written by Gijs Smit, a former student at Leiden. My supervisors, Dr. Vernon French at Edinburgh University and Prof. Paul Brakefield at Leiden University also read all of the chapters and made various comments and improvements.

To my parents

Luís and Maria de Lourdes

CONTENTS

ABSTRACT

The wings of the Nymphalid butterfly, *Bicyclus anynana*, have a series of eyespot colour patterns, each composed of a white pupil, a black centre and a gold outer ring. An eyespot pattern is organised around a group of signalling cells, the focus, that is active during the first hours of pupal development. Positional information, given to the cells around the focus, is translated into rings of differently pigmented scales. One hypothesis for the underlying mechanism is a concentration gradient of a diffusible morphogen produced by the focal cells, and interpreted in a threshold manner by the responding epidermis. If the diffusion gradient model is correct, when two foci are close together, the signals would summate and this effect would be apparent in the detailed shape of the pigment pattern formed. The morphogen gradient hypothesis was tested by measuring areas of fused eyespot patterns in *Bicyclus anynana*, by grafting focal cells close together, and also by using a mutation (*Spotty*) that produces adjacent fused eyespots. The results indicate that, in the region between two foci, there is nearly always an extra area of cells differentiating into part of the pattern. The same qualitative results were obtained using a computer model of two sources that, via diffusion, establish two overlapping concentration gradients.

I have investigated the potential for evolutionary change in the developmental mechanism of eyespot formation by applying artificial selection for various aspects of eyespot phenotype. Selection for colour composition of the large dorsal eyespot on the forewing, produced a line of butterflies with a narrow or no gold ring (BLACK) and another line with a reduced black centre and a broad gold ring (GOLD). Heritabilities were high, giving a rapid response in the selected eyespot and other eyespots also. Surgical experiments were then performed on pupal wings from the different lines at the time of eyespot pattern determination. Grafting foci between BLACK and GOLD line pupae, and inducing ectopic eyespots by damage, both

showed that the additive genetic variance for eyespot composition was at the level of the response component of the developmental mechanism.

The eyespots of *Bicyclus anynana* are normally circular in shape. By performing artificial selection on eyespot shape in two lines of butterflies, I produced elliptical eyespots (FAT and THIN). Realised heritabilities for this trait were low. The developmental nature of the response to selection was investigated by surgically testing for radial asymmetry in the signal component of the developmental mechanism specifying the eyespot. Removing and rotating the focus by 90 or 180 degrees and grafting it back into the wing epidermis did not influence eyespot shape. Also, local damage inflicted outside the focal region induced elliptical ectopic eyespots, characteristic of the FAT or the THIN selected line. Both experiments showed that differences between lines resulted from differences in the epidermal response to the focal signal. Thus our stock population has genetic variability for general epidermal properties (perhaps related to epidermal expansion during wing morphogenesis), but apparently not for the symmetry of focal signalling. Morphometric analysis of linear wing measurements and wing scale counts provided evidence that eyespot shape was correlated with changes in overall wing shape and with the density/arrangement of scale building cells around the eyespot region.

It has been suggested that the focal signal diffuses intercellularly, via gap-junctions. I explored this possibility by micro-injecting a fluorescent dye into a single cell in the pupal wing epidermis (in the area of the future eyespot pattern) and observed a rapid spread of the dye to several of the neighbouring cells, consistent with the presence and open state of gap-junctions at the relevant time of pattern formation.

FOREWORD AND ACKNOWLEDGEMENTS

This thesis is written in the form of a collection of separate papers that constitute the chapters. In the Introduction I give an overview on previous studies on pattern formation in butterflies and explain how all of the separate papers are integrated. Each of the chapters that follow have their own introduction, material and methods, results and discussion sections. Although some information may appear repeated in more than one chapter, these can be read independently without reference to any of the others.

I began to work on this project in mid November 1992 under the joint supervision of Dr. Vernon French at Edinburgh University and Prof. Paul Brakefield at Leiden University. The idea for this joint project arose in early 1992, by the time I finished my undergraduate research project in Leiden as an ERASMUS student. Paul Brakefield had been my supervisor and Vernon French, on a visiting trip, taught me how to operate pupae. This thesis was the natural follow up of the research I had just finished. After a brief period at the University of Edinburgh, I started with the intensive breeding and selection work at the University of Leiden where the butterfly husbandry facilities were established. Then I moved to Edinburgh and tried for several months to establish good breeding conditions to maintain reduced numbers of individuals from the selected lines, in order to perform grafting and manipulative experiments with the pupae. This was not possible for several reasons, among which was the use of a common greenhouse for rearing the larval food plants (maize) and other plants for other projects that were regularly sprayed with insecticide. Also, in the winter months, since the greenhouses were not artificially heated, growth of the maize was too slow to meet the larval demands. This period in Edinburgh was then followed by one more extensive period in Leiden where all the grafting and manipulative experiments were done.

I would like to thank both my supervisors, whose complementary work interests were the basis for a very stimulating research. They both accompanied the research throughout and helped on solving numerous problems with valuable

suggestions. They also read and made comments on all of the chapters. Chapters 2, 3 and 4 have already been submitted for publication, in very much the same format, with both Paul Brakefield and Vernon French as co-authors.

I also wish to express my enormous appreciation to Hans van Rijnberk for preparing the measuring program on the image analysis system. Prof. Hans Metz helped develop a mathematical test to support the morphogen diffusion hypothesis. It has been a pleasure working with him. I also thank Hans van Rijnberk, again, Peter de Jong and Mart Ottenheim with whom I had very helpful discussions on some of the analysis. Thanks also to Gijs Smit who produced the morphogen diffusion program, Catriona MacCallum, Patsy Haccou and Evert Meelis who helped with the discriminant analysis of chapter 4 and gave other statistical advice. Hans Roskam gave me access to his photographic records from museum collections of *Bicyclus*. Els Schlatmann and Bert de Winter grew lots of maize for hungry caterpillars. Pedro Pablos, Prof. Luis Fraser Monteiro and Gerard Mulder helped in discussing some of the ideas of chapter 5. David Spray, from the Department of Neuroscience, Albert Einstein College of Medicine, New York, performed the microinjections in chapter 6 and we were both helpfully assisted by Dr. M.B. Rook at the University of Utrecht. Jonathan Bacon at Sussex provided the space and the expertise for me to repeat the microinjection experiments in his lab. Prof. Maria de Lourdes Fraser Monteiro suggested the use of a mass spectrometry technique to identify a putative morphogen (Chapter 7). Adri 't Hooft, Peter Mulken and Fieneke Speksnijder from the photographic department in Leiden helped producing the photos. I also want to thank all the people in Edinburgh and in Leiden who helped in some way or another to make my life in the two places very enjoyable. Finally, I want to express my gratitude to Junta Nacional de Investigação Científica e Tecnológica (JNICT), Lisbon, who funded my work through grants from the Ciência and Praxis XXI programs.

CHAPTER 1

General Introduction

This thesis is about butterfly eyespot patterns..."Eyespot patterns?!", is the incredulous reaction I get every time I sit down in a pub, and casually inform new acquaintances of what I do for a living. Most of the time, they smile a lot, even laugh sometimes and then begin to ask the inevitable questions like: "Why?", "How do you get the money?", "What is the relevance of butterflies for human kind?" and so on. Every time I try a slightly different answer. In the beginning I used to focus on a really precise question I was trying to answer like "...finding out how the cells in a butterfly wing get their information to produce the different colour pigments in the special arrangements they do". But then, realising I was not really answering their questions I started developing this ability of moving very quickly away from my very "small" question and confronting them with more general issues like: "What makes the simple egg develop into a human being ?", or "Why do we have five fingers ?", or " How do the cells in the growing embryo begin to differentiate into the different tissues and organs ?". Some informed listeners then say, "It is all in the genes, in the DNA!" and I say, "but all the cells have the same genes and the same DNA, why do they start doing different things?"...Silence. The subject starts to grab them. Its like a little puzzle they had never thought about before. Then, it is much easier to go back to the butterflies and explain that what I am really doing is tackling these questions in a simpler and more accessible organism than the human body. The pattern in the wings of butterflies is a very good example of how cells, initially part of a two-dimensional, colourless and homogeneous sheet of tissue, will be transformed into scales on the adult wing that will incorporate a specific colour pigment according to their position. The pattern that is formed, from the combination of all these pigmented scale cells, is certainly controlled genetically and is a characteristic of each butterfly species. We can now ask two very different types of questions. The first is, "If all the cells in a wing have the same genetic information, what are the developmental mechanisms that

make one region of the wing produce an eyespot pattern and another region a band or chevron pattern?". The second question is, "If there are nearly 12,000 species of butterflies in existence today, most of them distinguishable on the basis of their colour pattern, and all descendant from a common ancestor, how have these mechanisms evolved?". This thesis attempts to contribute to both the understanding of the developmental mechanism underlying very common patterns found in butterfly wings, the eyespots, as well as disclosing genetic variability around this mechanism that could and can still give rise to the evolution of these elements. Below I give an overview of previous research on development and evolution of butterfly wing patterns in general. At the end of this chapter I describe my more specific aims for each of the chapters that follow within this large field.

The groundplan

Butterfly wing patterns are not just random patches of pigmentation. There is a relatively small number of pattern elements that can be identified across most species. Scwanwitsch (1924) and Süffert (1927) discovered, almost simultaneously and independently, this homology system known as the nymphalid ground plan, which was later modified by Nijhout (1991; Fig. 1). The nymphalid ground plan is a diagrammatic list of all the elements of the colour pattern and represents the maximum number of pattern elements that could be present in a butterfly. It basically consists of a system of bands and spots that run from the anterior to the posterior margins of each wing. The bands may be dislocated to a greater or lesser degree whenever they cross a wing vein. These bands are organised in pairs and each pair makes up a symmetry system. These are the basal (closer to the body) and the central symmetry systems. The term symmetry system derives from the pigment composition of the two bands in a pair, which are mirror images of each other. Additionally to the bands there is the discal spot, the system of border ocelli or eyespots, the chevron patterns and two marginal bands (only one shown in Fig. 1). Each element appears to be able to change independently of the others and it is the permutation of size, shape, colour and presence or absence of this relatively small set of pattern elements that is responsible for most of the diversity in wing patterns in butterflies and moths.

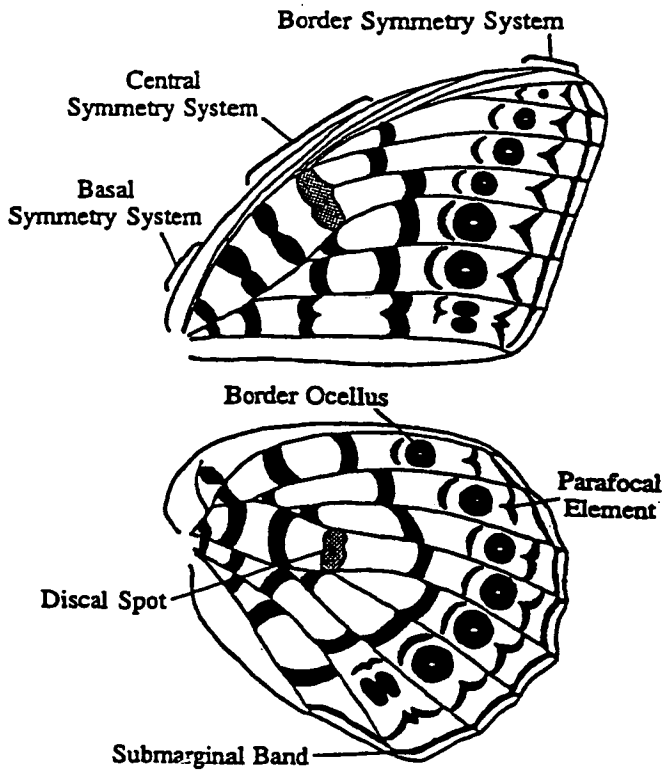

Figure 1. The nymphalid groundplan. Each wing cell (area created by the branching venation pattern) of the butterfly wing can potentially bear one of each of the following components: a basal symmetry system band, a border ocellus and a parafocal element (both of which are part of the border symmetry system), and one or two submarginal bands.

Pattern development in each wing-cell (an area of the wing bordered by veins) is also largely independent of that in other wing-cells. Nijhout (1991) proposed that dislocations of the bands happen because every piece of the band is independently produced in each wing-cell. Thus, pieces of band, as well as eyespots or chevrons can be present or absent in a wing-cell. Experimental studies (Nijhout 1980, French and Brakefield, 1992) have shown that artificially removing an eyespot on a wing does not affect development of the other eyespots nor of the rest of the pattern elements in the wing-cell. Similar experimental studies have not yet been performed for the rest of the pattern elements. However, genetic correlations calculated for the size of serially homologous (e.g. the group of eyespots) and non-homologous pattern elements (e.g. the eyespots, bands and chevrons) indicated no genetic correlations between non-homologous elements, and a varying degree of correlation between homologous elements (Paulsen 1994).

If portions of a symmetry system or border ocelli system develop largely independently on each wing region delimited by wing-veins, these veins must be an important element in pattern formation. In many species, veins mark compartment boundaries where pattern is interrupted from wing-cell to wing-cell. In other cases veins can be "transparent" to pattern, when for instance a large eyespot crosses a wing-cell with little or no distortion. An eyespot pattern, however, is always centred between two veins, in the middle of the wing-cell. To understand pattern development we have to know more about the development of the wing and its venation pattern.

Development of the wing

Within the larva a small group of invaginated cells form a growing pouch or "imaginal disc", consisting of two layers of epidermis which will form the dorsal and ventral surfaces of the wing (Fig. 2). Throughout development, each surface of the wing disc remains a monolayer of cells that grows and divides more or less continuously and independently of the rest of the epidermis of the larva. Each layer of cells produces a basement membrane and these fuse together over the entire inner surface of the disc. The venation and tracheation patterns of the imaginal disc become established during the last larval instar. In some species, including *Bicyclus anynana* and *Precis coenia*, a branching pattern of tubular lacunae forms between the fused laminae of the discs by local separation of the basement membranes. These lacunae are then invaded by fine tracheae that emerge from the large tracheal cluster at the base of the disc (Nijhout 1980b, A. Monteiro, pers. observ.). In other species, the sequence of events is reversed: the tracheae penetrate the disc before lacunae are evident (Nijhout 1991). Parallel to the margin of the wing disc there is the bordering lacuna, that marks the outline of the future adult wing, and is the end point of all the radial lacunae. Tissue distal to the bordering lacuna dies during the pupal stage. The initial tracheation pattern remains functional until about the middle of the pupal stage when it is replaced by a new set of tracheae that will provide the air supply for the adult wing. The two tracheation patterns are essentially the same with the exception that a few tracheae are lost in the final pattern (Nijhout 1991).

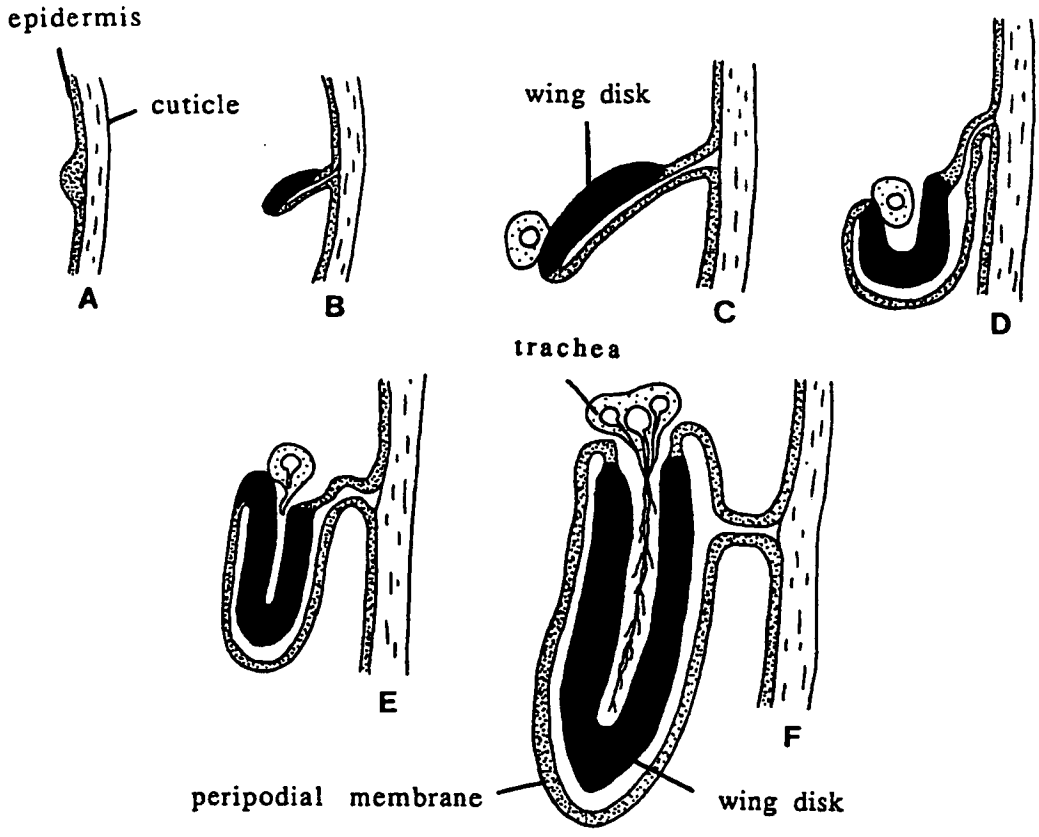

Figure 2. Development of lepidopteran wings, shown in cross sections of successive stages in the development of a wing imaginal disc within the caterpillar. The wing starts as a small thickening of the epidermis (A), which invaginates (B), thickens, and folds (C-E) to form a two-layered structure: the wing imaginal disc surrounded by a thin epithelial peripodial membrane. Midway through the last larval instar a bundle of tracheae invades the wing through the lacunae of the presumptive venation system (F). (After Kuntze 1935, in Nijhout 1991).

By pupation the imaginal disc evaginates and forms the pupal wing. During the end of the larval life and first half of the pupal stage there is extensive growth of the wing and its surface area enlarges to adult size. However, due to its confinement under the pupal cuticle, the surface of the wing is arranged in many fine folds that will only be stretched out when the wing expands after emergence of the adult (Nijhout 1991).

The differentiation of the scales that will carry the colour pattern happens during the first few days of pupal development and coincides with the mitotic activity in the pupal wing epidermis. Every cell in the epidermis will become either a scale cell or a normal epidermal cell. The scale cells become polyploid and greatly enlarged. They are organised in straight parallel rows that run perpendicular to the long axis of the wing and are separated by several rows of normal epidermal cells.

Likewise, the adult scales on butterflies' wings form straight rows overlapping like roof tiles. After enlargement, the scale cells start to send out a finger-like cuticular projection that flattens and forms a scale. Afterwards and just prior to adult emergence, and epidermal cell death, pigment is synthesised and deposited on these scales. The important events determining which cell produces which pigment have already happened days before, during the first few hours after pupation and will be explained below. The colours on the wings of butterflies are entirely due to the colour of their scales. Only one type of pigment is deposited in each scale making the colour pattern a finely tiled mosaic of single coloured scales. The colour of a scale may be due to the presence of chemical pigments, or it may be a structural colour that comes about when light interacts with regularly spaced physical structures in the scale (Nijhout 1985b). There is little contact between the two wing surfaces during development and in some species the wing pattern on the dorsal surface can be very different from that of the ventral surface.

Determination of the organising centres of the colour pattern

Pattern formation in an initially featureless system must start with the establishment of discontinuities that act as organising centres. For colour pattern in the wings of butterflies, discontinuities of interest are provided by the marginal and radial lacunae of the wing disc. In many species, the pattern develops on or next to the path of these lacunae, so that the venation pattern is also expressed in the colour pattern. Organising centres of patterns such as eyespots, centred in the middle of the wing-cell, must be established through some other mechanism. So far, it is not known how these organising centres develop but Nijhout (1990), adapting the lateral inhibition model of Meinhardt (1982), was able to model the establishment of dynamically stable centres of activator production, in the middle of a wing-cell. This model assumes that small concentrations of an activator diffuse continually from the veins bordering three sides of a wing-cell, and disturb the dynamics of the activator and its inhibitor already present in the wing-cell in steady state concentrations. The activator and inhibitor have slightly different diffusion coefficients and decay rates and interact as they diffuse. By varying the relative values of the two diffusion coefficients or decay rates it is possible to vary the number of stable points of activator concentration that form

as well as their positions in the wing-cell. A stable pattern can be produced at one or more points along the wing-cell midline, at points close to the veins at the border of the wing-cell, along the whole of the veins or along a stripe following the midline. Nijhout later proposed that, once these organising centres are established, in the imaginal disc, they could organise the pattern around them by generating a diffusible signal that would influence cells at relatively distant positions. There is no direct evidence that the lateral inhibition model is operating in the wing cell establishing these organising centres. However, Carroll and co-workers (1994) have shown that the pattern of expression of the gene product *Distal-less*, in the nymphalid *Precis coenia,* marks the centres of the presumptive eyespots. Further, the *Distal-less* expression pattern changes dynamically in the course of the last instar larvae and follows a very similar pattern to that predicted theoretically with the reaction-diffusion model described above (Nijhout 1994).

Colour pattern formation

Once the organising centres are established it is necessary for them to signal to the surrounding cells to differentiate the colour pattern. Nijhout (1991) proposed that these centres can either become sources or sinks of a morphogen. Both will produce a concentration gradient around them, but, whereas sources will have the highest concentration of morphogen at their centre, sinks, by degrading a morphogen already present in the wing, will have the lowest. Continuous gradient models can produce discretely distributed responses, like the rings in an eyespot, by translating the gradient into a discontinuous function. This is usually accomplished by arbitrary assumptions that one or more thresholds exist with gradient values above a threshold evoking a developmental response different from that evoked by gradient values below the threshold. Each colour ring of an eyespot would correspond to cells having perceived a certain range of morphogen concentrations (Nijhout 1978). According to a biochemical model proposed by Lewis and co-workers (1977), slight variations in the concentration of a gene activator can produce alternative steady states that are stable and heritable from one generation of cells to the next, and the transition from one state to the other is sharp, even with shallow signal gradients.

The morphogen concentration gradient hypothesis has been used in several modelling attempts to reproduce real butterfly wing patterns. Murray (1981) modelled vein-dependent patterns using this morphogen gradient model, where veins are the sources of morphogen. Bard and French (1984), modelled patterns on whole wings of several species with no vein dependent patterns. They used a combination of point sources and line sources or sinks for morphogen along the wing margins, to reproduce eyespots and continuous banding patterns across the wing. Nijhout (1990) identified the wing-cell as the unit of colour pattern formation and, therefore, has concentrated on modelling patterns within this sub-region of the wing. He has modelled the shape of most border ocelli and parafocal elements and was able to reproduce the vast majority of patterns seen in the butterflies, using an additive two-gradient model, from the "tool-box" of point and line sources or sinks mentioned above, and simple thresholds within a single wing-cell.

Experimental evidence for the existence of organising centres has been found for the eyespot pattern (Nijhout 1980a), but so far no conclusive evidence has yet been found for equivalent centres organising bands or chevron patterns. Work on the banding patterns has concentrated on two closely related moth species, *Ephestia kühniella* and *Plodia interpunctella* (Kühn and von Engelhard 1933; Wehrmaker 1959; Schwartz 1962; Wilnecker 1980; Toussaint and French 1988) with a simple band of the central symmetry system. Experimental work on the eyespot patterns began with *Precis coenia*: If cells at the centre of the presumptive eyespot pattern were killed, during the pupal stage, no eyespot developed; if they were excised and transplanted elsewhere on the wing, they induced an eyespot to develop in an ectopic location around the site of implantation (Nijhout 1980a). These experiments have now also been repeated in another nymphalid, *Bicyclus anynana* (French and Brakefield 1992, Monteiro et al. 1994).

Evolution of wing patterns

Fossils of butterflies exist (Walley 1986), but pigments are not preserved in the rock. If some specimens were to be found preserved in amber, for instance, the pigmented patterns would probably also have disappeared with time. It is, therefore, impossible to recreate evolution, and look back to see which was a butterfly's ancestral pattern

and the patterns that derived from it. Not all species, however, have the same degree of derivation and evolution of their colour pattern from the primitive pattern. Evolution proceeds more slowly if there is little natural selection acting on a large population (where random drift is minimised). Reconstruction of an ancestor can be done by means of the logical methods of phylogenetic systematics. This discipline attempts to identify monophyletic groups of species by first identifying primitive and derived traits among homologous structures and then using shared derived characters to identify clades (monophyletic groups) that share a common ancestor (Wiley, 1981). The characteristics of an ancestor can then be deduced from the distribution of primitive and derived traits among its descendants. Once this method is applied it is possible to map the evolution of many of the features of the wing pattern. However, it is impossible, by morphological data alone, to deduce the trajectory by which two patterns diverged from a common ancestor. This is because morphological evolution can proceed through many different paths. Additionally, not all paths are possible, since developmental mechanisms constrain the possible range of phenotypes (Maynard-Smith et al., 1985). The actual path of the trajectory is dictated by the action of natural selection and drift. To reconstruct the past it is necessary to understand the evolution of developmental processes that translate genes into phenotype. One way of beginning is to experimentally manipulate pattern in species and start uncovering the sources of additive genetic variance at the level of the developmental mechanisms.

This thesis

The approach followed in this thesis was to take a single species, apply artificial selection on some feature of its colour pattern and see how easily it changed in the direction we chose. Other patterns on the wing were monitored to see whether they remained stable or changed in response to selection. We can, in this way, not only identify sources of additive genetic variance that contribute to the between-species differences, but also begin to understand the developmental organisation of the whole pattern: which features are regulated independently and which suffer correlated changes.

The butterfly used in this work was *Bicyclus anynana*. The lab stock came from Nkhata Bay in Malawi in 1988 and has always been maintained at high adult numbers (>300) in the lab at 23° C. The generations are non-overlapping and are around 5 per year at this temperature. The larvae feed on maize plants which are grown in pots, and the adults on mashed banana. The butterfly is brown, with a lighter coloured band crossing the ventral surface of both wings (belonging to the central symmetry system). It has several eyespots on both the dorsal and ventral sides of the wings, chevron patterns and two distal bands along the margin of the wings.

In chapters 2 and 3, I describe selection experiments for colour composition and shape of the large dorsal eyespot on the butterfly *Bicyclus anynana*, quantify the heritability for this characters, measure correlated responses to selection and finally investigate at what level of the developmental system this variation occurred. In chapter 4, changes that occurred in wing shape and scale spacing around the eyespot region caused by selecting on the shape of the colour pattern are investigated. In chapter 5, further evidence is provided that eyespot patterns are consistent with the model of a morphogen concentration gradient established by diffusion. In chapter 6 it is shown that this diffusion could be possible via the cell interiors via gap-junctions and in chapter 7 I discuss the implications of this work and indicate future lines of research.

CHAPTER 2

Eyespot Colour Rings

ABSTRACT

The butterfly *Bicyclus anynana* has a series of distal eyespots on its wings. Each eyespot is composed of a white pupil, a black disc and a gold outer ring. We applied artificial selection to the large dorsal eyespot on the forewing, to produce a line with the gold ring reduced or absent (BLACK) and another line with a reduced black disc and a broad gold ring (GOLD). High heritabilities, coupled with a rapid response to selection, produced two lines of butterflies with very different phenotypes. Other eyespots showed a correlated change in the proportion of their color rings. Surgical experiments were performed on pupal wings from the different lines at the time of eyespot pattern specification. They showed that the additive genetic variance for this trait was in the response of the wing epidermis to signalling from the organizing cells at the eyespot centre (the focus).

INTRODUCTION

To understand diversity, it is critical to appreciate the differences in developmental mechanisms that underlie phenotypic variation. The nature of these mechanisms may provide an insight into which alterations in phenotype can result from genetic change. Thus, such an understanding can help to determine the limits and constraints on the phenotypes upon which selection can operate in the short term (Cheverud 1984).

We are interested in the potential for evolutionary change of butterfly wing patterns and, more specifically, in morphological variation of the eyespot patterns of

the nymphalid butterfly, *Bicyclus anynana* (Brakefield and French 1993; Monteiro et al. 1994). This species, and others of the genus, have a series of distal eyespots on the wings. All eyespots are considered homologous pattern elements and show high genetic correlations for several characters, presumably due to a common developmental mechanism (Nijhout 1991; Paulsen and Nijhout 1993; Paulsen 1994).

All eyespots in *B. anynana* have a white pupil, a black disc and a gold outer ring. These pigments are deposited in the scales just before adult emergence but the future pattern is specified in the wing epidermis much earlier, during the first few hours of pupal development. Through transplantation and damage experiments, in *Precis coenia*, Nijhout (1980) has shown that the cells at the centre of a future eyespot pattern, the focus, are responsible for organizing the pattern. Hence, early focal damage can abolish the eyespot, while an ectopic eyespot will form around a focus grafted into a different location. The mechanism of focal signalling is still not understood but a simple gradient model (Nijhout 1978, 1990) has been helpful in interpreting many experimental results. Here, focal cells produce a "morphogen" that diffuses away through gap-junctions, to form a radial concentration gradient. Cells at different distances from the focus would experience different morphogen concentrations at the time of pattern determination, leading them later to produce different pigments. The threshold responses to morphogen concentration would determine the extent of the different color rings and hence the total size and proportions of the eyespot. Alternatively, the focus may produce a gradient by functioning as a local sink for a morphogen present at high concentration throughout the wing epidermis, (see Nijhout 1985; French and Brakefield 1992).

By selecting on features of eyespot morphology in *B. anynana*, we have shown that there is substantial genetic variation present for eyespot size (Holloway et al. 1993; Monteiro et al. 1994), eyespot shape (Monteiro et al. 1997a) and position of eyespots on the wing (P. M. Brakefield, unpublished). In this study, we use selection experiments to estimate genetic variances for proportion (color composition) of the large posterior eyespot on the dorsal forewing of *B. anynana*. Correlated responses to selection, in the color composition of other eyespots, are also examined. Eyespot foci were then grafted between the divergent selected lines, to investigate whether the

response to selection produced a change in a) signalling from the eyespot focus or, b) the interpretation (or response) of the surrounding cells. Also, as local damage can induce ectopic eyespots (French and Brakefield 1992; Brakefield and French 1995), we tested for a difference between selected lines in the composition of eyespots formed in response to wing damage.

MATERIAL AND METHODS

Experimental animals

For selection, several hundred eggs were collected on the larval food plant (maize) from the stock population, and reared through to adult stage in a climate room, at 28° C, high humidity and 12h light: 12h dark photoperiod.

Selection procedure

Adult males and females were separated on the day of emergence and placed in separate hanging cages. The large posterior eyespot on the dorsal surface of the forewing was measured in the proximal-distal axis (parallel to the wing veins) for total diameter and for diameter of the black disc (Fig. 1A), using a micrometer eyepiece in a binocular microscope.

The butterflies were numbered with a black felt pen on the ventral surface of the hind wing. After roughly the first 100 males and females emerged and were measured, the mean ratio (and standard deviation) of black/total diameter was estimated for the whole generation. Assuming a normal destribution of eyespot ratios, two thresholds were determined for each of the sexes, so that approximately 100 low ratio and 100 high ratio individuals, of each sex, would have been selected for mating by the time the last emerged butterfly was measured. Selection, thus, started before all individuals had emerged (the total number of emerged butterflies in this generation was roughly 450 of each sex). The early age of the selected butterflies introduced in mating cages, as well as the chosen density of butterflies, maximizes the proportion of individuals which successfully pair (Monteiro et al. 1994). A

GOLD and a BLACK line were established from butterflies with low and high ratios, respectively. After mating had taken place, and in order to increase the selection intensity, only the 40 most extreme females from each line were allowed to lay eggs for the F1 generation. These females were removed from the mating cage and introduced in a cage with maize plants. Selection was performed for 9 generations. The average number of butterflies emerging in the F1, and subsequent generations, was around 600 in each line. Realized heritabilities for eyespot composition were estimated by regressing all generation means (up to generation 8), against the cumulative selection differential averaged between the sexes. The slope of the regression line estimates the realized heritabilities (Falconer 1989).

Correlated responses

In order to estimate correlated responses to selection, both the large posterior and the small anterior eyespot on the dorsal surface were measured in 9th generation butterflies. Both eyespots from a group of STOCK butterflies, raised in the same conditions, were also measured (100 from each sex). All measurements were made using an image analysis system (see Windig 1991).

Focal grafting experiments

Grafts were performed 3-5h after pupation, by moving the focus of the posterior dorsal eyespot to a different position on the wing of another pupa. A small square (0.25 mm^2) of focal epidermis plus cuticle was cut with a razor-blade knife, rotated 180° and transplanted into a similar square hole opened previously in the host wing. The 180° rotation was performed because polarity of the cells is already determined at this stage in development, conferring an opposite orientation of the scales to the grafted piece of tissue on the adult wing and, thus, leading to its easy identification. After adult emergence (at 28° C), the ectopic eyespots formed around grafted foci were measured in their total and black disc diameters and the ratio of black diameter/total diameter was calculated for each eyespot. Ectopic eyespots were included in the analysis only where a white pupil was present and the eyespot extended beyond the rotated scales of the grafted tissue.

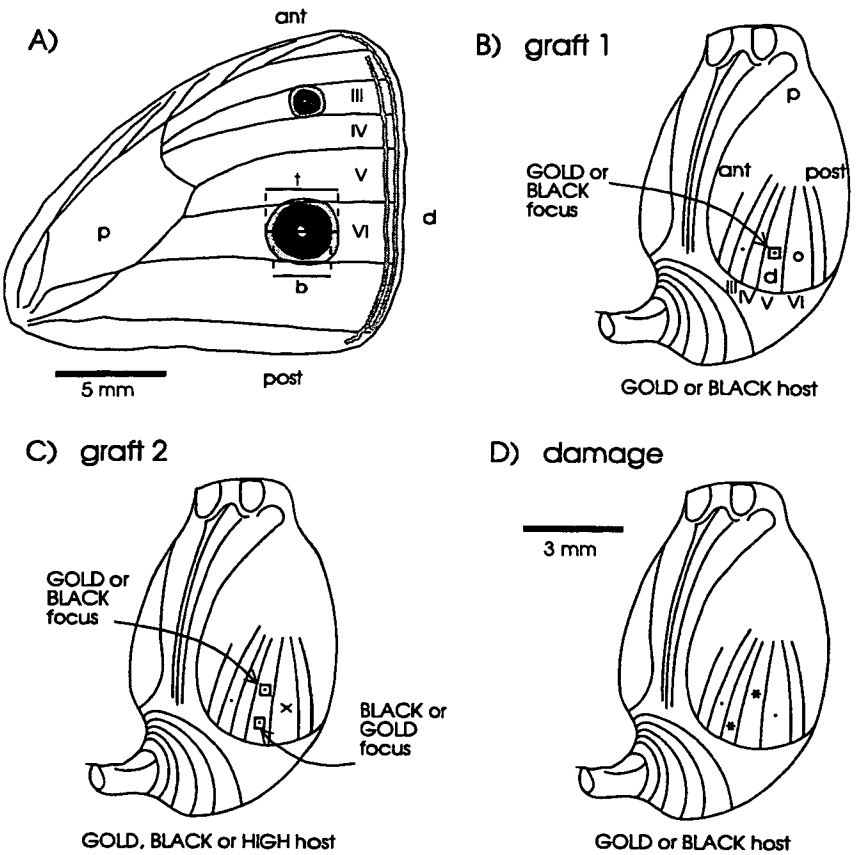

Figure 1. A) Dorsal surface of the adult forewing of *B. anynana* showing the small anterior and large posterior eyespots and the measurements of black (b) and total (t) eyespot diameters. III-VI, spaces between veins (wing-cells); ant, anterior; post, posterior; p, proximal; d, distal. B-D) Pupae showing grafting and wing damage operations. B) Graft Experiment 1: the posterior focus from a GOLD or BLACK pupa (square with dot) was grafted into the Vth wing cell. The posterior focus of the host pupa was removed (circle) to be grafted into another pupa. C) Graft Experiment 2: two foci from different lines were grafted into proximal and distal positions on the Vth wing cell. The posterior focus (cross) was also pierced to reduce eyespot size and prevent merging with the ectopic patterns. D) Wing damage experiment: the sites marked with asterisks were pierced at time periods 6, 12 and 18h after pupation.

Graft Experiment 1. Reciprocal grafts were performed, after 4 generations of selection, between GOLD and BLACK line pupae and also between pairs of pupae from the same line (Fig. 1B). In each case, the posterior focus from the left wing was grafted to a more anterior position on the left wing of the other pupa. For analysis, data was grouped into 4 categories: GOLD foci grafted into GOLD hosts, GOLD foci grafted into BLACK hosts, BLACK foci grafted into BLACK hosts, and BLACK

foci grafted into GOLD host, and the medians of the eyespot ratios were compared using the non-parametric Mann-Whitney test.

Graft Experiment 2. In this experiment, eyespot foci from different lines were compared directly on a common host wing (Fig. 1C). Pupae were used after 5 generations of selection and the posterior (left wing) foci from one GOLD and one BLACK pupa were grafted together into three different types of host: pupae from the GOLD, the BLACK or the HIGH line (a line selected for an enlarged posterior dorsal eyespot, showing enhanced epidermal response to a focus; Monteiro et al. 1994). Each experiment was replicated by using the right wing foci of the donor pupae and grafting them into the same positions on a second host pupa. The host sites to which the GOLD or BLACK foci were grafted remained the same between the replicates, but alternated with each experiment. For the following analysis, the replicates were treated as independent data points as there was no consistency in the correlation coefficients (Spearman rank) between the two eyespot ratios, calculated for each type of host (a test of homogeneity among coefficients showed significant heterogeneity; Sokal and Rohlf 1995).

Wing damage experiments

Ectopic eyespots were induced by wing damage to pupae of the 6th generation. At 6h, 12h or 18h (± 15 min.) after pupation, the left pupal wing was pierced with an unheated, finely-sharpened tungsten needle, at two sites (see Fig. 1D). Operated pupae were returned to 28° C, the emerged butterflies were frozen and then ectopic eyespots were measured. All analyses, except when indicated otherwise, were done using parametric tests on square-root transformed data, to make the variances homogeneous. Analysis of covariance (ANCOVAs) were performed on black disc diameters of ectopic eyespots taking total diameter as a covariate.

Response to selection on eyespot color composition

Both males and females responded to selection for a decrease (GOLD line) and an increase (BLACK line) in the relative size of the central black disc of the posterior dorsal eyespot (Fig. 2A). The butterflies from the GOLD and BLACK lines first showed non-overlapping distributions in the ratio of black diameter/total eyespot diameter in the 5th generation. Fig. 3 shows the changes in mean ratio through 8 generations of selection. For both lines and sexes, the estimates of realised heritability are similar: between 32 and 53%. Selection was stopped in the BLACK males after the 5th generation since most eyespots were composed only of the white pupil and surrounding black scales, with no outer gold ring. By the 8th generation some BLACK females lacked the outer gold ring, so it is likely that further selection would also produce completely black female eyespots. It is not clear whether prolonged selection of the GOLD line would eventually produce eyespots lacking the central black disc.

Correlated responses

The proportions of the small anterior dorsal eyespot diverged almost to the same extent as those of the selected eyespot (Table 1). Strong correlated responses to selection were also apparent in other eyespots (see Fig. 2B), indicating that a common developmental mechanism underlies eyespot color composition on all wing surfaces.

There was no significant change in posterior eyespot size between GOLD and BLACK lines measured at the end of selection (Males: mean GOLD (mm) = 2.31, SD = 0.36, mean BLACK = 2.29, SD = 0.30, with $F = 0.21$, p = ns, DF = 1, 201; females: mean GOLD = 3.30, SD = 0.43, mean BLACK = 3.28, SD = 0.40, with $F = 0.26$, p = ns, DF = 1, 222). Correcting these data for wing length in an ANCOVA did not change the result.

Eyespot color ring allometry

It is clear from Table 1 that eyespots in males have relatively larger black discs than in females, but it is also the case that the male eyespots are smaller in absolute size (see text above). Within the same sex, however, the smaller anterior eyespots are 'golder' than the posterior ones (Table 1). Since color composition may vary with the size of any particular eyespot, we performed ANCOVAs on the black disc diameters, using total diameters as the covariate, within each of the lines, to examine whether; a) anterior and posterior dorsal eyespots, or b) eyespots from males and females, differed in their color composition when they were of comparable size.

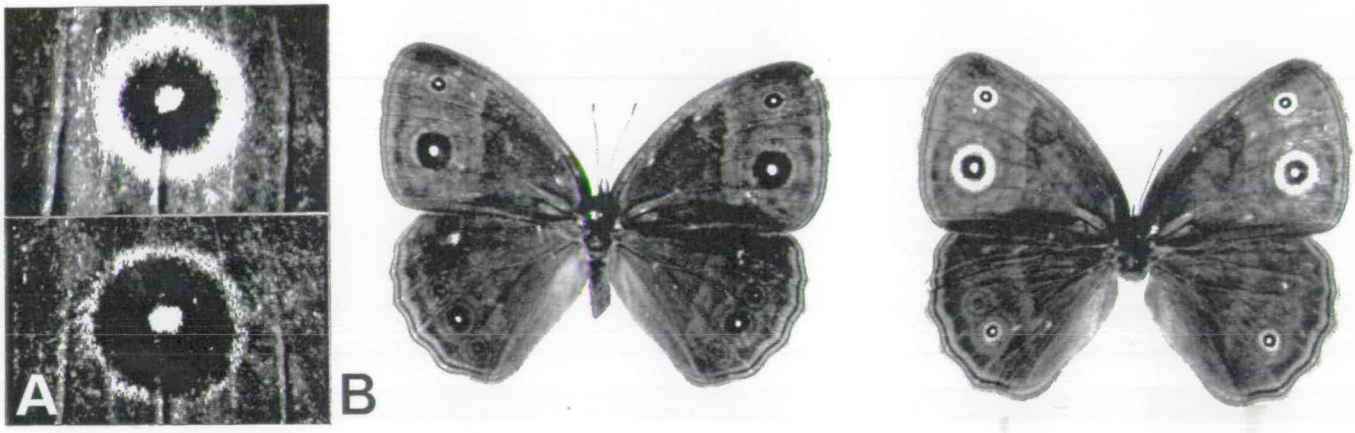

Figure 2. A) The target of selection for eyespot composition: GOLD (top) and BLACK (bottom) posterior eyespots on the dorsal forewing. B) Dorsal view of butterflies from the GOLD and BLACK selection lines.

We found that both anterior and posterior eyespots from males have a larger black disc than the corresponding female eyespots (Table 2a). There was one exception: male and female posterior BLACK eyespots had comparable black disc diameters (explained by both male and female posterior eyespots being almost entirely black in this line). For most ANCOVAs, the slopes of the regression lines of black diameter on total diameter were homogeneous between the sexes (i.e., the interaction term was not significant). In two cases, however, there was significant heterogeneity (Table 2a). Calculation of the adjusted black disc diameters (for total eyespot diameter) and significance testing was still performed using a common

regression line computed with a pooled regression coefficient within the groups. The high F values for differences in the elevation of the slopes (F-value for sex; especially in the STOCK posterior eyespot) indicated that, although the slopes were not parallel, their intercepts were sufficiently different for the analysis to be meaningful.

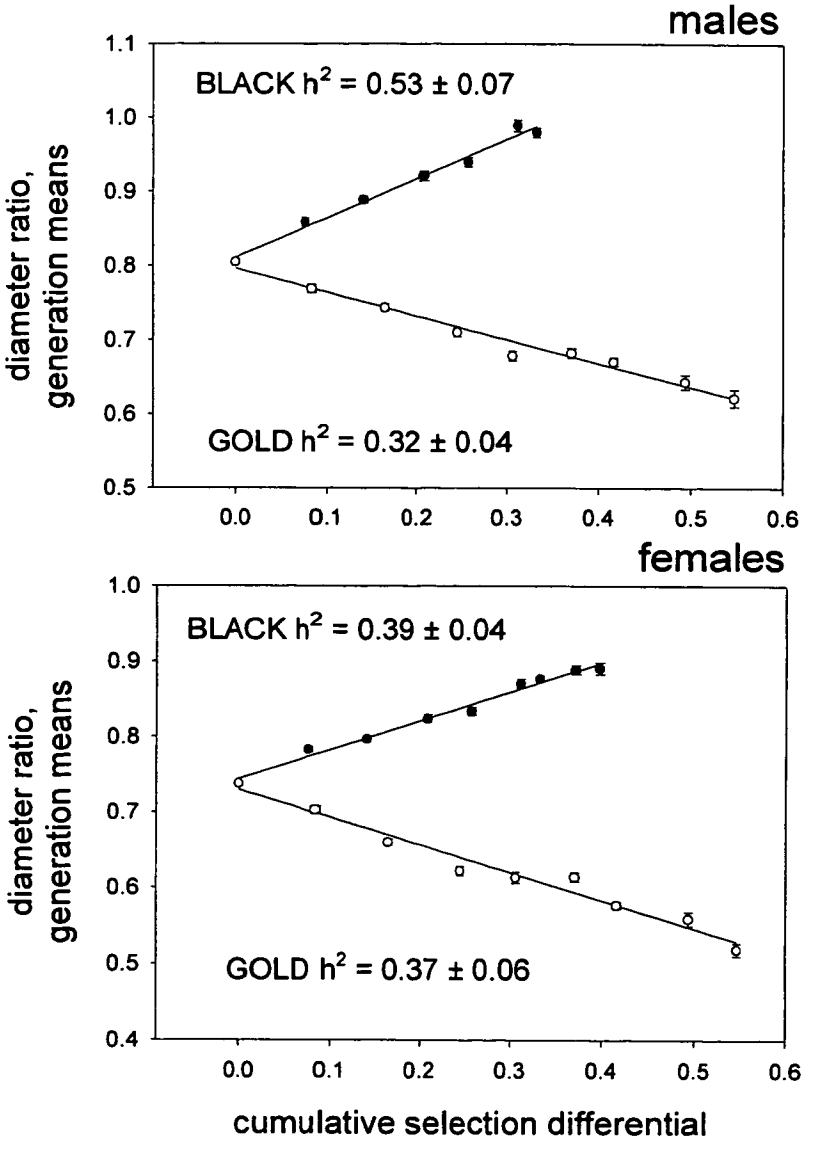

Figure 3. The change in eyespot composition (shown as mean ratio of black disc to total eyespot diameter) of BLACK and GOLD lines over 8 generations of selection. Estimates of realised heritabilities (h2 ± 95% CI) were calculated by the slope of the regression line of the diameter ratio generation means on cumulative selection differential. Bars around each generation mean correspond to 95% confidence intervals.

Table 1. Mean ratio of black disc-to-total eyespot diameter of the (selected) posterior and the anterior dorsal eyespots (± SD), after 9 generations of selection in GOLD and BLACK lines and in STOCK butterflies. Figures in brackets represent sample size.

	Males		Females	
Line	Anterior	Posterior	Anterior	Posterior
GOLD	0.55 ± 0.06	0.69 ± 0.05	0.52 ± 0.06	0.57 ± 0.05
	(137)	(137)	(114)	(114)
STOCK	0.71 ± 0.05	0.85 ± 0.05	0.66 ± 0.04	0.76 ± 0.04
	(100)	(98)	(100)	(99)
BLACK	0.86 ± 0.09	0.97 ± 0.06	0.79 ± 0.06	0.88 ± 0.06
	(78)	(68)	(110)	(110)

Table 2. Results of ANCOVAs performed on black disc diameters of a) male and female eyespots and b) anterior and posterior eyespots, taking total eyespot diameter as the covariate. The adjusted means for each test were always higher for males than for females (a) and higher for the posterior eyespot (b). The covariate (total diameter) was highly significant ($P < 0.000$) in all analysis with F values ranging from 487 to 1540 (for sample sizes see Table 1).

a) Eyespot	Line	Factors in ANCOVA	Signif. of F values	b) Sex	Line	Factors in ANCOVA	Signif. of F values
Anterior	GOLD	sex	***	Males	GOLD	eyespot	***
		sex*size	ns			eye*size	*
	BLACK	sex	*		BLACK	eyespot	***
		sex*size	*			eye*size	ns
	STOCK	sex	***		STOCK	eyespot	***
		sex*size	ns			eye*size	ns
Posterior	GOLD	sex	***	Females	GOLD	eyespot	ns
		sex*size	ns			eye*size	**
	BLACK	sex	ns		BLACK	eyespot	***
		sex*size	ns			eye*size	ns
	STOCK	sex	***		STOCK	eyespot	***
		sex*size	*			eye*size	ns

*** $P < 0.001$; ** $P < 0.01$; * $P < 0.05$; ns $P > 0.05$.

ANCOVAs performed within each sex (Table 2b) showed that when anterior and posterior eyespots were of a comparable size, the former were 'golder' than the latter. For GOLD females, however, the difference was not significant. The relationship between black centre and total diameter was colinear in most analyses, for both eyespots, even though there was little overlap in eyespot size between the two groups. In two cases there was a significant interaction effect: the slope for posterior GOLD eyespots, for each sex, was steeper than for anterior eyespots. In all cases, however, with the exception of the GOLD females, the adjusted means were very different between the eyespots (see F values in Table 2b). For further evidence that anterior eyespots, independently of their size, are really 'golder' than posterior eyespots, an ANCOVA was performed between the black centres of posterior eyespots in a line of butterflies selected for small posterior eyespots (LOW line, see Monteiro et al. 1994) and the black centres of STOCK anterior eyespots. These two eyespots were of comparable sizes in males (mean LOW posterior = 40.3, SD = 8.8; mean STOCK anterior = 40.8, SD = 7.6; T = -0.43, p = ns, df = 154). The ANCOVA showed that STOCK anterior eyespots were indeed 'golder' than LOW posterior eyespots (adjusted means of black centres: STOCK anterior = 28.9, SD = 0.3, LOW posterior = 33.6, SD = 0.3; F = 137.2, $p < 0.001$, df = 1, 176). There was no interaction effect between the two regression lines (F = 0.13, p = ns, df = 1, 175). Thus, in summary, anterior eyespots are 'golder' than posterior eyespots, even when through selection both eyespots achieve a comparable size, and males produce 'blacker' eyespots than females, throughout their overlapping range of sizes.

Ectopic eyespots induced by grafted foci

The ectopic eyespots induced by grafted foci were analysed to determine whether differences in eyespot composition between GOLD and BLACK selected lines resulted from differences in focal signal or in epidermal response.

Graft Experiment 1. The reciprocal grafts between pupae (Fig. 1B) showed that GOLD or BLACK foci in a BLACK host induced eyespots with a very narrow gold ring (large black-to-total diameter ratio) while, when grafted into a GOLD host, they each produced eyespots with a reduced black disc and a broad gold ring (small

Table 3. The 'goldness' and 'blackness' (ratio of black disc/total diameter) of eyespots induced by a grafted focus in Experiment 1. The comparison 'GOLD into BLACK' indicates a GOLD line focus grafted into a BLACK line pupa (a ratio of zero means that only gold scales were present outside the grafted tissue). n, number of scorable results from each category of graft operation. The Mann-Whitney (M-W) test statistics are given.

	Comparison (focus into host)	n	Ratio (median)	M-W (for ratio)	Size of ectopic eyespot (median)	M-W (for size)
a	GOLD into BLACK	27	1.00	W = 1207.5	37.0	W = 628.5
	BLACK into GOLD	33	0.00	***	52.0	***
b	GOLD into GOLD	36	0.35	W = 1411.5	61.5	W = 1954.5
	BLACK into GOLD	33	0.00	*	52.0	*
c	BLACK into BLACK	13	1.00	W = 285	43.0	W = 301.0
	GOLD into BLACK	27	1.00	ns	37.0	ns
d	GOLD into GOLD	36	0.35	W = 750.5	61.5	W = 1447.0
	GOLD into BLACK	27	1.00	***	37.0	***
e	BLACK into BLACK	13	1.00	W = 520	43.0	W = 244.0
	BLACK into GOLD	33	0.00	***	52.0	ns

*** $p < 0.001$; ** $p < 0.01$; * $p < 0.05$; ns $P > 0.05$

ratio). The four different categories of graft were arranged in pair-wise comparisons and the eyespot ratio medians were compared using the non-parametric Mann-Whitney test (Table 3). It is clear that there is a major effect of host 'environment' on eyespot color composition (Table 3, a, d & e) while the origin of the focus has little effect (Table 3, b & c). In grafts to GOLD hosts, however, BLACK foci produce somewhat 'golder' eyespots than GOLD foci (Table 3, b). This is explained by a positive correlation between size (total diameter) of an induced eyespot and its ratio ($r_S = 0.331$, $P < 0.01$; for all eyespots induced on a GOLD host), coupled with the finding that eyespots induced by the BLACK foci were smaller than those induced by GOLD foci. Other significant size differences (e.g. Table 3 a, d) do not affect the results of the ratio analysis since there, the smaller eyespot is also the 'blacker'.

Graft Experiment 2. The double graft of foci from BLACK and GOLD pupae (Fig. 1C) resulted in formation of two ectopic eyespots on the host wing (Fig. 4A). The data from the three different hosts were pooled and then split into two categories: all hosts where the GOLD focus was grafted to the proximal site (and BLACK to distal) and those with the GOLD focus grafted distally (and BLACK proximally). The data were analysed with a Wilcoxon paired comparison test where the eyespots induced by the GOLD and BLACK foci in the same host made up a data pair, with the null hypothesis of no difference in the composition of the eyespots. The ratio of black-to-total diameter for the BLACK focus-induced eyespot was subtracted from that of the GOLD focus-induced eyespot, a negative value indicating that BLACK foci induced a 'blacker' eyespot. The differences were then ranked from smallest to largest, irrespective of their sign. The original sign of the differences was assigned to the ranks and the sum of the positive and negative ranks calculated. The smallest sum in absolute value, Ts, is the test statistic (Sokal and Rohlf, 1995). There was a strong position effect (Table 4): whichever focus was grafted into the proximal position yielded the ectopic eyespot with the largest proportion of gold. The effect of host site was much stronger than any effect of the foci in controlling the color composition of induced eyespots, thus the data could not be examined in a pair-wise manner as had been initially planned. The enlarged gold ring in the proximal eyespots may be related to their smaller size: a GLM analysis of square-root transformed total diameter data (to produce homogeneous variances ; chi-square = 9.86; df = 11; p = ns) with 4 factors (site of operation, type of focus, type of host, sex) showed that proximal eyespots were smaller than distal ones, GOLD foci induced smaller eyespots than BLACK foci, and BLACK hosts as well as male hosts formed the smaller eyespots (Table 5).

No parametric test could be performed on the ratio of black-to-total diameters since the variances for the different groups were heterogeneous and the data highly skewed. A series of non-parametric comparisons were then performed, for each grafting site, to compare the effect of the GOLD and BLACK foci, both within each host line (GOLD, BLACK and HIGH) and with all hosts combined (Table 6). This analysis did not detect any affect of line of origin of focus on eyespot color

proportions but it was evident that a BLACK host produced 'blacker' eyespots than a GOLD host.

Table 4. Analysis of the two ectopic eyespots induced in Graft Experiment 2 by grafting foci into proximal and distal positions: Wilcoxon sign-ranked test for paired data, to compare differences in color composition of eyespots induced by the GOLD and BLACK foci (see Results for details). n, number of host wings bearing two scorable ectopic eyespots.

Focus position	n	Sum of positive ranks	Sum of negative ranks	Wilcoxon sign-ranked tabled Ts
GOLD-proximal	38	108	633	194 (> 108)
BLACK-distal				p = 0.005
BLACK-proximal	31	411	85	118 (> 85)
GOLD-distal				p = 0.005

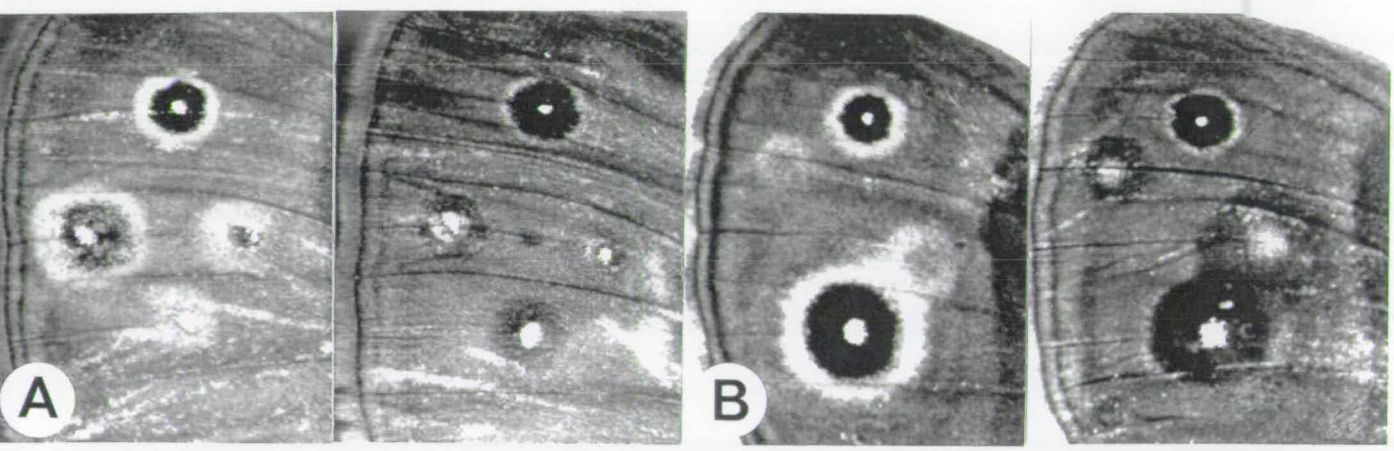

Figure 4. A) Graft Experiment 2: a GOLD and a BLACK focus were grafted into a proximal and a distal position respectively on a GOLD host (left) and BLACK host (right). B) Ectopic eyespots induced by damage during the pupal stage on GOLD (left) and BLACK (right) line butterflies.

Table 5. GLM analysis on size of ectopic eyespots resulting from Graft Experiment 2. The analysis was performed with 4 factors (site of operation, line of grafted focus, line of host and sex). The eyespot diameters were square-root transformed. Analysis of interaction terms (not shown) showed a significant ($p < 0.05$) interaction between host line and sex.

Source	DF	F	p	Levels within factors	Means	SD
Site	1	7.53	**	proximal	6.87	0.09
				distal	7.22	0.09
Focus	1	5.50	*	GOLD	6.90	0.10
				BLACK	7.19	0.08
Host	2	29.74	***	GOLD	7.50	0.09
				BLACK	6.23	0.15
				HIGH	7.40	0.06
Sex	1	27.41	***	males	6.72	0.10
				females	7.37	0.07
Error	231					

*** $p < 0.001$; ** $p < 0.01$; * $p < 0.05$

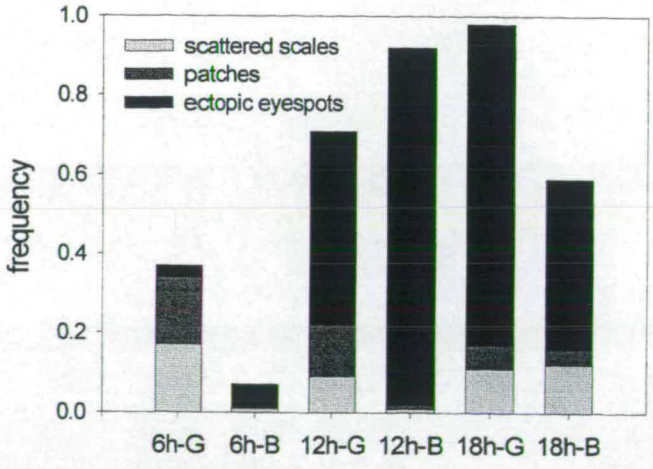

Figure 5. Frequency of the different types of ectopic pattern induced by wing damage (data from the two sites is combined). Wings of GOLD (G) and BLACK (B) pupae were pierced either at 6, 12 or 18h after pupation.

We conclude from Graft Experiments 1 and 2 that it is mainly the epidermal response to a focal signal that has been changed in the GOLD and BLACK lines as a result of artificial selection. The source of the focus seems to have no influence on the relative extent of black and gold scales.

Table 6. Comparisons between the ratio of black-to-total eyespot diameters (median) produced in Graft Experiment 2 by a GOLD or BLACK grafted focus, per site insertion of graft and type of host pupae. Values within brackets correspond to sample size.

		Host pupa			
Site	Focus	GOLD	BLACK	HIGH	All hosts
Proximal	GOLD	0.000 (19)	0.789 (5)	0.000 (37)	0.000 (61)
	BLACK	0.000 (10)	0.778 (9)	0.000 (30)	0.000 (49)
	Kruskal-Wallis	H = 1.69 df = 1, p = ns	H = 0.02 df = 1, p = ns	H = 0.26 df = 1, p = ns	H = 0.16 df = 1, p = ns
Distal	GOLD	0.000 (13)	0.773 (9)	0.536 (35)	0.554 (57)
	BLACK	0.247 (19)	0.837 (14)	0.590 (34)	0.571 (67)
	Kruskal-Wallis	H = 0.04 df = 1, p = ns	H = 0.53 df = 1, p = ns	H = 0.32 df = 1, p = ns	H = 0.15 df = 1, p = ns

Ectopic patterns induced by wing damage

Wings of BLACK and GOLD line pupae were damaged in two positions (Fig. 1D) and the resulting patterns ranged from a few scattered gold or black scales, to a more compact patch of gold or gold and black scales, to a fully differentiated ectopic eyespot with a black centre and an outer gold ring (Fig. 4B). Damage at 6h produced mostly scattered scales or patches, whereas operations at both 12h and 18h induced mainly eyespots (Fig. 5). We have analysed the proportions of gold and black in ectopic eyespots only, and compared them between selection lines.

A GLM analysis on ectopic eyespot size (not shown) demonstrated that ectopics produced at 12h were larger than at 18h; proximal ectopics were larger than

distal ones; females produced larger ectopics than males and at 18h, GOLD line ectopics were larger than BLACK line ectopics. The color composition of eyespots induced in the BLACK and GOLD lines could not be compared using an analysis of covariance (because the slopes of the regression of black diameters against total ectopic eyespot diameters were not parallel over the lines), so the ratios of black-to-total eyespot diameters were compared by means of two-sample Mann-Whitney non-parametric tests. In all comparisons of median ratios (per time of operation, sex and site of operation; Table 7), induced eyespots on the GOLD were 'golder' than those on the BLACK butterflies. These results support the hypothesis that the response properties of the epidermis have been changed by selection for GOLD and BLACK eyespots.

Table 7. Color composition of ectopic eyespots induced by damage to GOLD and BLACK pupae. A Mann-Whitney test was performed between the medians of the ratio of black/total diameters of the GOLD and BLACK ectopics for each position (see Fig.1D, 4B), age at cautery (12h and 18h) and sex. Numbers in brackets indicate sample size.

		Males		Females	
Age	Line	Proximal	Distal	Proximal	Distal
12h	GOLD	0.95 (8)	0.74 (15)	0.65 (22)	0.68 (25)
	BLACK	1.00 (25)	1.00 (32)	1.00 (32)	1.00 (31)
Mann-Whitney		W = 67.0 ***	W = 187.5 ***	W = 345.0 ***	W = 450.0 ***
18h	GOLD	0.50 (58)	0.43 (57)	0.45 (29)	0.42 (21)
	BLACK	1.00 (18)	1.00 (24)	0.77 (6)	1.00 (13)
Mann-Whitney		W = 1728 ***	W = 1676.5 ***	W = 474.0 *	W = 237.5 ***

*** $p < 0.001$; * $p < 0.05$

The effect of sex and site and time of operation on color composition of the ectopic eyespots was analysed within each line by an ANCOVA of black disc

diameters, using total diameter as a covariate (not shown). For both lines, 18h ectopics were 'golder' than 12h ones. In addition, distal ectopics were 'golder' than proximal ones in the GOLD line and, in the BLACK line, males produced 'blacker' ectopics than females.

The color composition of ectopic eyespots and control posterior eyespots of the same butterflies were compared by an ANCOVA (not shown). The analysis showed that GOLD line 12h ectopics (both proximal and distal) showed a larger black disc than control eyespots, whereas 18h ectopics were on average 'golder' than their control eyespots. For the BLACK line, female 12h and 18h ectopics were always 'blacker' than control eyespots, whereas in males, 18h ectopics were 'golder' than the corresponding control eyespots.

DISCUSSION

Substantial additive genetic variation is present for eyespot color composition, even in our laboratory stock of *B. anynana*. The estimates of heritability are similar to, although a little lower than, those for eyespot size in both the ventral and dorsal large posterior eyespot (Holloway et al. 1993; Monteiro et al. 1994). Selection in the BLACK line reached its phenotypic limit, especially in males, by the 5th generation, producing mostly 'black' eyespots. No limit was reached in the GOLD line as all eyespots still had a (reduced) central area of black scales in the 8th generation (Fig. 3).

All other eyespots, on both wing surfaces, changed their color composition in the direction of selection. Butterflies from the GOLD line became much more striking in appearance, whereas BLACK line butterflies became dark and less conspicuous (Fig. 2B). Similar strong correlated responses to selection were found in experiments for eyespot size in *B. anynana* (Holloway et al. 1993; Monteiro et al. 1994).This shift, indicating strong genetic correlations among all eyespots, supports the idea that eyespots are developmental homologues formed by a common developmental mechanism (Nijhout 1991).

The proportions of the different colored rings in an eyespot are mainly determined by the response properties of the wing epidermis. Both focal grafting and wing damage results support this conclusion. Thus, any focus or local damage in BLACK wing epidermis induces a 'black' eyespot, with a very narrow gold ring. When a GOLD pupa is used, the focus or damage will induce an eyespot with a small black disc and a broad gold ring.

Using the unselected stock, French and Brakefield (1995) grafted anterior and posterior foci into different positions in the wing and found that posterior foci always induced 'blacker' ectopic eyespots that anterior foci. They argued that the color ring proportions of the eyespot depended on the identity of the focus and not on the responding epidermis. This analysis, done with ratios, without attending to the total eyespot size, is only partly correct. It is now clear that the grafting of a posterior foci, into any given site, will induce 'blacker' eyespots only due to the fact that they will also induce larger eyespots than anterior foci, when grafted into the same site.

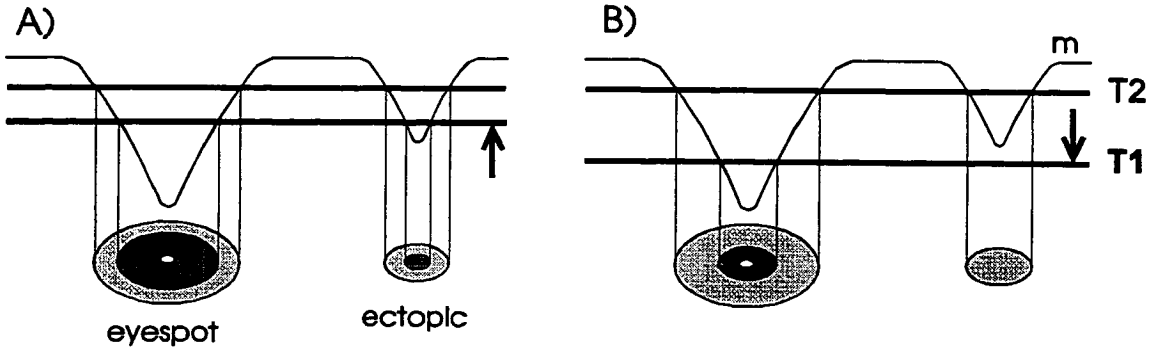

Figure 6. Gradient model of eyespot specification involving two thresholds of response to concentration of morphogen (m). Cells experiencing morphogen concentration < T1 later form black scales; between T1 and T2, gold scales (stippled) and above T2 the background brown scales. In this version of the model, the focus acts as a local sink, producing a pit in morphogen concentration, and hence an eyespot pattern. Appropriately-timed local damage also depletes morphogen (see text), leading to an ectopic pattern. Selection in A) the BLACK line and B) the GOLD line may raise or lower the T1 threshold and hence change color composition (but not size) of the normal and ectopic eyespots.

In relation to the gradient model of eyespot formation (see Introduction), the present results indicate that genetic variation for color composition affects threshold levels of response of the epidermal cells to the focal signal. Figure 6 illustrates a sink variant of the gradient model, where responding cells have two thresholds of sensitivity to morphogen concentration. A narrow gold ring can be produced by selection bringing the two thresholds closer, while separating them leads to a 'golder' eyespot. Change is shown only in the lower threshold (T1), as there was no difference in eyespot outer diameter between the BLACK and GOLD lines. In previous selection experiments for eyespot size (Monteiro et al. 1994), the major change was in focal signal but changes in response (i.e. in threshold T2) had also occurred. There may be a strong genetic coupling of the two thresholds as the size-selected lines maintained a similar color ring composition: no difference for the males and black-to-total diameter ratios of 0.76 for the HIGH line and 0.70 for the LOW line females (Monteiro et al. 1994). In the present experiments, selection on ratio (to produce GOLD and BLACK lines) would uncouple changes to T1 and T2. It remains unclear, however, why only T1 was altered, while T2 (and eyespot size) was unchanged.

Apart from differences of response between the selected lines, within individuals there were differences across the wing epidermis. Eyespots induced by a grafted focus at a distal site were 'blacker' than eyespots of a comparable size induced more proximally. Response thresholds are, thus, not uniform across the wing epidermis (similar results were found in French and Brakefield 1995, for equivalent positions). We also found a difference in color composition for the normal anterior and posterior eyespots of *B. anynana*: anterior eyespots are 'golder' that posterior ones of a comparable size, indicating a difference of the response in these different wing regions. When in a separate experiment (see chapter 5), two identical posterior foci (from the left and right wings) were grafted into the anterior and posterior wing cells, distal to the normal eyespots, they induced 'blacker' eyespots on the posterior site (adjusted means from an ANCOVA for black disc diameter (total diameter as covariate) = 53.0 and 45.4 for posterior and anterior grafts respectively; $F_{1,45}$ =

11.14, $P < 0.01$). Also, eyespot color composition varies with the sex of the butterfly: males normally have a narrower gold ring than females.

The frequency and size of ectopic eyespots induced by focal damage at different times and sites were similar to the results of previous studies (French and Brakefield 1992; Monteiro et al. 1994; Brakefield and French 1995). Eyespot induction by damage, although not well understood, can be interpreted in terms of the gradient model (Fig. 6; see French and Brakefield 1992, Brakefield and French 1995 for discussion).The large differences in the color pattern of ectopics produced in the BLACK and GOLD lines, mimic the respective eyespot phenotypes. The relationships between eyespot composition and size for these ectopic patterns were, with one exception, comparable to those for the control eyespots. In terms of the model, this suggests that cells respond according to the same thresholds and the same morphogen gradient is established around the natural focus and around an injury, presumably by diffusion. Further speculation (e.g. why ectopics tend to be 'golder' when induced at 18h rather than 12h) seems unprofitable until there is more direct evidence for the model.

This study shows that our lab stock has substantial additive genetic variance affecting the response thresholds of wing epidermis to signalling from the eyespot focus. Artificial selection can produce rapid responses to yield lines with more or less 'black' eyespots or those with much more prominent outer gold rings: phenotypes not present in the stock or in field collected material of *B. anynana* (P. M. Brakefield, personal observation). The different *Bicyclus* species show substantial variability in the proportions of gold and black on their eyespots (Condamin, 1973). All phenotypes, however, fall well within the range of the selected eyespot phenotypes of *B. anynana*. There is no indication that these species-differences involve epidermal response thresholds, although this could be investigated by cross-species focal grafts. Some species have completely black dorsal eyespots and ventral ones with only a narrow gold ring (e.g. *B. angulosus* and *B. cottrelli*). Others have a broad gold ring on both wing surfaces (e.g. *B. ena* and *B. trilopus jacksoni*). In these latter species, the background color surrounding the eyespots also tends to be light in color, reducing the conspicuousness of the gold ring. Visual selection in the field may tend

to favour an intermediate eyespot phenotype in most *Bicyclus* species, perhaps because of its effect on conspicuousness. However, variation in time and space or disruptive selection (sexual selection vs. visual selection by predators) may account for the occurrence of high additive genetic variance for eyespot color composition and size (Monteiro et al. 1994), giving strong potential for evolutionary responses.

CHAPTER 3

Eyespot Shape

ABSTRACT

Bicyclus anynana normally has circular-shaped eyespots on its wings. By performing artificial selection on eyespot shape in two lines of butterflies, we produced elliptical eyespots (FAT and THIN). Realized heritabilities for this trait were low. The developmental nature of the response to selection was investigated by surgically testing for radial asymmetry in the signal component of the developmental mechanism specifying the eyespot. Removing and rotating the signalling centre of the eyespot (the focus) by 90 or 180 degrees and grafting it back into the wing epidermis did not influence eyespot shape. A change in the response to the focal signal was investigated by local damage inflicted outside the focal region and the shape of the ectopic eyespots induced was characteristic of the FAT or the THIN selected line. Both experiments showed that differences between lines in eyespot shape resulted from differences in the epidermal response to the focal signal. We conclude that our stock contained genetic variability for eyespot shape which influenced general epidermal properties (perhaps related to epidermal expansion during wing morphogenesis), but apparently not the mechanism of focal signalling.

INTRODUCTION

Cells in a butterfly's wing epidermis differentiate to produce the diverse and spectacular color in the particular arrangements that characterize each wing surface of each species. The underlying developmental mechanisms are not fully understood.

Experimental work on wing patterns has mainly concentrated on the specification of the simple eyespot pattern (see Nijhout 1980, 1985; French and Brakefield 1992, 1995; Monteiro *et al.* 1994; Brakefield and French 1995). In previous work we have examined quantitative genetic variation of the developmental system to understand which of its components controls the size and color composition of an eyespot pattern (Monteiro *et al.* 1994; Monteiro et al 1997b). Here we investigate the underlying developmental mechanism controlling eyespot shape. Only by studying the developmental mechanisms involved in the translation of genotype to phenotype can we have a complete understanding of evolutionary change, morphological diversity and its associated limitations and constraints.

The pigments that make up an eyespot are deposited in precise spatial relation to a reference point, or "focus", midway between the wing veins. During development, the focus provides "positional" information to the surrounding cells that determines the nature of the differentiation they will undergo and their subsequent production of a specific pigment (Nijhout 1978, 1980). Hence elimination of the focus at an early pupal stage can remove the eyespot, and grafting it to a different position results in the surrounding host cells responding to the focal signal and forming an ectopic eyespot (Nijhout 1980; French and Brakefield 1992, 1995; Monteiro *et al.* 1994). The focus may signal by producing a diffusible morphogen that forms a gradient in the surrounding epidermis (Nijhout 1980, 1991). Progressively lower morphogen concentrations would occur in concentric rings of cells around the focus, and these cells would respond to produce and deposit, later in development, different pigments, forming the concentric eyespot color pattern. Also, at a particular stage, the epidermis of the pupal wing may respond to local damage (piercing with a fine needle) by producing an ectopic eyespot with its characteristic color rings (see Nijhout 1985; Monteiro *et al.* 1994; Brakefield and French 1995). It is not clear how local damage can mimic a natural focus, to initiate formation of an eyespot. If one turns the focal source model upside down, we obtain an equally plausible "sink model". Here, the focal cells degrade morphogen present at high levels throughout the epidermis where the lowest levels of morphogen will be found at the focus. Local damage might, using this model, produce an artificial sink for

morphogen and, in this way, mimic the action of a focus (French and Brakefield 1992).

The experiments described here are concerned with the genetic and developmental aspects of eyespot formation on the wings of a nymphalid butterfly, *Bicyclus anynana.* Selection experiments were used to estimate genetic variance for shape of the large posterior eyespot on the dorsal forewing. Correlated responses to selection, in the shape of the smaller anterior eyespot on the same wing surface, were also examined. After selection for elliptical eyespots, focal rotation-grafts and wing damage experiments were performed on pupae of the divergent lines, to investigate whether the selection produced radial asymmetry in the focal signalling or epidermal response components of the developmental process that specifies the (normally circular) eyespot.

MATERIAL AND METHODS

The experimental animals

Bicyclus anynana were reared at 28°, 12D:12L, 80-90% RH.

The selection on eyespot shape

In each generation, virgin butterflies were selected on the basis of the shape of the large posterior eyespot on the dorsal surface of the forewing. Using a stereo microscope fitted with an ocular micrometer, eyespot total diameters were measured along two perpendicular axes, crossing the central white pupil: along the wing cell midline (parallel to the wing veins) and orthogonal to it. Parents for the next generation were selected on the basis of the ratio of eyespot diameter along the midline to diameter across the midline. A FAT (large ratio - elongated proximal-distally) and a THIN (small ratio - elongated anterior-posteriorly) line were selected for nine generations, starting from a single large population from the STOCK. Truncation selection was applied in both sexes. For the first two generations 40 females and 80-100 males with the most extreme phenotypes were selected within

each line from a total of around 900 (P) or 350 (F1) individuals. The selection pressure was increased for the remaining generations by reducing the number of selected females to 25 and that of males to 60-80 (chosen from a total of 300 to 600 individuals). This alteration in the selection procedure was taken after preliminary realized heritability estimates were calculated with the data from the previous generations, and found to be low. For the ninth generation, 40 selected females from each line were allowed to lay eggs and all progeny were measured in an image analysis system, together with 100 butterflies of each sex of the STOCK population. Measurements of the small anterior as well as the large posterior eyespot were made, to estimate correlated responses to selection. Realized heritabilities were estimated at generation three and eight by regressing all previous generation means against the cumulative selection differential, averaged between the sexes (see Falconer 1989).

Grafting of a focus

For the surgical experiments, pupae from the FAT and THIN lines were used, after eight generations of selection. Pupation times were recorded every half hour. Pupae were operated 3 to 4.5 hours after pupation, when the epidermis of the dorsal surface of the forewing is still attached to the pupal cuticle which is sufficiently hardened to permit cutting and manipulation. A square piece of cuticle and epidermis was cut around the focus of the posterior eyespot of the left forewing, lifted with fine forceps, rotated either 90° or 180° and lowered back in place (Fig. 1). The operated pupae were returned to 28° and, after emergence, the butterflies were frozen. The sex was scored and the large operated eyespot was measured in the two diameters: along and across the wing cell midline.

Damage experiments

The left forewing of each operated pupa was damaged twice at different time periods. First, the anterior and posterior eyespot foci were pierced with a fine tungsten needle at 6h after pupation, to reduce the size of the normal eyespot (see French and Brakefield 1992). The pupa was returned to 28° and then pierced again, either at 12h or at 18h, to induce eyespots at two or three non-focal sites (see Fig. 1). Emerged

butterflies were frozen and their ectopic patterns measured along and across the wing. All measurements were done blind, with no knowledge of selection line.

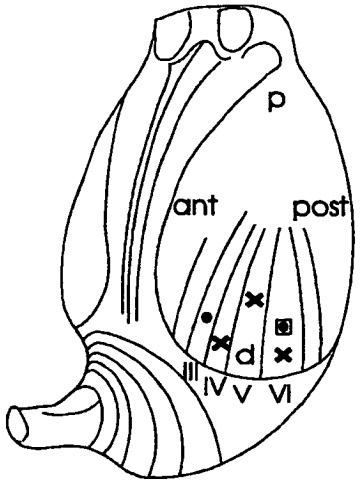

Figure 1. The grafting and damage operation sites on the pupal left forewing. The rotated graft tissue is indicated by a square, including the focus (filled circle) of the large posterior eyespot. Crosses mark the positions of wing damage. Spaces between veins are labelled II-V and damage sites are designated from anterior to posterior IIId, IVp and Vd. ant, anterior; post, posterior; p, proximal; d, distal.

RESULTS

The change in eyespot shape

For each selection line and each sex, the white pupil, black disc and gold ring had a different shape within the same eyespot: the outer gold ring was always the "fattest" (with the highest shape ratio; see Table 1), while the white pupil was always comparatively "thin" in shape. The shape of these components in the selected large posterior eyespot, however, changed to a similar extent in the selected lines relative to STOCK butterflies (Fig. 3a; Table 1). A greater shape change (from STOCK eyespots) was achieved in the FAT line than in the THIN line, probably partly due to the larger selection differential applied to FAT line butterflies (21% greater; see Fig. 2). The anterior eyespot diverged in shape only in the FAT line, where it became "fatter" in both the outer gold ring and the black disc. THIN anterior eyespots in each sex retained the same shape as STOCK butterflies.

Table 1. Shape of the posterior and anterior eyespots in FAT and THIN selected lines after nine generations of selection and in the STOCK population.Table gives mean values of the ratio of proximal-distal to anterior-posterior diameters for the white pupil (White), black disc (Black) and outer gold ring (Total) of the eyespots. F and P values are from a one-way ANOVA between the ratios of the three groups (FAT, THIN and STOCK). Pair-wise comparisons were done using the Bonferroni method (T = THIN; S = STOCK; F = FAT).

	males						females					
		posterior			anterior			posterior			anterior	
line	n	Total	Black	White	Total	Black	n	Total	Black	White	Total	Black
FAT	103	1.15	1.10	0.97	1.18	1.12	121	1.11	1.07	0.97	1.18	1.11
STOCK	100	1.04	1.01	0.90	1.12	1.07	100	1.01	0.97	0.94	1.10	1.03
THIN	92	1.00	0.94	0.86	1.12	1.05	146	0.95	0.91	0.85	1.10	1.05
	F	194.7	173.0	15.8	18.9	17.3		328.2	276.2	33.1	61.6	25.1
	P	***	***	***	***	***		***	***	***	***	***
Pair-wise compar.		all ≠	all ≠	all ≠	T = S	T = S		all ≠	all ≠	F = S	T = S	T = S

*** $P < 0.001$

Realized heritabilities

The two selection lines progressively changed in eyespot shape, over eight generations of selection (Fig. 2). The slopes of the regression of shape (mean ratio of diameters) against cumulative selection differential estimated realized heritabilities which ranged between 13 and 17% (see Fig. 2). Realized heritabilities calculated up until the third generation (with the first four points on the x-axis) gave slightly higher estimates (FAT males: 0.22 ±0.02; THIN males: 0.19 ± 0.06; FAT females: 0.12 ± 0.06; THIN females: 0.21 ± 0.02). The decrease in heritability, especially in the males, with the continuation of selection was partly due to a plateau being reached from the fifth generation onwards i.e., there was no further divergence between the lines. The eyespots of males (but not females) in both lines appeared to have reached the limit of their circular distortion. The reduction if the number of selected butterflies from the 3rd generation onwards could also have lead to a more rapid plateauing and loss of additive genetic variance due to drift and stronger inbreeding effects (Weber 1990a).

The grafting experiments

The grafting experiment tested for an asymmetry in the focal signalling component of eyespot development in the selected lines. If eyespot shape reflects differences in anterior-posterior vs. proximal-distal signalling, it should be changed by a 90°, but not by a 180° rotation of the focus. Of the 234 operated pupae (from the two lines, with a 90° or 180° rotation) a total of 153 produced adults where the graft had healed, forming appropriately rotated white scales, and was surrounded by a large scorable eyespot pattern (Fig. 3b). A general linear model (GLM) analysis was carried out on the data for the ratio of eyespot diameters and three factors were included; 1) selection line (two levels: FAT and THIN), 2) rotation of the graft (two levels: 90° and 180°), and 3) sex. The data were first transformed by raising all values to the power of -0.095 (Taylor's power law, see Fry 1993) to obtain homogeneous variances in the eight groups (Bartlett's test: chi-square = 13.9, df = 7, p = ns). Analysis showed that no significant part of the eyespot shape variation was explained by graft rotation

or sex and there were no significant interaction effects (Table 2; Fig. 4). This means that for a butterfly of either sex, focal orientation doesn't influence the shape of the final eyespot. Selection line was the only significant factor: butterflies will have a "thin" eyespot if coming from the THIN line and a "fat" eyespot if emerging from the FAT line (see Fig. 3b).

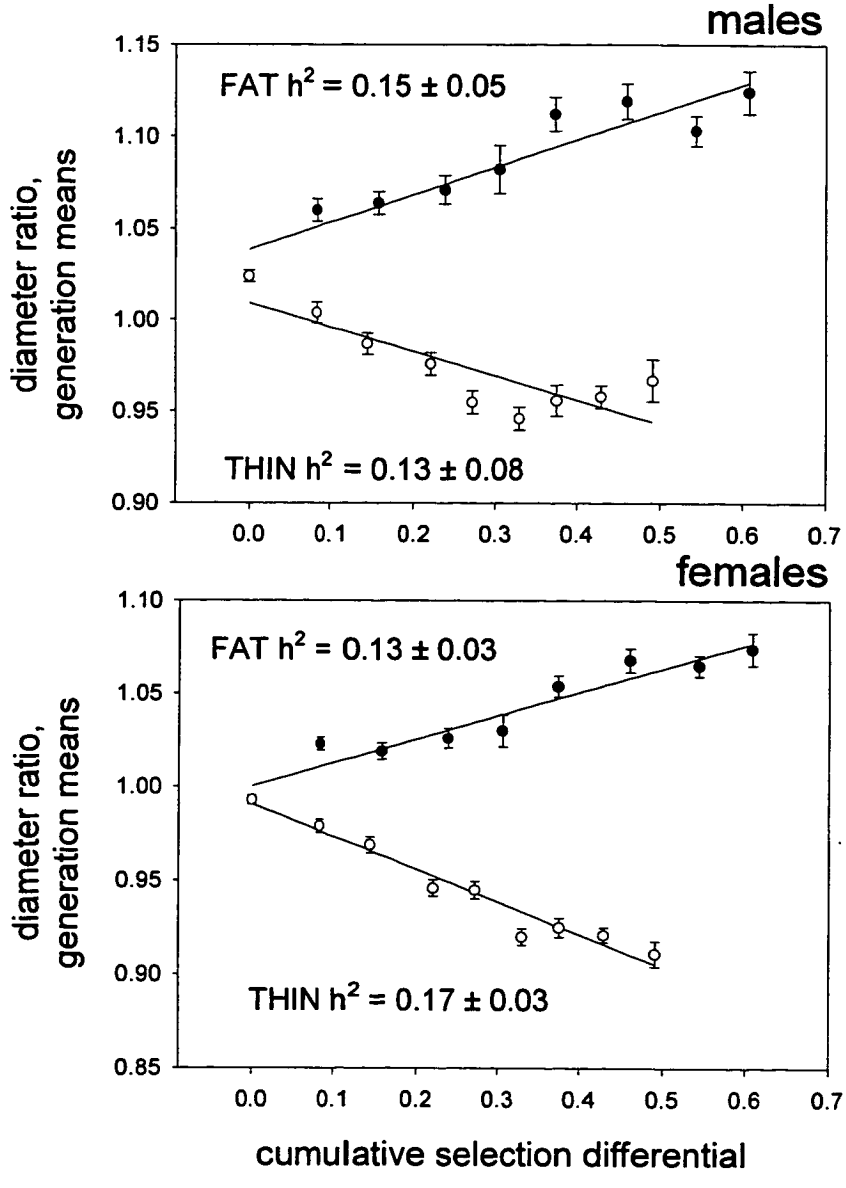

Figure 2. The change in eyespot shape (shown as mean diameter ratio) of FAT and THIN lines over eight generations of selection. Estimates of realised heritabilities (h^2 ± 95% CI) were calculated by the slope of the regression line of all generation means on cumulative selection differential. Bars around each generation mean correspond to 95% confidence intervals.

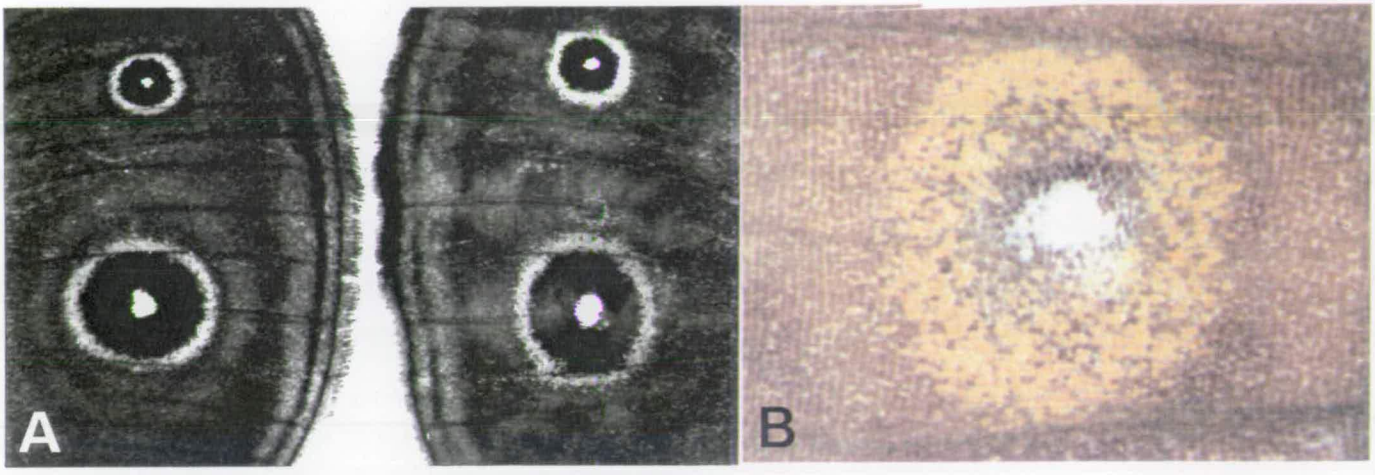

Figure 3. Selected eyespots and focal graft rotation. a) A FAT (left) and a THIN wing showing the small anterior and the large selected posterior eyespot. b) A typical result from a 90° focal rotation on a pupa from the THIN line: the resulting adult eyespot is "thin" in shape.

Table 2. General linear model analysis on eyespot shape after focal rotation with three factors: selection line (FAT and THIN), rotation of the graft (90° and 180°) and sex.

Source	DF	F	P
line	1	91.39	***
rotation	1	0.41	ns
sex	1	0.09	ns
line*rotation	1	0.97	ns
line*sex	1	1.61	ns
rotation*sex	1	1.21	ns
line*rotation*sex	1	2.32	ns
error	144		
total	151		

*** $p<0.001$

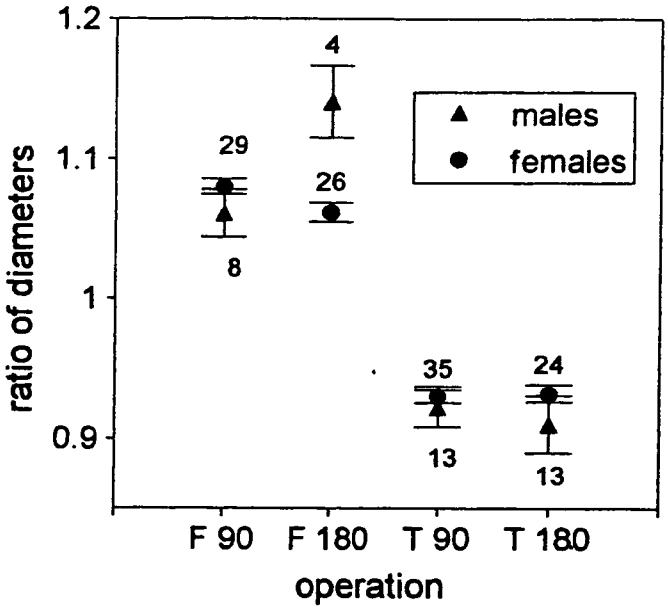

Figure 4. Shape of eyespots from the FAT (F) and THIN (T) lines after focal rotation by either 90° or 180°. Means with asymmetrical 95% confidence intervals for the ratios in the untransformed scale. The means have been adjusted by the GLM analysis (Table 2), to account for unbalanced data. Numbers of scorable animals are shown in brackets.

The damage experiments

These experiments tested whether FAT and THIN lines differed in the shape of eyespots induced by piercing the pupal wing epidermis. As in previous experiments (Brakefield and French 1995), such damage at 12-18h after pupation induced ectopic patterns consisting of scattered gold scales (not analyzed further), gold patches (GP), gold and black patches (GBP) or ectopic eyespots (EE) with a black disc and outer gold ring. GP, GBP and EE were measured in their total diameters, along and across the wing cell midline. EEs were also measured in their black disc diameter along the same two axis. In order to test whether the shape of ectopic patterns differed between the FAT and THIN lines, a GLM analysis was done on the ratio of their total diameters. Three factors were included in the analysis: line (with two levels: FAT and THIN), site (three levels: IVp, IIId and Vd; see Fig. 1) and hour of cautery (two levels: 12h and 18h). Sex was initially included as one of the factors but due to two empty cells (the males were missing in both the FAT and THIN line for the IIId site

and the 12h operation) the full GLM design with interactions could not be calculated. The GLM performed without the interaction terms showed that sex didn't account for a significant difference between the ratios and it was thus removed from the subsequent analysis. The 12 remaining groups of data showed homogeneous variances (Bartlett's test: chi-square = 15.3, df = 11, p = ns).

The shape of ectopic patterns differed significantly between the lines, the sites and the times of operation (Table 3), with a significant interaction term between time and site of operation. There was a consistent difference between selected lines: FAT butterflies produced "fatter" ectopic patterns than THIN butterflies at the three sites and the two times of operation (Fig. 5; a, b). Also, patterns occurring at the proximal site (IVp) were "fatter" than those at the distal sites, and patterns induced at 12h were "thinner" than those produced at 18h except at one of the sites (Fig. 5b, c). A summary of the results, with all the interacting factors, is shown in Fig. 5d.

A similar analysis was then performed on the measurements made on the black discs of the ectopic eyespots (Table 4). All groups showed equal variances (Bartlett's test: chi-square = 15.9, df = 11, p = ns). The same pattern was found as in the previous analysis on total ectopic diameters, but the difference between the lines was no longer formally significant and a new significant interaction effect appeared between line and site. Fig. 6a shows that the black disc patterns of the FAT line were only distinct and "fatter" than those from THIN at one site (Vd); at the other sites the line means were similar. FAT line ectopics were "fatter" than those in the THIN line at each of the time periods. As for the total-diameter ratios, the black discs were "fatter" at the proximal site and when induced at 18h (Fig. 6b, c). The overall picture is given in Fig. 6d.

Table 3. General linear model analysis on shape of ectopic patterns with three factors: selection line (FAT and THIN), site of operation (IIId, IVp and Vd) and time of operation (12h and 18h) - Based on the ratio of total diameters of all ectopic patterns.

Source	DF	F	P
line	1	8.51	**
site	2	12.14	***
hour	1	16.04	***
line*site	2	0.10	ns
line*hour	1	0.56	ns
site*hour	2	12.25	***
line*site*hour	2	0.17	ns
error	262		
total	273		

**p<0.01; ***p<0.001

Table 4. General linear model analysis of shape of ectopic eyespots with three factors: selection line (FAT and THIN), site of operation (IIId, IVp and Vd) and time of operation (12h and 18h). Based on the diameter ratio for black discs of ectopic eyespots.

Source	DF	F	P
line	1	3.71	ns
site	2	14.30	***
hour	1	11.13	**
line*site	2	6.82	***
line*hour	1	0.32	ns
site*hour	2	1.26	ns
line*site*hour	2	2.90	ns
error	170		
total	181		

**p<0.01; ***p<0.001

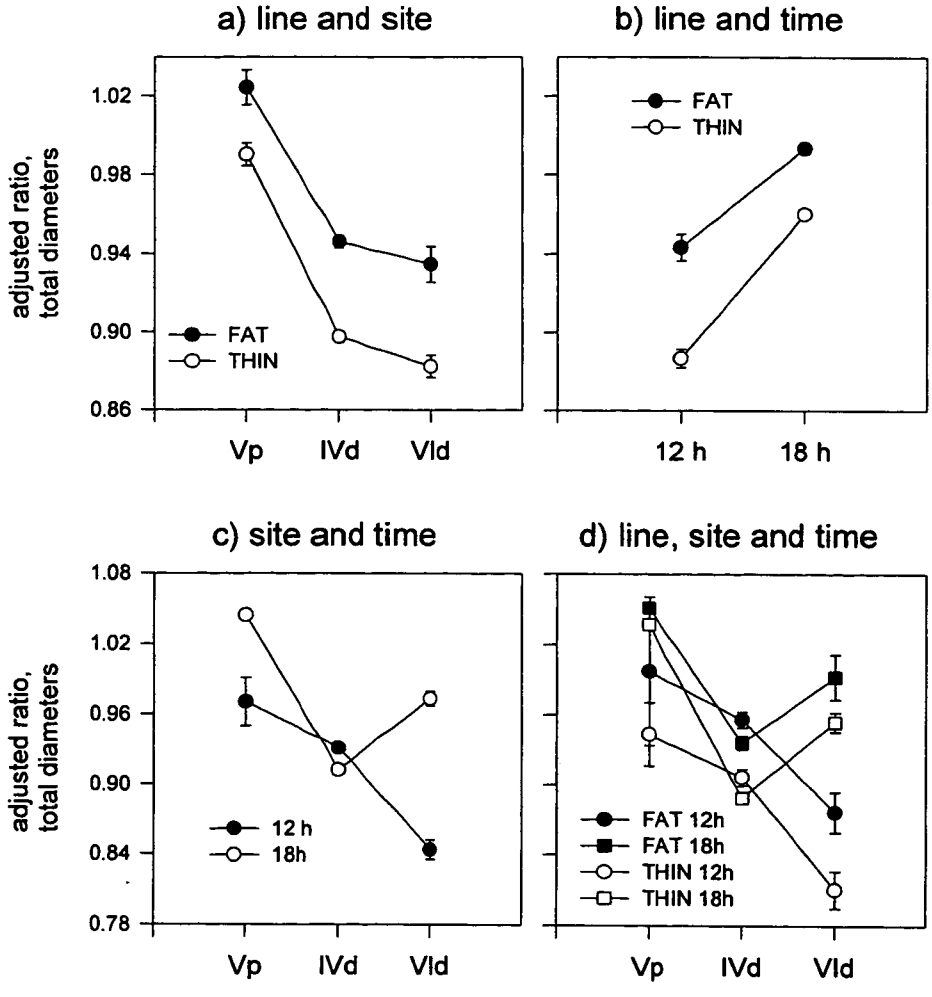

Figure 5. Graphic representation of the GLM analysis of shape of ectopic patterns produced by damage (Table 3). These are the adjusted means (of the unbalanced data set calculated through the GLM analysis) ± 95% confidence intervals of diameter ratios. a), b) and c) only plot the relationship between two factors (the third factor is confounded in the data) whereas d) shows the means from all the groups used in the analysis, separated by the three factors.

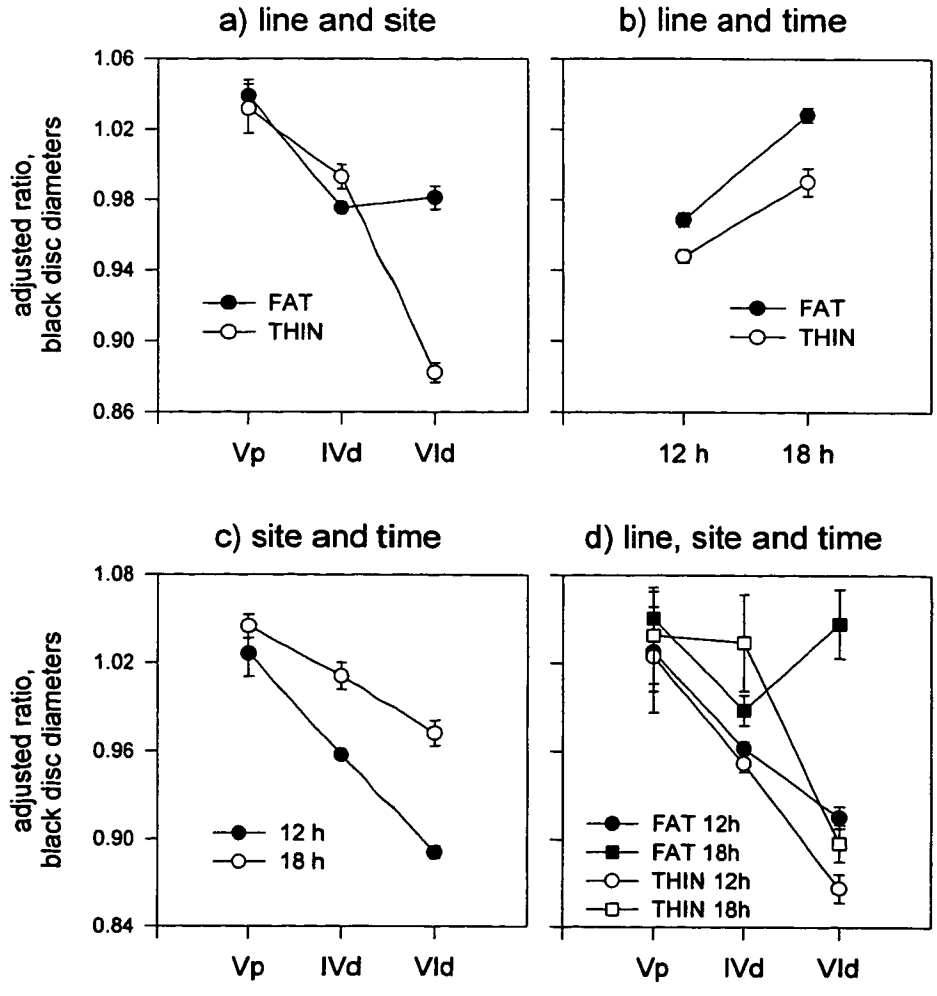

Figure 6. Graphic representation of the GLM results of Table 4. These are the adjusted means (due to the unbalanced data set calculated through the GLM analysis) ± 95% confidence intervals of shape of black discs of ectopic eyespots. As in Fig. 5, a), b) and c) only plot two factors (the third factor is confounded in the data) and d) shows the means from all the groups used in the analysis, separated by the three factors.

The area of all ectopic patterns (calculated by multiplying the product of the two radii by Pi) varied between sites ($F = 35.8$, $df = 2, 264$, $p < 0.001$; in a GLM with site, line and time of operation as factors), with the largest patterns produced at site IVp and the smallest at site IIId. Areas also varied with the time of operation ($F = 106.0$, $df = 1, 264$, $p < 0.001$), the largest ectopics being produced at 12h. There was, however, no difference in size of ectopic patterns induced in the FAT and THIN

selected lines ($F = 0.4$, $df = 1, 264$, $p = 0.51$). The consistent difference in shape of the ectopic patterns (at all three sites) and in the central black regions (at one site) support the conclusion, drawn from the grafting experiments, that selection had altered eyespot shape through modifying epidermal response to the underlying signal.

DISCUSSION

Selection succeeded in generating two forms of elliptical eyespots, but the realized heritabilities for shape were low or moderate and decreased over the generations. This phenomenon, corresponding to a declining response, indicated that selection either reduced or exhausted the available genetic variation for eyespot shape present in the STOCK. Selection for shape of the large posterior eyespot lead to correlated changes in the shape of the small anterior eyespot on the same wing surface. Correlated changes in eyespots not directly targeted by selection were observed in previous selection experiments for eyespot size (Holloway *et al.* 1993; Monteiro *et al.* 1994) and eyespot color composition (Monteiro et al. 1997b). These correlated responses were always in the same direction as that in the directly selected eyespot but were usually of a smaller magnitude. They indicate a common developmental mechanism for all eyespots, that is regulated or fine-tuned in each wing region by a partially independent set of genes. Heritabilities for eyespot shape are lower than those estimated for either size or color composition in the same stock at 28° (Holloway *et al.* 1993; Monteiro *et al.* 1994; Monteiro et al. 1997b).

Formation of the eyespot pattern can be analysed in terms of the signal from the central focus and the response to it of the surrounding epidermis (Nijhout 1980, 1991). In relation to eyespot shape, the genetic variation present in the STOCK influences the response component of the developmental mechanism. This is clear from the grafting results which provide no evidence that the orientation of the focus influences eyespot shape. Furthermore, the results of local damage demonstrate that ectopic eyespot shape is influenced by the properties of the general epidermis of the wing, particularly in the site adjacent to the selected eyespot (Vd). It is intriguing that there appears to be no genetic variation present for the symmetry of focal signaling,

whereas the results of selection for eyespot size revealed genetic variation in the strength of the focal signal (Monteiro *et al.* 1994).

It is likely that eyespot shape would be influenced by the shape of the central focus which must be established, midway between wing veins, earlier in wing development. Nijhout (1990, 1991) proposed that focus formation is based on reaction-diffusion processes (see Meinhardt 1982) spreading from the veins and distal wing margin. This model suggests that the focus resolves from an elongated to a small circular region. It is notable that a similar change is seen in the expression pattern of the regulatory gene, *Distal-less*, that marks the position of the focus in the larval wing imaginal disc (Carroll *et al.* 1994; Nijhout 1994). Nijhout (1990) suggests that variation in timing of focus formation could yield foci of different shapes but the present results give no indication of relevant genetic variation affecting this process.

The genetic variation for eyespot shape that was available in the STOCK for selection influenced the epidermal response. Ectopic eyespots were "fat" in the FAT line and "thin" in the THIN line. The shape differences between lines were especially evident in ectopics produced just distal to the selected eyespot. Due to selection, properties of the epidermal cells changed, making them respond in a similar manner to a focal signal or to local damage. One possible basis for effects on eyespot shape could be the initial specification of a circular region of cells around the focus or site of damage, and then a deformation of this region as the pupal wing epidermis expands, eventually to form the cuticle of the larger and differently-shaped adult wing. Expansion is likely to involve both cell divisions and cell elongation and may differ in extent, orientation and timing in different parts of the wing surface. It is interesting to note that, for each line, ectopic patterns were "thinner" and larger if induced at 12h than at 18h. After 18h damage the pattern was small but closer in shape to the outer border of a normal eyespot. According to the diffusion gradient model (Nijhout 1990), the outer edge will be the last region of the eyespot to be specified. Just as the time at which an ectopic eyespot is initiated may influence its final shape, there may be a proximal-distal difference in the properties of the epidermis which underlies the effect of site on the shape of ectopic eyespots. If the

shape differences between eyespots and ectopic patterns produced in pupae of the FAT and THIN lines results from differences in epidermal morphogenesis during the pupal stage, there may be differences between the lines in cell division or cell packing within the epidermis, and in resulting adult wing shape (Monteiro et al. 1997c). The response to selection implies genetic variability for the parameters of epidermal morphogenesis but the low heritabilities indicate that genetic variability was low.

CHAPTER 4

Eyespot Shape and Wing Shape

ABSTRACT

The African butterfly, *Bicyclus anynana* normally possesses circular eyespots on its wings. Artificial selection lines, which express ellipsoidal eyespots on the dorsal surface of the forewing, were used to investigate correlated changes in wing shape. Morphometric analysis of linear wing measurements and wing scale counts provided evidence that eyespot shape was correlated with localized shape changes in the corresponding wing-cell, with overall shape changes in the wing, and with the density/arrangement of scales around the eyespot area.

INTRODUCTION

Recent studies describing patterns of morphological diversity between groups of nymphalid butterflies have found that, despite the great diversity of wing shapes present, most of this variation was explained by allometric size-scaling effects, i.e., large species were mainly allometrically changed versions of smaller ones (Strauss, 1990, 1992). It thus appears, that significant evolutionary constraining forces have been governing the sources of wing shape variation. In this paper, we address a developmental mechanism of morphological diversification that can account for some of the small, size-independent differences in butterfly wing shape and illustrate that, through artificial selection on wing patterns, it is possible to change morphology in localized areas of the butterfly wing.

Quantitative genetic studies of butterfly wing colour patterns (e.g. Brakefield, 1984; Kingsolver and Wiernasz, 1987; Wiernasz, 1989; Holloway and Brakefield, 1995; Monteiro et al., 1994) have not previously been coupled with studies of butterfly wing shape (Ricklefs and O'Rourke, 1975; Johnson and Walter, 1978; Strauss, 1990 and 1992). Both wing pattern and shape (together with wing venation patterns) have played a major role in taxonomic and evolutionary studies of the Lepidoptera (e.g. Strauss, 1990) and it is important to establish whether these are independent characters, or whether they may be coupled through common developmental mechanisms. In this paper we demonstrate a correlation between colour pattern and wing shape in the Nymphalid butterfly *Bicyclus anynana*. We also show that there is substantial genetic variation for wing shape present in this species and discuss the potential for natural selection on colour patterns in the evolution of wing shape.

The nymphalid butterfly *B. anynana* has large eyespots near the margin of the adult dorsal and ventral wing surfaces. Each eyespot has a white pupil, a black central disc and an outer gold ring, and is centred midway between adjacent wing veins. The eyespot patterns are determined at early pupal stage (approximately 24h after pupation in *B. anynana* reared at 28° C: French and Brakefield, 1992) by a developmental mechanism consisting of a focal signal that is produced by cells at the centre of the presumptive eyespot and interpreted by the neighbouring cells, leading them to produce different colours with increasing distance from the focus (see Nijhout, 1980a; French and Brakefield, 1992). The nature of the signal is unknown, but a simple, plausible model involves a diffusible "morphogen" that forms a conical concentration gradient around the focus (Nijhout, 1991).

Adult wing colour arises from pigment deposited at very late pupal stage in the cuticle of the overlapping rows of cover scales: large, flattened protrusions from specialized scale-building cells. In nymphalid butterflies, the scale-building cells are first distinguishable in the early pupa as enlarged cells in regular parallel rows running anterior-posterior across the pupal wing epidermis (Nijhout, 1980b, 1991).

The eyespots of *B. anynana* are approximately circular in shape. We applied artificial selection on the shape of the large eyespot of the dorsal forewing (Monteiro

et al. 1997a). Nine generations of selection led to strong divergence of a FAT and a THIN line with elliptical eyespots elongated in the proximal-distal and anterior-posterior axes, respectively. The divergence demonstrated additive genetic variance for eyespot shape, although estimated values for heritability were only moderate (around 15%). In order to examine whether selection had resulted in asymmetry in signalling from the eyespot focus, we rotated foci on FAT and THIN pupae by 90 degrees and 180 degrees but found no effects on the final shape of the eyespots (Monteiro et al. 1997a). These results suggested that selection had acted, not on the focus, but on the response of the pupal wing epidermis to focal signalling or to its subsequent development to give the adult wing.

Here we test by morphometric analysis whether the shape of the adult wing (or part of the wing) in FAT and THIN lines is distorted in a corresponding manner to the "stretching" observed for the eyespot colour pattern. We also investigated whether changes in the matrix of scales had occurred in the region of the selected eyespot and hence whether the change in eyespot shape was due to scale re-arrangement in the wing epidermis, rather than to the addition of extra pigmented scales along a particular axis.

MATERIAL AND METHODS

The butterflies

Samples of eggs from butterflies of the ninth generation of FAT and THIN selected lines, and from the unselected STOCK population, were reared on young maize plants at 28° C. About 100 newly-emerged butterflies of each sex and line were frozen and stored for measurement.

The measurements

An image analysis system (see Windig, 1991) was used to perform the linear measurements of the butterfly wings shown in Fig. 1. Additionally, this system enabled the measurement of wing area, wing maximum length and the maximum

orthogonal length. Also the point of intersection of these latter two lines and the segments of the lines from that point to the distal edge (sub-maximum and sub-orthogonal lengths, respectively). From the maximum length, sub-maximum orthogonal length and sub-maximal length, a measure of wing base length was calculated by squaring (maximum length - sub-maximum length) and adding the square of sub-orthogonal length. Data were stored automatically for later analysis by the MINITAB or SPSS statistical packages.

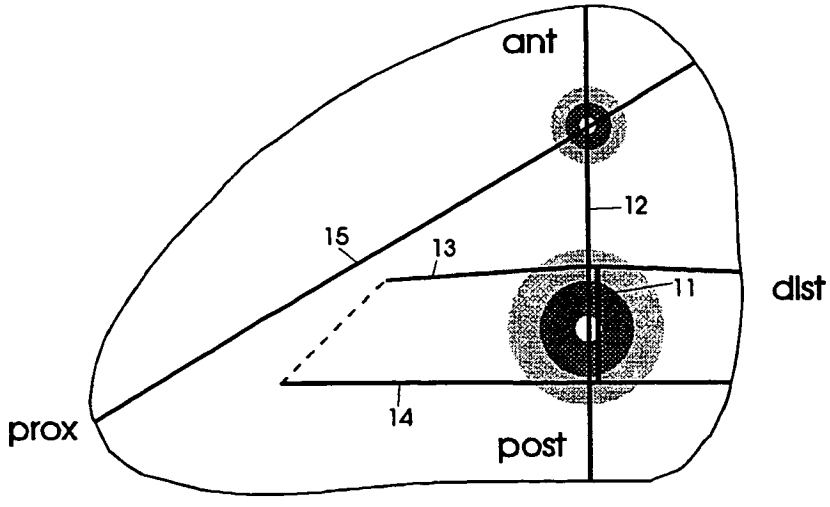

Figure 1. The dorsal surface of the forewing of *B. anynana*, showing anterior (ant) and posterior (post) eyespots, each consisting of white pupil, black disc and outer gold ring. prox, proximal; dist, distal. Measurements were made of the anterior-posterior (12) and proximal-distal (15) extent of the wing, and along (13, 14) and between (11) the veins that define the "wing-cell" within which the posterior eyespot is centered. Also the anterior eyespot (outer and black disc diameters) and posterior eyespot (outer, black disc and white pupil diameters) were measured in anterior-posterior and proximal-distal axes (measurements 1-4 and 5-10, not shown).

The measurements (Fig. 1) were chosen in reference to the following questions:

1- Has selection for posterior eyespot shape lead to changes in the shape of the corresponding wing-cell (measurements: 11, 13 and 14)?

2- Has the whole wing changed shape (12, 15, and wing base length)?

3- Has the small anterior eyespot also changed shape (1 - 4)?

4- Have the white pupil, black discs and total diameters of both eyespots in the dorsal surface changed shape in a proportional way (measurements 1 - 10)?

The analysis

A discriminant function analysis was performed to address the first two questions. The analysis separates the three groups of individuals (FAT, THIN and STOCK), using measurements for these individuals on several variables, by calculating two uncorrelated linear combinations of these variables and summarizing all information in two functions. The first function will explain the largest differences between the groups (Simon, 1983; Norusis, 1985; Manly, 1986).

Separate discriminant function analyses were performed here for males and females since males have smaller, more pointed wings than females. A total of six variables were used:

- wing cell height (11) (w-cell-h);
- wing height - wing cell height (12-11) (w-height);
- wing length (15) (w-length);
- average wing cell length ((13+14)/2) (w-cell-l);
- wing base length (w-base-l)
- wing area

Scale counts

We examined whether selection for eyespot shape lead to changes in the matrix of cover scales, that is whether the arrangement of scales in the wing-cell of the selected eyespot, had changed in FAT and THIN wings. 70 wings (around 35 per selected line, 17 for each sex) were attached to microscope slides with Euparal and the number of cover scales were counted in two perpendicular axes, at regular intervals along the wing-cell, starting at the outer edge of the white pupil of the eyespot (Fig. 2). The scale density in the scale rows which run anterior-posterior was measured every 50 micrometer units (m.u.). This vertical scale was scored as the number of cover scales per 100 m.u. centred around the wing-cell midline (Fig. 2a). The horizontal scale density along the wing cell midline was estimated by counting the number of scale rows that fitted in every 50 m.u., using the white pupil as the starting point (Fig. 2b). The measure of vertical scale density includes half the total number

of scale building cells present in the row on the pupal wing (the other half form the ground-scales; Nijhout, 1980b).

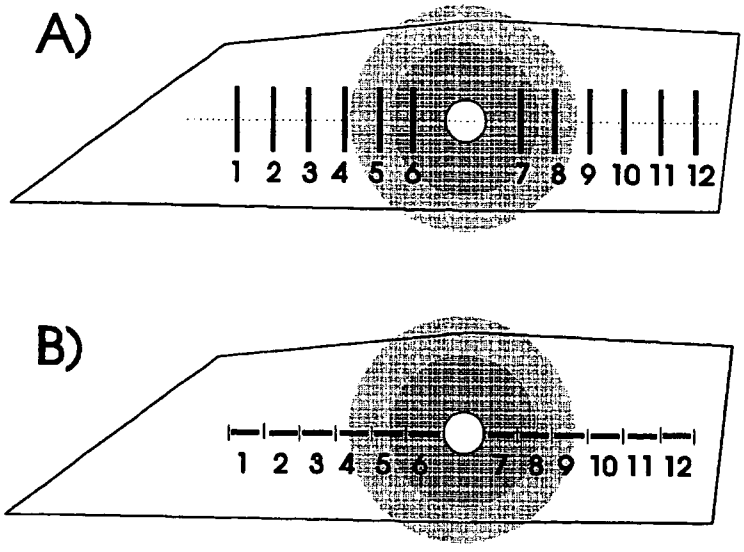

Figure 2. The wing-cell of the selected posterior eyespot. Scale counts were carried along a) vertical transects of 100 micrometer units (m.u.), separated by 50 m.u. and b) consecutive horizontal transects of 50 m.u. along the wing-cell midline. The measurements were made to either side of the white pupil, starting from its outer edge.

RESULTS

The change in eyespot shape

Shape was measured as the ratio of the eyespot width to height (diameter along wing-cell midline to diameter across wing-cell midline), for both eyespots on the dorsal surface (Chapter 3). The shape of the selected posterior eyespot, in each of its components - the outer gold ring, black disc and white pupil - changed in the selected lines relative to STOCK butterflies (Fig. 3). Within a line, however, an eyespot had always a "fatter" outer diameter compared to the shape of the black disc and white pupil (usually always "thin" in shape).

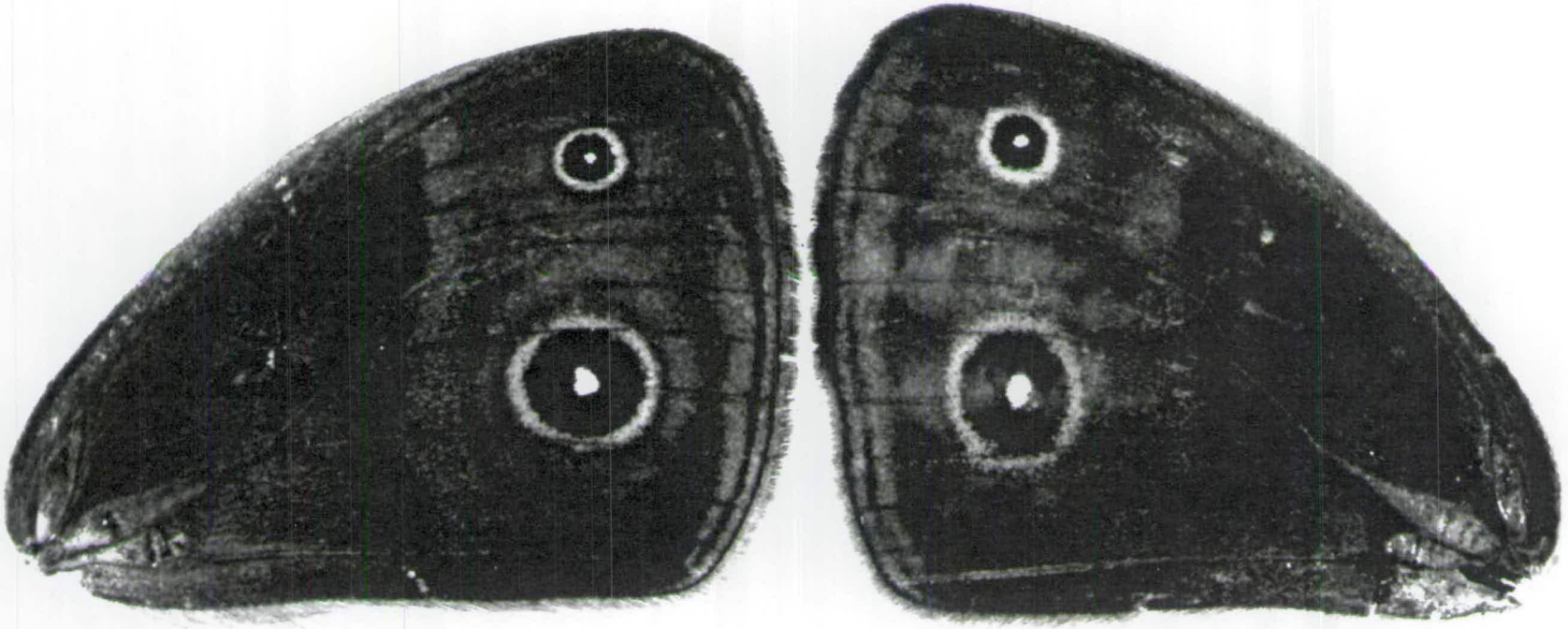

Figure 3. The dorsal surface of a FAT (left) and a THIN forewing of *Bicyclus anynana*.

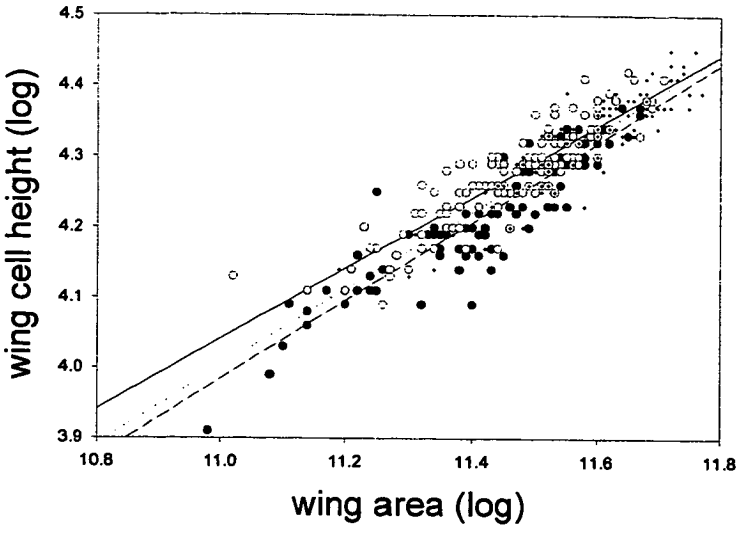

Figure 4. Relationship between wing cell height and wing area for females of THIN (open circles), FAT (closed circles), and STOCK wings (crosses). Measurements are logarithms of pixels and square pixels, respectively. Continuous, dashed and stippled lines are regression lines for THIN , FAT and STOCK, respectively.

The anterior eyespot diverged in shape only in the FAT line where it became "fatter" in both its black and outer ring diameters. For both anterior and posterior eyespots and within lines, males had "fatter" eyespots that females. There was no difference in the size (area) of the selected eyespot between the two selected lines ($F = 0.55$, p = n.s., DF = 1, 458; from a GLM analysis with line and sex as factors).

Discriminant analysis

Differences in wing area occurred between the lines (males: $F=35.97$, $p<0.001$, DF = 2, 292; females: $F=50.23$, $p<0.001$; DF = 2, 365): mean wing areas for FAT, THIN and STOCK were 71184, 76303, and 80740 for males and 93101, 96393 and 108078 for females, respectively (measurements in square pixels). For the analysis to discriminate the wings in terms of shape and not size, it was necessary to correct each variable for overall wing size. All raw linear measurements and areas were first transformed into natural logarithms. This ensures that the variances of individual measurements are independent of their mean values and linearizes allometric relationships among characters (Bookstein et al., 1985; Strauss, 1987). A pooled

within-group regression of the logged linear measurements on logged area (see Fig. 4) was used to produce size-free variables (the residuals). An analysis of covariance was first performed on each of the variables separately to check if there had been any change in the slope (in the allometric relationship between the linear wing measurements and wing area due to selection). All variables, except w-cell-l in both sexes, were co-linear across the three lines. For smaller wings, w-cell-l was shorter in FAT butterflies and longer in STOCK wings, but in larger wings the relationship was reversed. THIN wings fell in the middle of the two crossing regression lines. Despite this crossing of the lines (whether real or due to measurement error), the residuals were obtained in the same way as for the rest of the variables (thus some size-dependence will remain in the residuals for w-cell-l). Residuals from 364 females and 293 males were used in two separate analyses. Two discriminant functions were produced in each analysis. Function 1 accounted for 88.1% and 76.7% of the total between-groups variability, in males and females, respectively, while function 2 accounted for the remaining 11.9% and 23.3%. Both functions together separated the three groups (test based on Wilks' lambda. Males: $^2 = 109.3$; $df = 10$; $p < 0.0001$, females: $^2 = 127.0$; $df = 10$; $p < 0.0001$) and Function 2 alone contributed to further group separation ($p < 0.01$, for both sexes). Function 1 explains 28% and 23%, in males and females respectively, of the total size-independent variance in wing shape. A further 5.0% (males) and 8.4% (females) of the variation was accounted for by Function 2.

The average scores for Function 1 were negative for FAT, positive for THIN and around zero (males) for STOCK butterflies (Table 1). Butterflies with an average negative discriminant score -FAT- had larger w-lengths, w-cell-l and w-base-l (i.e. those variables negatively correlated with the function; Table 2) and smaller w-cell-h and w-heights than those wings with an average positive score - THIN - butterflies. The latter had shorter w-lengths, w-cell-l and w-bases and larger w-cell-h and w-heights (see also Fig. 3). STOCK butterflies were intermediate.

Table 1. Average discriminant function scores

Disc. function	sex	FAT	THIN	STOCK
1	males	-0.753	0.769	0.077
	females	-0.757	0.515	0.162
2	males	-0.139	-0.188	0.317
	females	-0.111	-0.240	0.487

Table 2. Pooled within-groups correlations between discriminating variables and canonical discriminant functions.

variables	males (F1)	males (F2)	females (F1)	females (F2)
w-cell-h	0.367*	0.048	0.767*	-0.250
w-height	0.671*	0.285	0.357	0.742*
w-length	-0.644*	0.382	-0.552*	0.294
w-cell-l	-0.109	-0.420*	-0.267*	0.059
w-base-l	-0.021	0.786*	-0.224*	-0.092

* Denotes largest absolute correlation between each variable and any discriminant function (F1 and F2).

The variables more highly correlated with Function 1 were those that varied most between FAT, THIN and STOCK wings and, therefore, contributed to a greater extent to the separation of the three groups. In males, w-length, w-height, and w-cell-h, in decreasing order of importance, most effectively separated the wings from the three groups. W-base-l and w-cell-l were poorly correlated with this function. In females w-cell-h was the most important discriminator variable, followed by w-length, w-height, w-cell-l and w-base-l.

The average scores for Function 2 were negative and quite similar for FAT and THIN and positive for STOCK. In males, the variables more strongly correlated with this function were w-base-l (positive) and w-cell-l (negative). Thus STOCK wings have a relatively longer w-base-l and shorter w-cell-l than either FAT or THIN wings. In females, w-height (positive) was the only variable more highly correlated

with Function 2 than with Function 1. STOCK wings had a larger w-height relative to the selected lines.

In summary, FAT and THIN wings diverged in shape from STOCK wings. This divergence was mostly accomplished by antagonistic changes in linear wing measurements in the selected lines (Function 1). Parallel changes in wing shape occurred in each sex. In females, however, localized changes in the dimentions of the wing-cell (w-cell-h) where the selected eyespot occured, were the most important, whereas more gereral wing-shape changes such as w-height and w-length were evident in males. Wing shape differences between both selected lines and STOCK butterflies (Function 2) could have arisen due to some size-dependency of the residuals which was not completely removed from the initial data regression analysis (see M & M above).

Scale counts

Scale density was measured in equally spaced intervals along perpendicular axes, within the posterior eyespot wing-cell, of both FAT and THIN wings. However, since THIN wings were larger than FAT wings, two measurements taken at the same absolute distance from the pupil in the two lines, will correspond to different topological regions of the wing. To compare like with like, the absolute values of the distances from the pupil (50 m.u., 100 m.u., etc.) were divided by wing-cell size (measurement 14 in Fig. 1). The transformed data were then grouped into 13 classes prior to analysis by ANOVA. Class width was calculated by starting from the lowest corrected distance to each side of the pupil and adding increments of 0.14 units. These increments were chosen on the basis of frequency histograms of the corrected distances, so that natural groups of data (closest to the focus) would all fit into the same class. Some of the classes that were more distant from the pupil, and only contained data from females, were removed from the analysis.

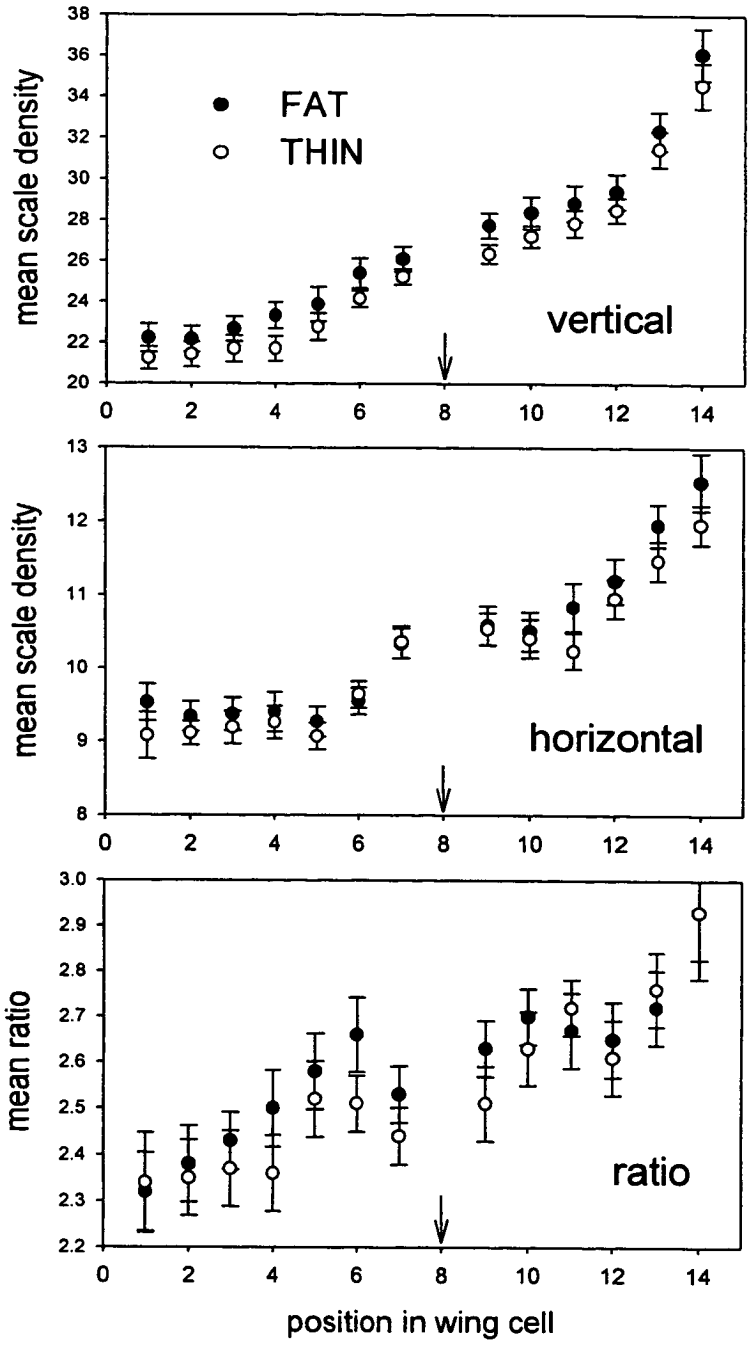

Figure 5. Scale counts along the wing-cell of the posterior eyespot (mean values ± 95% CI) in the FAT and THIN lines (males and females combined). Arrow represents the white pupil's position. Position 1 is the one closest to the body while position 14 is at the margin of the wing. Top graph - number of scales per 100 m.u. in vertical transects along the wing-cell; Centre - scale number per 50 m.u. in horizontal transects along the wing cell; Bottom - ratio of scale densities (vertical / horizontal counts). Sample size per line in all positions except first and last in each graph is above 23 (mean = 31).

A GLM with the data on vertical scale density (i.e. density along a scale row) was done using three factors (sex, line and position along wing-cell; Table 3a). Scale density varied with distance from the pupil; there were more scales per 100 m.u. in the distal part of the wing cell than in the proximal part. The relationship was more or less linear (Fig. 5, top) until positions 13 and 14, where scale density rose steeply - the area close to the wing margin was composed of very narrow scales. FAT wings had a higher vertical scale density than THIN wings (Fig. 5, top) along the whole of the wing-cell. Males had a higher scale density than females and the interaction terms were not significant (Table 3a).

A GLM was performed on horizontal scale density (spacing of scale rows) with the same three factors (Table 3b). In both lines, scale counts varied with the position along the wing cell, with a higher density of scales occurring towards the margins (Fig. 5, centre). Scale density was more or less constant in positions 1 through 6, when abruptly, in position 7, the density increased. Positions 7 and 9 always corresponded to measurements made in the region of black scales to either side of the white pupil (position 8 - arrow). The black scales have a characteristically uniform and tight packing, different from either gold or background scales. The density of scales from position 10 onwards increased linearly towards the margin. There was a significant line effect (Table 3b): FAT wings had a higher mean scale density than THIN wings. This difference, however, was not so apparent in the area bordering the white pupil but only closer to the body or to the margin (Fig. 5, centre). The significant interaction between line and position (Table 3b) was probably due to this effect. Males had a higher scale density than females and the significant interaction between sex and position was due to a smaller difference between males and females occurring close to the body (positions 1 and 2) and around the pupil (7 and 9) relative to the margin (Fig. 6).

Table 3. General linear model on scale density, with 3 factors: line (FAT or THIN), sex and position along wing-cell (13 different positions).

	a) vertical scale densities			b) horizontal scale density			c) ratio of vertical to horizontal scale densities.		
Source	DF	F	P	DF	F	P	DF	F	P
line	1	59.65	***	1	23.98	***	1	10.95	**
sex	1	36.53	***	1	210.66	***	1	25.80	***
position	12	252.85	***	12	168.50	***	12	29.73	***
line*sex	1	0.18	ns	1	1.12	ns	1	2.52	ns
line*position	12	0.41	ns	12	2.40	**	12	1.47	ns
sex*position	12	0.79	ns	12	2.64	**	12	1.01	ns
line*sex*position	12	0.54	ns	12	0.56	ns	12	0.66	ns
error	683			722			683		
Total	734			773			734		

*** $P < 0.001$, ** $P < 0.01$

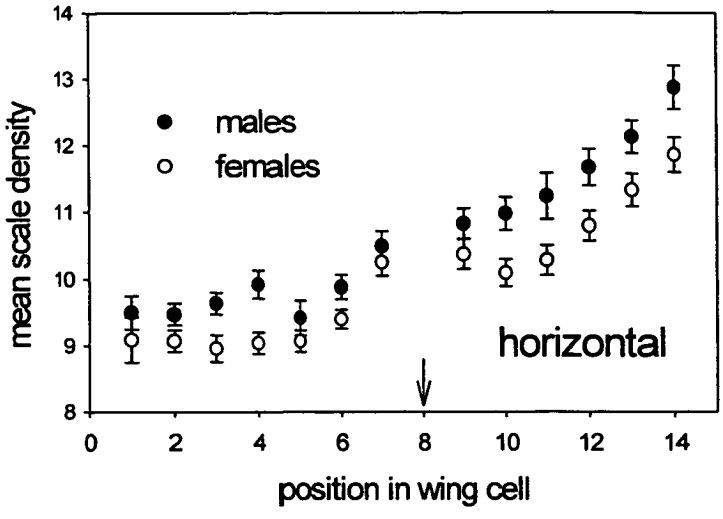

Figure 6. Horizontal scale counts along the wing cell of the posterior eyespot (mean values with 95% CI) for males and females (FAT and THIN combined). Arrow represents positin of the white pupil. Sample size per sex from positions 2-14 is above 12 (mean sample size = 30).

The next and most interesting question is whether the ratio of scale densities, that is the ratio of vertical to horizontal scale counts, varies between the lines. These were calculated by dividing vertical measurements 1,2,3,...etc. (Fig. 2a) by horizontal measurements 1,2,3,... (Fig. 2b) respectively, and regrouping the data into the previously calculated distance classes. A GLM with 3 factors (line, sex and distance from focus), performed on the ratio of scale densities data showed (Table 3c) a significant effect of position, line and sex. None of the interaction terms were significant. Scale ratio increases towards the margin (Fig. 5, bottom) and FAT wings have a heigher average ratio than THIN wings. This difference between the lines, however, is most striking in the middle of the wing-cell, around the pupil. Males have a lower general scale ratio than females.

To understand the extent to which distortion in scale spacing could account for the change in eyespot shape we correlated eyespot shape with scale ratio. We took an average ratio of scale densities closest to the focus (average density of positions 6 and 7 for the vertical scale density and positions 5+6 and 7+8, for the horizontal scale counts; Fig. 2) and compared it to the ratio of eyespot diameters on

the same 70 wings. The correlation between eyespot ratio and scale ratio was 0.49 (significantly different from zero: $t = 4.50$, $p < 0.001$). Thus a significant but small part of the variability in eyespot shape is associated with differences in scale spacing.

DISCUSSION

Shape of the adult wing

The morphometric analysis of the selected lines shows that the wings have changed shape in a parallel manner to the change in the selected eyespot: THIN wings are stretched in the anterior-posterior and compressed along the proximal-distal axis while FAT wings responded in an opposite way. The responses to FAT and THIN selection have been largely symmetrical judging from the intermediate position of STOCK wings. The response included general changes in wing shape such as those in w-length, w-height and w-base-l, and more localized and intense changes (w-cell-h and w-cell-l) for the wing-cell within which the target eyespot is located. The localized changes, especially in w-cell-h, were more apparent in females, while the males were more effectively discriminated on the basis of more general shape changes such as w-height and w-length. The difference between the sexes may result from part of the genetic factors involved being sex-linked.

This result shows that there is additive genetic variance present for the morphology of localized regions of the wing. A similar result was found by Weber (1990b, 1992) when selecting antagonistically on wing dimensions in Drosophila. He found that well defined allometries were easily broken. Wing regions were more easily contracted or expanded in some dimensions than others but all sub-regions of the wing revealed significant, locally acting, genetic variation. He found that very small regions (less than 100 cells across; Weber, 1992) could respond almost independently, with disproportionately smaller correlated changes happening in the remainder of the wing.

We have shown here that, within a species of butterfly, there is potential for evolution of wing shape, independently of allometric size-scaling effects which seem

to account for most wing shape variation within and between species (Strauss, 1990, 1991). This potential could also have been used, during evolutionary history, to adjust the wing shape of butterflies in response to selection for changes in aerodynamic performance or for particular flight patterns (Dudley and Srygley, 1994; Kingsolver and Koehl, 1994).

It is not clear why selection for eyespot shape lead to decreases in overall wing size (area) of FAT and THIN wings. The correlation between eyespot shape and wing area was negative for each sex of FAT, THIN and STOCK (but only significant for THIN females: $F = 6.16$, $p < 0.05$), implying an allometric relationship between size and eyespot shape with the "fatter" eyespots occurring in the smaller butterflies. After nine generations of selection a bias of selecting slightly smaller butterflies for the FAT line relative to THIN could account for the significant size changes. The reduced size of the selected (FAT and THIN) versus unselected (STOCK) butterflies, may be due to inadvertent selection for faster developers. A parallel study using molecular markers (M. van Eeken, unpublished data) showed only a small loss of heterozygosity, and high egg fertility in the selected lines relative to STOCK, implying that our method of selection was effective in minimizing the effects of drift and inbreeding.

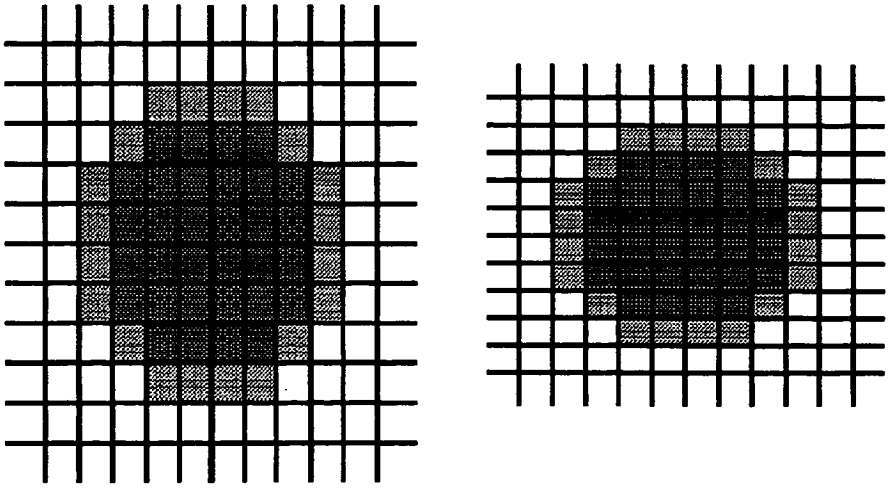

Figure 7. The "shape" of the matrix of scale-cells around the eyespot area. Left - THIN, right - FAT. See text for explanation.

Through scale counts we found that vertical scale density varied within a butterfly wing. Inside the studied wing cell, scale spacing along a row decreased from proximal towards the margin. Rows of scales also occurred closer to each other near the margin than proximally in the wing-cell. On average, throughout the wing-cell, FAT wings had a higher scale density along both horizontal and vertical axes. This could be due to a difference in the size of the epidermal cells and, hence, also explain the observed differences in wing area. We also found that there were localized differences between FAT and THIN wings in the ratio of scale densities around the eyespot area. This effect can be visualized with reference to a matrix of scales, with columns and rows of rectangular cells (Fig. 7). Each rectangle corresponds to the average space taken by a single cover scale. The scale can be larger or smaller than the rectangle if it overlaps with the neighbouring scales or if it has some space around it. FAT and THIN wings differ from each other in the size of each rectangle within this matrix. The size scaling of the matrix in FAT and THIN wings occurred in a proportionate way throughout most of the wing cell but, in the region around the focus, the shape of the rectangles (ratio of scale densities) changed. In this area, FAT wings have more scales within a row (vertical density) but a similar spacing of rows from that of THIN wings, i.e., the rectangles became "flatter".

Development of the wing

The FAT and THIN lines of *B. anynana* were generated by artificial selection on eyespot shape. The elliptical eyespots reflect changes in the developmental properties of the wing epidermis, rather than asymmetry in the central focus that induces the pattern of scale cell pigmentation during the early pupal stage (Monteiro et al., 1994). The timing of early pupal development is best known in another nymphalid butterfly, *Precis coenia*, where apolysis of the pupal wing epidermis begins at 12h after pupation at 26° C and coincides with the start of a period of cell divisions (Nijhout, 1980b). The appearance of rows of enlarged scale-building cells begins at 20h and is complete 16h later. Sporadic mitosis still occur after this period in the undifferentiated epidermal cells but no significant changes in cell number or cell arrangements take place in the period between 36 and 48h (Nijhout, 1980b).

Signalling from the focus to specify the colour pattern in *Precis* begins prior to pupation and is completed about 48h later (Nijhout, 1980a), and thus fully overlaps these cellular events.

Our results show that change in eyespot shape is associated with corresponding changes in wing shape (particularly in the region of the eyespot) and in the matrix of wing scales comprising the eyespot. At present, it is not clear to what extent these differences in adult wing morphology result from differences in the early pupal wing (in shape and in the establishment of the rows of scale-building cells), or in the morphogenesis that occurs during and after eyespot specification, as the pupal epidermis grows and expands to form the adult wing. Similarly, the change in eyespot shape may reflect asymmetry in the propagation of the focal signal through the pupal epidermis, or a subsequent deformation of the epidermis (after pattern specification).

Evolution of eyespot shape

In our FAT and THIN lines, quantitative genetic variation underlies the production of ellipsoidal eyespots, but this is not the only potential source of variation for changing eyespot shape in butterflies. The ringlet butterfly (*Aphantopus hyperantus*), an European satyrine, is polymorphic for a locus with a recessive allele that changes the shape of all eyespots in the wing margin from circular to ellipsoidal - "FAT" (Ford, 1945; Collier, 1956; Revels, 1975). It is unknown whether this gene is causing similar wing-shape scale matrix changes as in *B. anynana*, in a single step, or whether it is affecting the focal determination mechanism. Genetics of species of Heliconius, Hypolimas, Papilio and other genera also show that single genes can produce extensive change of colour pattern elements without influencing wing shape (see Sheppard et al., 1985; Nijhout et al., 1990 and Nijhout, 1991).

Examination of photographs of about 60 species of *Bicyclus* (there are around 80 species in the genus; Condamin, 1973) showed that their eyespots are nearly always circular in shape. Only two species (*B. ena* and *B. procures*) appear to have slightly "fat" anterior eyespots. Additive genetic variation for eyespot shape (as in our stock of *B. anynana*), does not seem to have been an important factor in

diversification in colour pattern or wing shape within this genus. However, this may not always be the case. Wherever changes in either colour pattern or wing shape are favoured through selection, correlated responses of the type we have demonstrated in *B. anynana* may lead to biases in the pattern of evolution of certain combinations of pattern and wing shape. The outcome will depend on the developmental and genetic basis of the correlations and on the strengths of directional and stabilizing selection.

CHAPTER 5

Eyespot Patterns and Morphogen Gradients

ABSTRACT

The wings of the Nymphalid butterfly, *Bicyclus anynana*, have a series of eyespot colour patterns, each composed of a white pupil, a black disc and a gold outer ring. An eyespot is organised around a group of signalling cells, the focus, active during the first hours of pupal development. Positional information, given to the cells around the focus, is translated into rings of differently pigmented scales. One hypothesis for the underlying mechanism is a concentration gradient of a diffusible morphogen produced by the focal cells, and interpreted in a threshold manner by the responding epidermis. If the diffusion gradient model is correct, when two foci are close together, the signals would summate and this effect would be apparent in the detailed shape of the pigment pattern formed. The morphogen gradient hypothesis was tested by measuring areas of fused eyespot patterns in *Bicyclus anynana*, by grafting focal cells close together, and also by using a mutation (*Spotty*) that produces adjacent fused eyespots. The results indicate that, in the region between two foci, there is nearly always an extra area of cells differentiating into part of the pattern. A near perfect match of the extent of extra pattern differentiating was obtained by means of computer simulations of diffusion from two sources that establish two overlapping concentration gradients on a plane.

INTRODUCTION

The identification of cells that have acquired a different fate during early development of the colour pattern on the wings of butterflies is easy. Each scale cell receiving different positional information early in development, will identify itself on

the adult pattern, by synthesising a different colour pigment. The resulting patterns are complicated and varied and seem to be produced by apparently rich and unconstrained developmental mechanisms.

One of these patterns, the eyespot, has been the object of considerable study. Nijhout (1980) identified cells at its centre, the focus, that organise the pattern during early pupal development. Damaging the focus can remove the adult eyespot or reduce its size. Grafting the focus to another site on the wing induces the formation of an ectopic eyespot. Nijhout (1978, 1980) proposed that the different colour rings in an eyespot result from a concentration-dependent response to a single morphogen being produced and diffusing from the focus. High concentrations closer to the source activate different genes, and later different pigment synthesis pathways, from the ones turned on by lower concentrations further away.

Here we attempt to prove that there is a concentration gradient underlying differentiation of an eyespot pattern. If the morphogen gradient hypothesis is correct, the contours of adult eyespot patterns are spatial indicators of where a threshold-dependent expression pattern of underlying genes involved in pigment synthesis pathways, took place. Additionally, low levels of morphogen were present in epidermal cells positioned beyond that sharp outer contour, in the "tail" of the concentration gradient. These cells, however, received too low a concentration to differentiate into part of the pattern. This implies that if a sub-threshold area of the wing receives morphogen from a second source (also individually influencing this area at sub-threshold levels), the two concentrations can summate, pass the threshold level, and produce an area of pattern.

In the following experiments, we use natural and artificially created fused eyespot patterns of the nymphalid butterfly *Bicyclus anynana* to detect whether this additive effect is present. Also, individual eyespot fusion patterns were compared with patterns generated by a computer simulation of diffusion from two point sources. First, the strength of individual point sources, the level of the thresholds and decay rates were adjusted in the diffusion model in order reproduce the final size of individual eyespots. Then, the interaction of two point sources with adjusted strengths, in order to reproduce the size of each eyespot in a fused pattern, was

simulated on the computer and the shape of the experimental and modelled fused patterns were compared.

METHODS

The butterflies

We used 4 different lines of butterflies: the STOCK, the selected HIGH and LOW lines and the *Spotty* mutant line. The HIGH and LOW lines were previously selected for a larger and smaller size, respectively, of the posterior eyespot on the dorsal forewing of *Bicyclus anynana* (Monteiro et al. 1994). The size difference in these lines is mainly due to differences in the focal cells. *Spotty* is a single, autosomal allele showing incomplete dominance that causes the appearance to two extra eyespots in both dorsal and ventral surfaces of the forewing, between the normal anterior and posterior eyespots. An homozygous mutant line was used for the experiments below. These individuals have the black and gold regions of the eyespots fused and display the characteristic pattern of an outer gold rim enclosing a single black ellipse with a row of four white pupils (Brakefield and French 1993).

All butterflies were reared at 28° C, 12L:12D light cycle and high (90%) relative humidity. Pre-pupae from all lines were timed for their individual pupation times within ±15 minutes.

Grafting and wing damage operations

We aimed to analyse fusion patterns between the normal eyespots on the dorsal forewing of *B. anynana* and additional ectopic eyespots induced by foci grafted into an adjacent, more distal, position in the same wing-cell. The foci used for grafting came from the HIGH line in order to produce large ectopic eyespots. Both posterior foci of HIGH line donor pupae (from left and right wings) were grafted into distal positions, next to the normal anterior and posterior foci, respectively, of STOCK pupae (Fig. 1a). Grafting operations were performed 3 to 5 hours after pupation.

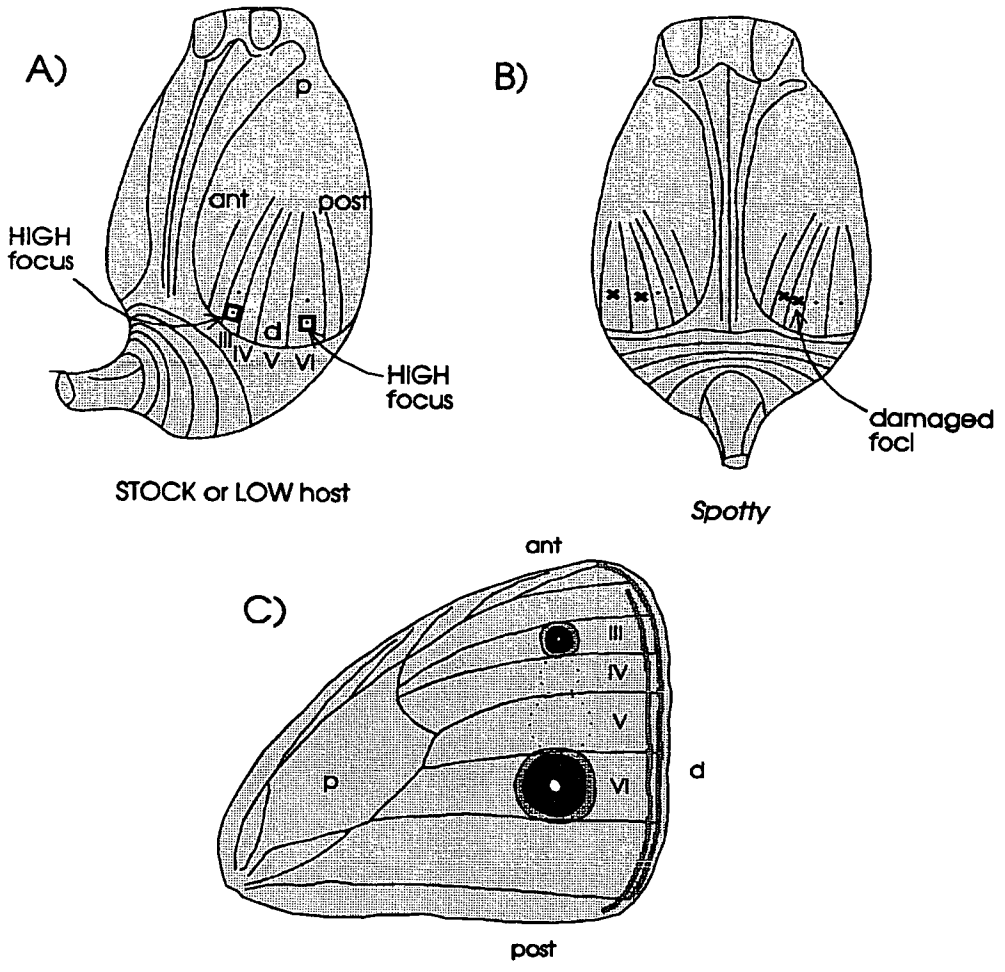

Figure 1. Schematic representation of pupae from Bicyclus anynana and dorsal surface of adult forewing. A) Foci from the HIGH line were grafted onto two distal sites on the wing of STOCK or LOW host pupae. Dots on the wing indicate foci; squares, pieces of grafted tissue; wing-cells are labelled from III-VI; p, proximal; d, distal; ant, anterior; post, posterior. B) Pupa from *Spotty* line showing wing-cells where damage was applied to foci, by piercing with a fine needle. The undamaged foci, on right and left wings, will fuse together in pairs. C) Adult wing with normal anterior and posterior eyespot patterns. *Spotty* mutants have two additional eyespots (represented by the dashed circles) on wing-cells IV and V.

Control operations were made in order to measure the proximal-distal symmetry of isolated ectopic eyespots, unfused with the normal eyespots. In these operations, the anterior and posterior foci in the host pupa were pierced with a fine tungsten needle before grafting the two foci into distal positions. The eyespots resulting from the damaged foci become very reduced or absent (see French and Brakefield 1995) and cannot fuse with the eyespots from the grafted foci. In some control operations, LOW

line pupae were used as hosts for HIGH line foci. The small dorsal eyespots characteristic of the LOW line also prevent them from fusing with the ectopic eyespots from grafted foci.

Butterflies from the *Spotty* line were used to study fusion patterns between eyespots in adjacent wing-cells, i.e., between the anterior-posterior axis of the wing. The fusion patterns were studied in two pairs of eyespots: the normal anterior eyespot and the one just posterior to it (in wing-cells III and IV; see Fig. 1c) and the normal large posterior eyespot and the one just anterior to it (in wing-cells VI and V). In order to obtain isolated two-eyespot fusion patterns, instead of the fusion of all four eyespots, two of the foci were damaged early in development. Using a fine tungsten needle, at 4-5 hours after pupation, the two most anterior foci were damaged in one wing and the two most posterior foci were damaged in the other wing (Fig. 1b). Control operations were performed in some animals in order to measure anterior-posterior symmetry of each individual eyespot, isolated from its neighbours. Foci in alternate wing-cells were damaged at 4-5 hours after pupation.

Measuring the fused patterns

After adult emergence, the eyespot patterns in operated wings were drawn on paper with a camera lucida attachment. Contours of the white pupil, the black disc and the outer gold ring of the eyespots were drawn on paper, along with the position of the veins and the distal wing margin. The fused patterns were divided into two outer halves and the inner, coalescing part, as shown in Fig. 2a. The control STOCK eyespots and grafted eyespots were divided into proximal and distal halves and the isolated *Spotty* eyespots into anterior and posterior halves. Photocopies of the drawings were cut along the outer (gold) contour and the patterns further divided into the parts mentioned above. To calculate whether the pattern had been extended by summation of the focal signals, we assumed that i) each of the fused eyespots would, in isolation, have perfect radial symmetry and ii) fusion would not affect the size of the outer half of the eyespots. For each fused pattern, the two outer eyespot halves were flipped over the middle segment and the overlap (piece D in Fig. 2b) deducted from their combined area, which was then compared with the middle segment (piece

B) to give the extra pattern. The areas were estimated by cutting the tracings of eyespot patterns into the appropriate sections and weighing the pieces of paper with an accuracy of 0.1 mg. The paper used was of high quality, with little variability in weight between sheets and high weight homogeneity across the surface of each sheet.

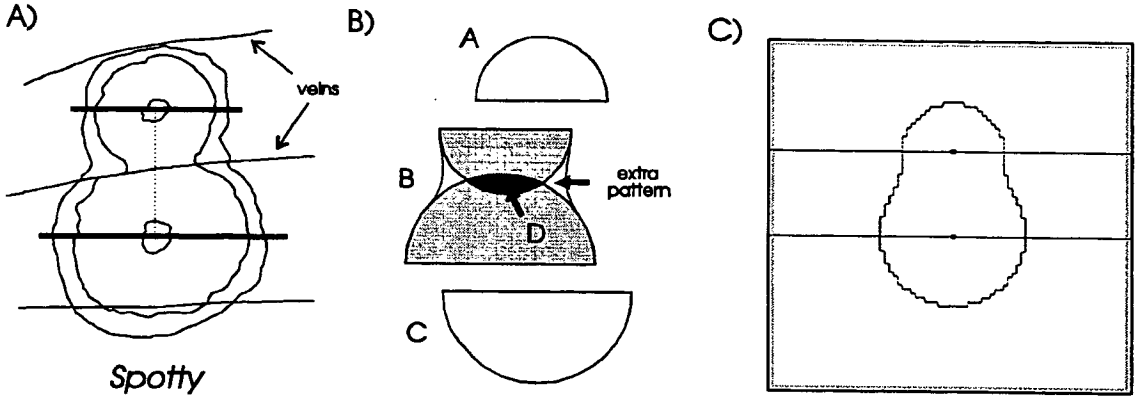

Figure 2. A) Drawing of a *Spotty* fusion pattern between eyespots V and VI. Two lines perpendicular to the dotted line connecting the centre of the two pupils, were added, dividing the pattern in three parts. B) The calculation of extra pattern was made by cutting the paper drawing in parts A, B and C, then flipping parts A and C over part B (undersides of paper shown in a shade of grey); drawing the contours of the overlapping part, D, in either A or C and cutting it out. The area of extra pattern = weight B - weight A - weight C + weight D. C) The same fusion pattern as in A) modelled by a computer diffusion simulation. Constant source cells (squares) have *p*-values of 22.8 and 110.3, respectively; threshold value is 1 and decay rate is 0.009. The pattern has reached equilibrium.

Modelling approaches

Our reference model assumes that a morphogen is produced at one or two relatively small sources. This morphogen spreads out by homogeneous diffusion, while decaying at a constant relative rate. The variously coloured eyespot regions are supposed to correspond to different, adjacent, ranges of morphogen concentration. We shall refer to the values of the morphogen concentration at the boundary between two such ranges as thresholds. We use both a numerical and an analytical approach to solve the diffusion equations. We only considered constant strength sources, point sources in the analytical solution, and sources the size of a single grid cell in the numerical simulation. In appendix B we show that for sufficiently narrow sources the

difference between constant strength and constant level sources should be negligible (see also Bard and French 1984).

Analytical approach

Appendix A derives the equilibrium distribution m of morphogen around a point source given by $m = cK_0(\lambda r)$, with r the radial distance from the source, $c = S/D$, S the source strength in mol per unit of time, D the diffusion coefficient, $\lambda = \sqrt{k/D}$, k the decay constant, and K_0 is the so-called "modified Bessel function of the second kind of order zero". Graphs of K_0, tables and handy approximation formulas can be found in Abramowitz and Stegun (1965). Let T denote the threshold value of morphogen concentration bounding the eyespot colour contour under consideration. Then the points on the contour all satisfy $m = T$. Dividing through by T makes the model contour be given by the relation

$$p\,K_0(\lambda r) = 1, \qquad (1)$$

with $p = c/T$. Not unexpectedly, the contour is a circle with radius depending on the two parameters p and λ. Notice that it is not possible to estimate p and λ separately from an estimate of radius. Given a radius and the value of either λ or p, we can calculate the value of the other parameter by taking recourse to tables of K_0. If we have more that one source it is possible to do better.

The model formulation excluded any interaction between the morphogen molecules away from the source. We can, therefore, get the local morphogen concentration due to more than one point source by simply adding the contributions from the various sources. In the case of two sources $m = c_1K_0(\lambda r_1) + c_2K_0(\lambda r_2)$, with r_1 and r_2 being the radial distances from each point along the contour to the respective sources, and c_1 and c_2 the corresponding source strengths. The model contour satisfies

$$p_1K_0(\lambda r_1) + p_2K_0(\lambda r_2) = 1, \qquad (2)$$

with $p_i = c_i/T$. Unfortunately, equation (2) is more easily written down than solved but it permits the application of a numerical method described below where it is possible to determine λ from a fusion contour of two eyespots.

Computation of lambda

From a drawn fusion contour of two eyespots we can determine the radius for several points along that contour to the centre of the two white pupils (r_1 and r_2 from expression (2), above) but we cannot determine p_1, p_2 and λ simultaneously. However, Expression (2), which describes the relation between all these variables, has the form of a linear equation. By plotting $K_0(\lambda r_1)$ against $K_0(\lambda r_2)$, and if the diffusion gradient hypothesis is correct, λ is the value that maximises the correlation coefficient between the two Bessel functions.

For each fusion pattern several r_1 and r_2 measurements were made along the outer contour line at similar spaced intervals (at approximately 30 points). A series of correlation coefficients between the two Bessel functions were calculated, each time with a different λ, until the maximum correlation coefficient was reached. The λ used to obtain this coefficient was taken to be the correct λ parameter for the particular fused pattern. In order to have an idea about the shape of the plot of the Bessel functions if another type of signalling model was operating, λ was calculated for a fusion pattern produced by the interception of two drawn circles.

Numerical approach - diffusion model

Computer simulations of diffusion in two dimensions from two sources with different constant strengths and at different distances from each other were used to model and attempt to match observed patterns of fused eyespots. A square grid of 80 by 80 "cells" was used. Constant rate sources were used for all simulations, e.g., in each iteration of the program, a fixed number of "morphogen units" were added to a "source cell" that started the diffusion process. Diffusion was simulated by making the source cells, and every other cell in the grid pass 50% of its contents, in each iteration, to four surrounding cells. A decay rate for morphogen (where a fixed percentage of morphogen units from each cell in the grid is subtracted per iteration)

was introduced in the model so that a stable gradient was eventually reached. This equilibrium situation occurs when the net amount of morphogen diffusing to each cell, in each iteration, equals the amount that is removed due to decay. The program then displays contour lines around cells with similar chosen morphogen levels or thresholds. The simulated patterns were printed on paper and the extra pattern was calculated in the same way as for the camera lucida drawings of the eyespot patterns.

Strength of the sources

The size of a single eyespot pattern, according to the diffusion model described above, will depend on 1) the strength of the focus; 2) the threshold level for the outer contour and 3) the decay rate. Assuming that the pattern is determined only after reaching equilibrium, additional variable parameters such as the diffusion coefficient (the percentage of morphogen diffusing in each iteration to the neighbouring cells) and the relative time of onset of diffusion will not affect the size of the final pattern. From previous selection experiments on eyespot size (Monteiro et al. 1994), we found that differences in focal strength were the major size determinant. In our diffusion simulations we have, thus, assumed a constant threshold level and a constant decay rate for all patterns and only varied the strength of the sources and the distance between them. In order to relate final eyespot size with focal strength (of a constant rate source) we used formula (1) already presented above (see "Analytical Approach"):

$$p\,K_0(\lambda r) = 1,$$

In this case, we standardised and approximated λ to the nearest integral digit from all the separate estimates obtained (see results on "Estimating Lambda"). This digit was one. We have now an expression that relates the radius of a single eyespot to the morphogen production rate of its focus $p = 1/K_0(r)$.

To gauge the numerical simulation of the diffusion model in function of the mathematical expression we took several radii (3, 4 and 5cm) and obtained their corresponding p values. Then, we introduced these same p values in "source-cells" in the computer model and progressively adjusted the decay rate so that the final size of the modelled circular patterns were perfect scaled versions of the original radius.

Since arbitrary threshold levels had already been set to one in the analytical approach, the same threshold level was used in the numerical simulation (the contour of the pattern at equilibrium will surround all "cells" containing more than one morphogen unit). The appropriate decay rate for this threshold was found to be 0.009 (0.9% of the morphogen units in each cell are removed per iteration of the model).

When modelling fused patterns, with two "source-cells", we observed that when the two sources were well separated (at comparable distances to the real fused eyespots) there was a negligible influence from one source-cell on the radius of the outer half of the other eyespot. The size of these outer radii was compared to the radii produced by these sources when placed alone in the grid. This observation enabled individual p values to be assigned to each of the foci, in real fused patterns, by taking an average of the eyespot radius at several points along the outer unfused half of each eyespot in the pattern.

Calculating eyespot symmetry

Some eyespot patterns are not symmetric about the line connecting their centres. The computer simulations of fused patterns created by diffusion from two closely placed sources was only performed for the most symmetric patterns obtained from *Spotty* and operated STOCK butterflies. Symmetry of the fused pattern in *Spotty* individuals was evaluated by measuring the proximal and distal halves of the pattern (divided by an anterior-posterior line between the centres of the two white pupils) along three transects (see Fig. 3a). The difference between distal and proximal sides was calculated (e.g., r1-r2, r3-r4 and r5-r6; Fig. 3a) and the variance of the differences was used to rank each pattern. The five most symmetric patterns, for each of the fusion patterns (containing the small anterior and the large posterior eyespot, respectively), were used for modelling. Anterior-posterior symmetry of the fused patterns resulting from focal grafts, was calculated as above, across the dividing axis running proximal-distal between the two pupils. Because the grafted distal focus sometimes produced a pattern whose outer contour was flattened close to the wing margin, two extra measurements were added to the symmetry estimate (r7 and r8; see Fig 3b). Proximal-distal symmetry of the control eyespot on the non operated wing

was also measured. Additional to the variance component described above, the variance of r1, r2 and r7 and the variance of r5, r6 and r8, were also calculated. These three variance components were grouped and ranked. Symmetry of the control eyespot was separately assigned a rank. The average rank for a butterfly (mean of the 4 ranks) was calculated. The 5 butterflies with the smallest ranks were used for modelling.

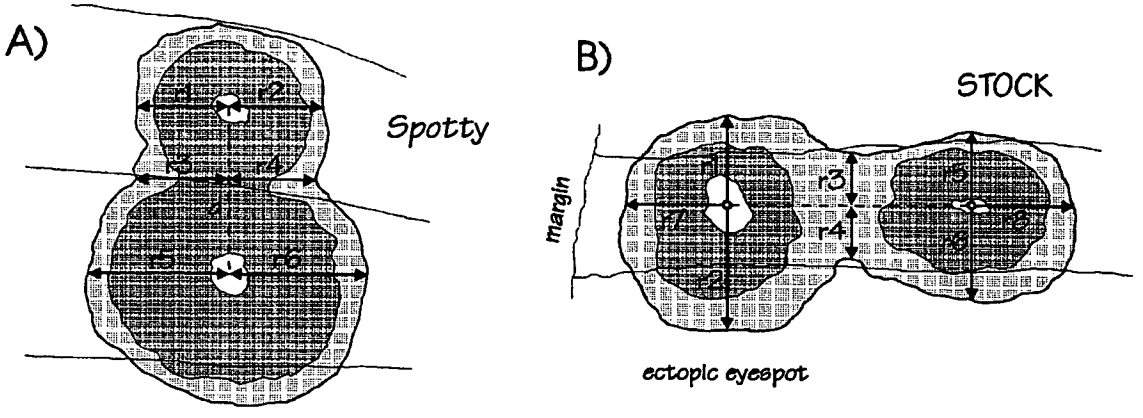

Figure 3. Measurements performed on the hand-drawn fusion patterns in order to choose the most symmetric patterns to use for computer modelling. A) In *Spotty* patterns proximal-distal symmetry was calculated via measurements r1-r6 (see methods); d, distance between the centres of the white pupils. B) In fused patterns along the wing-cell, anterior-posterior symmetry was calculated via measurements r1-r6, and the degree of flatness close and away from the wing-margin was estimated using additional measurements r7 and r8.

RESULTS

Symmetry of isolated eyespots

The proximal and distal halves of isolated eyespots resulting from grafted foci are similar in size (Table 1A), except for grafts placed adjacent to the damaged anterior focus, where an extension of the proximal side may result in nearby damage (see Brakefield and French 1995). The normal anterior and posterior eyespots are asymmetrical with a larger distal half (and the anterior eyespot also has a larger posterior half). When isolated, the more posterior of the extra eyespots of the *Spotty*

individuals (in wing-cell V; Fig 1c) has a larger anterior half (complete isolation of the other extra eyespot was not possible because of insufficient damage applied to the adjacent foci). These results have the following implications for the calculation of the area of extra pattern formed in each fused pattern:

1) In fusion patterns between grafted foci and normal eyespots, there will be an over estimation of extra pattern.

2) In fusion patterns of *Spotty* butterflies, expressing eyespots V and VI (Fig. 1c) there will be an underestimation of the area of extra pattern.

3) In fusion patterns of *Spotty* butterflies, expressing the eyespots (III and IV; Fig. 1c) there will probably be an overestimation of the extra pattern.

Fused patterns

The grafting of a focus distal to the normal anterior or posterior eyespot resulted in the formation of an ectopic eyespot pattern (with a white pupil, black disc and outer gold ring) that fused with the adjacent eyespot (Fig. 4a, b). The damage to pairs of foci in *Spotty* mutants greatly reduced these eyespots and resulted in restricted fusion patterns involving the undamaged anterior or posterior pairs of eyespots (Fig. 4c).

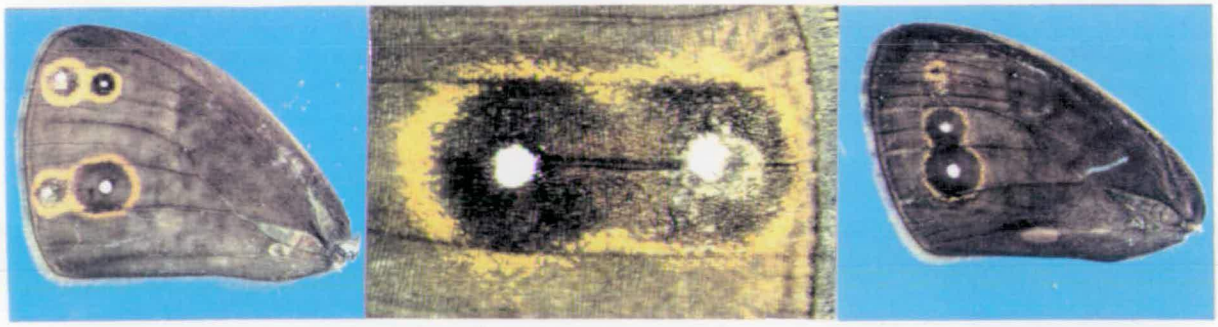

Figure 4. The operated wings of *Bicyclus anynana*. A) A STOCK wing showing ectopic eyespots induced by grafted HIGH foci fusing with the normal anterior and posterior eyespots. B) A posterior eyespot fused with an eyespot induced by a piece of rotated focal epidermis. C) *Spotty* wing where the two most anterior eyespots are

reduced in size, due to early damage to their foci, and were unable to fuse with the two most posterior ones.

Table 1. The symmetry of isolated eyespots in STOCK, LOW and *Spotty* wings, measured as mean weight differences of paper drawings of proximal and distal and anterior and posterior halves. T-test measures whether the difference between halves significantly deviates from zero. n = number of scored patterns. See grafting positions and wing-cell notations in Fig. 1.

A) distal / proximal symmetry	larger half	n	t-test	significance
IIId-graft + damage to anterior focus	proximal	36	4.70	***
IIId-graft in LOW line host	=	6	0.43	ns
VId-graft + damage to posterior focus	=	37	1.15	ns
VId-graft in LOW line host	=	16	1.11	ns
anterior eyespot	distal	67	4.55	***
posterior eyespot	distal	65	8.53	***
B) anterior / posterior symmetry				
anterior eyespot (wing-cell III)	posterior	20	5.04	***
Spotty eyespot (wing-cell V)	anterior	25	3.42	***
posterior eyespot (wing-cell VI)	=	25	0.05	ns

***, $p < 0.01$; ns, $p > 0.05$

Estimation of the areas of the different parts of the fused patterns revealed that, in most cases, there was an area of extra pattern formed (Fig. 5). For the fusion patterns resulting from the grafts, distal to the anterior eyespot, fusion resulted in a

local extension of the pattern, equivalent to an average increase of 6.9% in total area of the fused eyespot pattern (SE = 0.8%; significantly different from zero: $n = 68$, $t = 8.13$, $p < 0.001$). Fusion with posterior eyespots produced an increase corresponding to 5.6% of the total area (SE = 0.4%; $n = 71$, $t = 15.15$, $p < 0.001$). From the symmetry results calculated above, these two values are likely to be overestimations of the real extent of extra pattern. For the *Spotty* individuals, the effect of fusion increased the total pattern area by 1.1% (SE = 0.3%; $n = 27$, $t = 4.33$, $p < 0.001$) for the two posterior eyespots and by 5.1% (SE = 0.6%, $n = 10$, $t = 8.11$, $p < 0.001$) for fusion of the two anterior eyespots. Also from the symmetry results, the latter value is a likely to be an overestimate and the former an underestimate. The average area of extra pattern that forms due to the fusion of two eyespots will be somewhere between 1.1 and 5.1%.

Estimating lambda

The parameter λ was estimated from a series of contour measurements and found to have values rather near to one (Table 2). The control pattern had a value of λ three to four times larger. The plots of the Bessel functions (Fig. 6) also show that the data fit well into a straight line, whereas the control pattern doesn't. In this case, points will always be found lying on two straight lines parallel to the axes (apart from some measurement error), whatever value of lambda is chosen (the "optimal" lambda will depend on the places where the measurement points are chosen). The points either lie on circle 1 or on circle 2. For points on circle 1, r_1 = radius of circle 1 is constant, r_2 varies. This gives the straight line parallel to the r_2 axis. The points lying on circle 2 give the straight line parallel to the r_1 axis. This control pattern can represent a model based on a simple cell to cell relay system.

The Bessel plots (Fig. 6) support the diffusion model due to the good straight-line fit of the data and also give the best possible use of the contour information in testing against alternative plots to the diffusion gradient model. This method, however, may not be able to separate all possible alternative models.

Diffusion model

In order to investigate the potential causes of the variability around estimates of extra pattern obtained above and whether their magnitude is compatible with a diffusion mechanism, individual fusion patterns were modelled in a diffusion program. The most

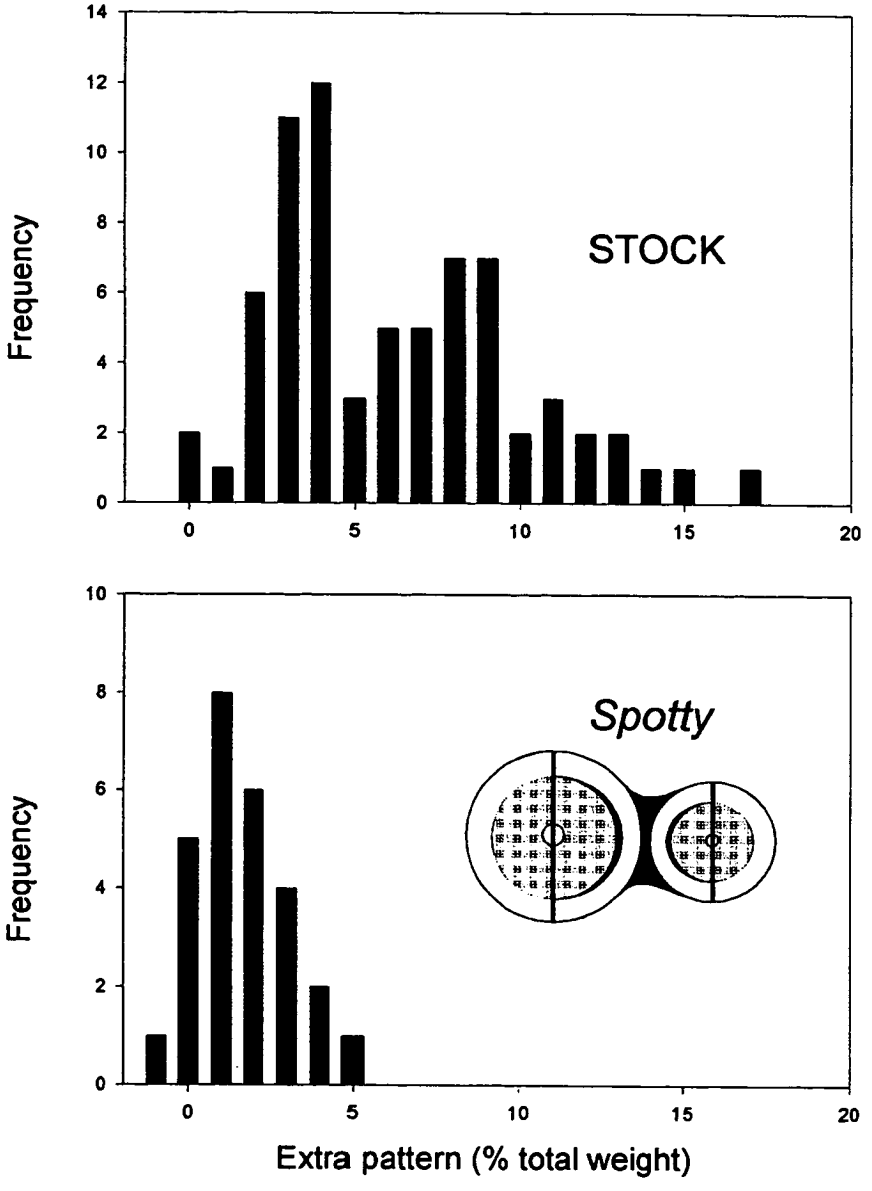

Figure 5. The amount and frequency of extra pattern produced in all operated individuals (measured as a percentage of the total paper weight of the fused pattern) in STOCK and *Spotty* hosts

likely parameters affecting variability of the estimates between fusion patterns are differences in focal strengths and the distance between the foci. Differences in threshold values between individuals exist (see Chapter 3) and differences in decay rates are also possible. These differences, however, are probably less important and they were assumed constant. The five most symmetric fusion patterns from each type of *Spotty* fusion and from the fusion of posterior and distal ectopic eyespots were used for modelling. No fused patterns between ectopic and anterior eyespots were used because of the high degree of asymmetry and small size of the total fused pattern. There was a close correspondence between the observed and modelled increase in area of extra pattern (Fig. 7; $r = 0.917$, $n = 15$, $F = 68.38$, $p < 0.001$, pooling *Spotty* and grafts). It was striking, however, that the higher values obtained of extra pattern were always underestimates of the modelled values. This problem will be addressed in the discussion.

Table 2. Estimated lambdas for the most symmetric fused patterns. n is the number of equidistant points along the contour used to calculate r_1 and r_2 (see "Estimating Lambda" in the M & M section). Control refers to a drawn pattern of two circles that intercept. * identifies the patterns shown in Fig.6.

fused pattern	estimated λ	correlation coefficient	n	average λ
Spotty III + IV	0.35*	0.97	27	0.51
	0.45	0.97	27	
	0.65	0.96	28	
	0.55	0.96	28	
	0.53	0.96	25	
Spotty V + VI	0.51*	0.97	30	0.69
	0.53	0.94	32	
	0.95	0.91	34	
	0.61	0.94	35	
	0.86	0.94	30	
Graft + posterior eyespot	0.89*	0.98	31	0.78
	0.75	0.96	34	
	0.64	0.97	33	
	0.79	0.97	34	
	0.84	0.94	33	
Control	3.62*	0.83	29	3.62

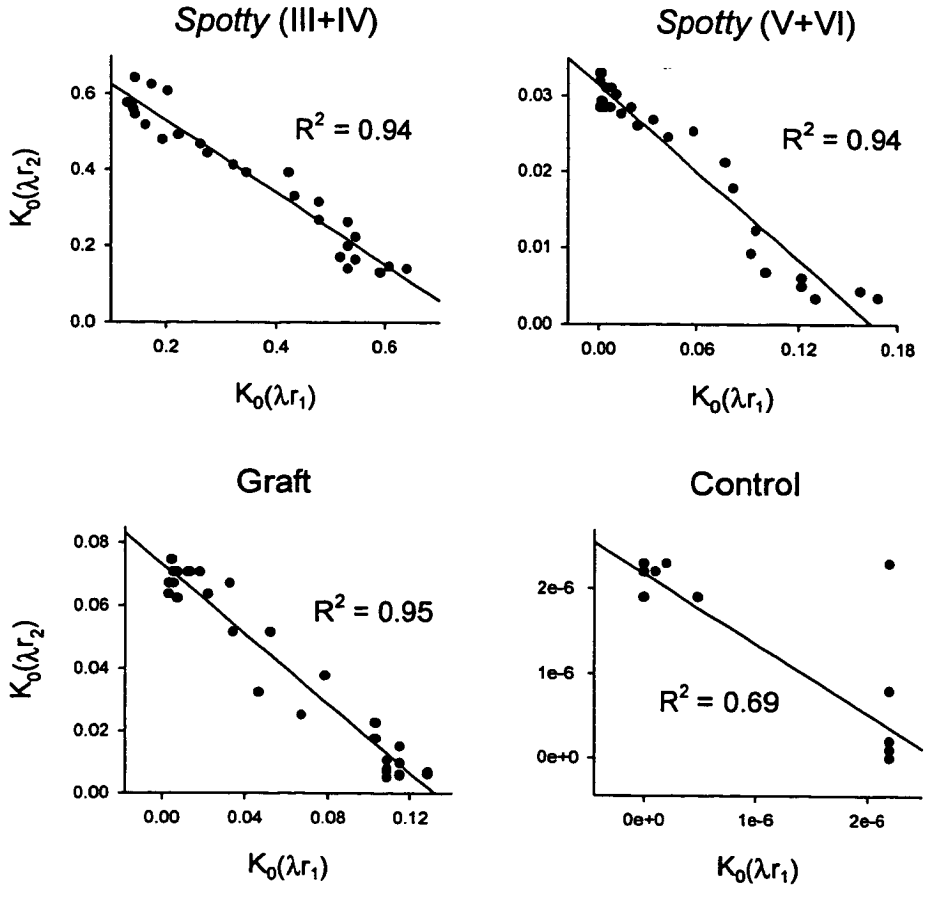

Figure 6. Bessel plots with a chosen λ that maximises the correlation coefficient between the two Bessel functions. r_1 and r_2 are the distances from several points along a fused contour to the centre of each white pupil (or to the centre of the drawn circles in the control pattern -bottom right). The top two graphs are for *Spotty* fused patterns, the bottom left for a large posterior eyespot fused with an ectopic eyespot. The control pattern is a drawing of two intercepting circles (to introduce some noise in the measurements one of the centres of the circles was moved slightly off centre).

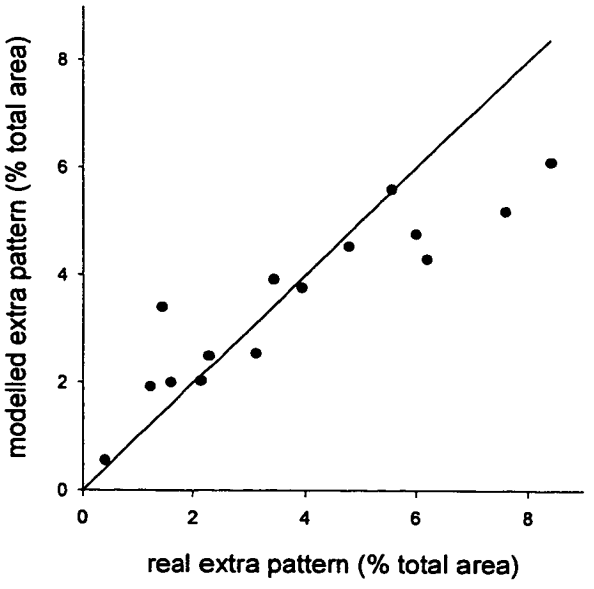

Figure 7. The correlation between extra pattern calculated from the hand drawings of the fused patterns (real extra pattern) and the extra pattern calculated from the computer model drawings (see Fig. 2c). Extra pattern is measured as a percentage of the total weight of the fused pattern.

DISCUSSION

When two eyespot foci are close on the wing surface they can produce a fused pattern in which more cells than just those expected from the intersection of two circles differentiate as part of the pattern. These results are consistent with the presence of a long-range morphogen gradient established from each focus, and influencing cells beyond the visible eyespot outer contour line, at sub-threshold concentrations. In the area of overlap of the two gradients, there is an additive effect that can raise the morphogen levels above the threshold.

An alternative model for long-range patterning from a signalling group of cells is the cascade model. In this model signalling occurs via a sequence of short-range interactions where cells receiving signal A generate signal B, which is perceived by the neighbouring cells, leading them to produce signal C and so on. Propagation of a signal (and therefore determination of its final range), will depend mainly on the type of signal rather than on the amount received (reviews in Perrimon

1995; Blair 1995). The experiments described in this paper, along with following lines of evidence, strongly indicate that the focus provides one long-range signal, rather than merely the first of a cascade of short-range signals:

1) Strong and weak artificially selected foci induce respectively larger and smaller eyespot patterns (Monteiro et al. 1994). It is difficult to imagine how variability in the first signal produced in the focal cells, could control final eyespot size, via a cascade of several signals. In the gradient model, a stronger focus would produce a larger concentration gradient affecting a broader area.

2) Progressively later damage applied to the focus, in early pupal development, leads to a progressive increase in adult eyespot size (Nijhout 1980a; French and Brakefield 1992; Monteiro et al. 1994). If eyespot size is dependent on a cascade of signals, only the first of which is produced in the focus, it is difficult to imagine how late damage to the focus can still affect eyespot size. With a gradient model, the later the damage the smaller the effect on the final eyespot size, until the complete gradient is established.

3) Damaging a focus often leads to a small pattern on the adult wing consisting only of scale cells containing pigment from the outer colour rings (French and Brakefield 1992). Early damage to a focus might result in a very shallow concentration gradient, that can only rise above the lower thresholds of gene activation - producing the outermost colour rings in an eyespot. Influencing the production of the first signals in a cascade model should always affect first the appearance of the outer colour rings, which is not the case.

Morphogen gradients have been known to exist since *bicoid* was discovered in the early syncytial state of the *Drosophila* embryo (Driever and Nusslein-Volhard 1988). At this stage of development, the egg is still devoid of cell membranes and large proteins can diffuse freely in the common cytoplasm. Only more recently has proof accumulated that even in solid tissue (Gurdon et al. 1994) or in an epidermal layer (Heemskerk and DiNardo 1994, Katz et al. 1995, Zecca et al. 1995; Nellen et al. 1996; Lecuit et al. 1996), cells are responding to particular substances, synthesised some distance away, in a concentration dependent manner. Most of these studies have used one or several of the following methods: 1) molecular techniques

to either increase or reduce gene expression of the putative morphogen and monitor these effects in the expression domain of target genes; 2) ectopic expression of the morphogen to monitor the response of target genes; 3) inhibition of protein synthesis in a layer of cells between the signalling cells and the responding cells to look for expression of target genes, beyond the non-responding cells; 4) artificial activation of the receptor system for the morphogen (mimicking reception morphogen) to test whether the activated cells can then relay the signal.

The *Drosophila* growth factor *decapentaplegic* (*dpp*) was recently presented as a long-range morphogen, inducing the expression of one of its target genes, *optomotor-blind* (*omb*), in a concentration dependent manner, at least 20 cell diameters away from the *dpp* producing cells (Nellen et al. 1996). It later appeared, however, that cell proliferation, from an initial population of cells that received a short-range signal, may be responsible for the enlargement of the *omb* expression pattern. This was accomplished by daughter cells maintaining either the expression of the transcript or the stability of the *omb* protein (Lecuit et al. 1996).

Although the present experiments provided an innovative and inexpensive way of testing the morphogen gradient hypothesis in the butterfly wing, it is inevitable that some of the above described molecular techniques will have to be applied, once a putative morphogen is identified in this system. Some lines of evidence, however, seem to indicate that epidermal cell growth in this system might not be as confounding as it was for *dpp* in the *Drosophila* wing: in the butterfly wing there is little scope for cell division carrying the signal away from the focus and certainly not to areas outside the wing-cell within which the focus lies. This is because landmarks such as veins, attached to the epidermis and frequently crossed by the adult eyespot pattern, are already present by pupation, before focal signalling starts, and separated by circa 1 mm of epidermal tissue (the average radius of the posterior eyespot in *B. anynana* corresponds to about 0.7 mm or 90 cell diameters on the pupal wing epidermis; French and Brakefield 1994). Histological studies on another nymphalid butterfly, *Precis coenia*, showed that cell divisions in the pupal wing epidermis occur randomly throughout the wing and not by cell growth from the eyespot centres. The extra tissue is accommodated underneath the hard cuticle by

epidermal pleating in regular rows (Nijhout 1980b, 1991). In *Precis*, cell growth overlaps the period of focal signalling and it is likely that the same happens in *B. anynana*. Expansion of the matrix of cells during focal signalling doesn't seem to alter the shape of the gradient as predicted from the computer simulations on a fixed matrix. This may indicate that concentrations are constantly and naturally being adjusted relative to the new position of a cell in the expanding epidermis. Such continuous reading of the levels of a morphogen gradient, as the gradient is being established, has already been found in other systems (Gurdon et al. 1995).

Computer simulations of diffusion from two point sources, interacting at an equivalent distance and with equivalent strengths (predicted mathematically) to real foci, matched the fusion patterns to a high degree. The matching was measured by the extent of extra area that differentiated in the real eyespot fusion's and in the model. To calculate this area in real patterns, assumptions about perfect eyespot radial symmetry were made, which was not always the case. For the simulations, however, only the most symmetric patterns were used, and under or overestimations of extra pattern were minimised. The proximal-distal asymmetry found in some of the control eyespots is probably related to the different epidermal cell arrangements encountered along this axis (see Chapter 4). Anterior-posterior asymmetry found in the *Spotty* V eyespot could be an artefact of the damage inflicted in the closest neighbouring focus on the IV wing-cell. This type of asymmetry in the anterior eyespot, however, is not understood.

Computer simulations of butterfly wing patterns, involving morphogen concentration gradients, have previously been performed for the whole wing pattern (Bard and French 1984) and for the pattern occurring in individual wing cells (Murray 1981; Nijhout 1990, 1991). None of these studies, however, attempted to use the detailed analysis of the pattern produced through these diffusion models in order to rule out or evaluate alternative types of signalling mechanisms. When Bard and French (1984) simulated whole wing patterns containing adjacent eyespots, using a similar diffusion model to the one presented here, they actually concluded that the single diffusion gradient model was insufficient in explaining the observed patterns. Their modelled patterns would very readily lead to A-P elongation and fusion of

adjacent eyespots, whereas the real eyespot patterns were normally elongated along the P-D axis and did not fuse. From our simulations, it became clear that the correct adjustment of the diffusion model, for a wide range of focal strengths, with an appropriate combination of threshold value and decay rate, was absolutely critical in determining the success of the simulations. i) The decay rate determines the shape of the morphogen gradient; ii) the threshold, the place along this curve where slight differences in concentration are translated into different colours and iii) the interaction of the two determines the extent of the additivity effect when two such curves are close together. Despite the determinism of this model, it is possible that veins, situated between adjacent eyespots, might also have played a role.

In their experiments, a higher threshold level along the veins would make an elliptical morphogen contour be interpreted as a circular pattern. Veins could also have acted as sinks, producing a similar effect. In our simulations, the model predicts less additive effects than those actually observed. The discrepancy is apparent from the last four points in Fig.7, which all fall bellow the reference line. Three out of these points correspond to fusions between eyespots III and IV of *Spotty* butterflies. In these patterns, a wing vein crosses the line connecting the two foci. The veins, in this case, could have slightly lower threshold values and lead to the appearance of additional extra pattern, not accounted for by the model.

A few undetermined issues still remain when simulating focal signalling. The first is whether concentration gradients can be read before equilibrium is reached. The second is whether a focus is a constant level or constant rate source of morphogen. Although these two types of sources are conceptually quite different, and constant level sources biologically more plausible (see Nijhout 1991), the patterns at equilibrium in our simulations were the same. Finally, we still don't know whether diffusion occurs intracellularly (via gap-junctions) or, as presumably happens for *dpp*, through the extracellular fluid, binding to cell membrane receptors as it diffuses. These two modes of spreading through tissue may need different modelling approaches due to the different organisation of the physical space allowed for diffusion.

As already mentioned, although these experiments argue for the existence of a long-range morphogen gradient (possibly the longest range of all systems studied so far), molecular evidence and discovery of the morphogen will still be necessary to prove the case. Carroll et al. (1994) have started cloning *Drosophila* homologues of important patterning genes in the imaginal disc of *P. coenia*, and looking at their expression patterns. The dorsal-ventral, anterior-posterior and proximal-distal axis of the butterfly wing disc are specified in a similar way to those in *Drosophila*. For instance, the *apterous* gene is expressed in dorsal cells, the *engrailed*-related gene, *invected*, in the posterior domain, and *wingless* in presumptive wing-margin cells. The gene *Distalless* (*Dll*) is expressed in the centre of the leg imaginal disc in the fruitfly, which gives rise to the most distal structures of the leg, and also in a distal zone in the wing disc of *P. coenia*. But, more interestingly, *Dll* is also expressed in the future centres of the eyespot patterns in this butterfly and also in *Bicyclus anynana* (Brakefield et al., submitted). Since *Dll* is a homeodomain protein, it binds to the DNA of cells where it is produced, and cannot be the morphogen discussed in this paper. Future research, however, into down-stream or up-stream genes targeted or regulating *Dll* might provide exciting progress in this field.

APPENDIX A

The stationary diffusion profile

We start from the diffusion model

$$\frac{\partial m}{\partial t} = D\left[\frac{\partial^2 m}{\partial x_1^2} + \frac{\partial^2 m}{\partial x_2^2}\right] - k\, m \qquad \text{(A1)}$$

Since we concentrate on the rotationally symmetric case we transform to polar co-ordinates (see e.g. Crank 1975):

$$\frac{\partial m}{\partial t} = \frac{1}{r}\frac{\partial}{\partial r}\left[r\, D\frac{\partial m}{\partial r}\right] - k\, m, \qquad r > 0\,. \qquad \text{(A2)}$$

To this equation we have to add a boundary condition at zero representing a source at $r = 0$, producing a mass S per unit of time. This mass should equal the mass flowing per unit of time over an infinitesimally small circle surrounding the source. For a rotationally symmetric mass profile, the diffusion flux over a circle of radius r equals

$$-r\, D\frac{\partial m}{\partial r}.$$

Therefore we get the boundary condition

$$\lim_{r\to 0} -r\, D\frac{\partial m}{\partial r} = S. \qquad \text{(A3)}$$

Since there is only one source of morphogen we may add the second boundary condition

$$\lim_{r\to \infty} m = 0\,. \qquad \text{(A4)}$$

At equilibrium (A2) can be replaced by

$$\frac{1}{r}\frac{d}{dr}\left[r\,D\frac{dm}{dr}\right]-k\,m=0, \qquad r>0. \tag{A5}$$

Differentiating out the left most expression, and multiplying the whole equation with r^2/D, leads to

$$\left[r^2\frac{d^2m}{dr^2}+r\frac{\partial m}{\partial r}\right]-\frac{k}{D}r^2\,m=0. \tag{A6}$$

As a final step we absorb the factor k/D by setting $z=\sqrt{k/D}$ to arrive at

$$\left[z^2\frac{d^2m}{dz^2}+z\frac{\partial m}{\partial z}\right]-z^2\,m=0. \tag{A7}$$

Abramowitz and Stegun (1965) tell us that the solutions of (A7) can be written as a weighted sum of the Bessel function $K_0(z)$ and $I_0(z)$. (A4) excludes I_0. Therefore, we have to consider solutions of the form cK_0 only. To determine c we use formula 9.6.8 from Abramowitz and Stegun: $K_0(z) \approx -\ln(z)$. First we substitute $z = \lambda r$, with $\lambda=\sqrt{k/D}$. This tells us that near $r = 0$

$$\frac{dK_0(\lambda r)}{dr}\approx-\frac{1}{r} \tag{A8}$$

Substituting (A8) for m in (A3) finally tells us that

$$m(r) = c\,K_0(\lambda r), \tag{A9}$$

with $c = S/D$.

APPENDIX B

Comparing fixed strength with fixed level sources

We consider the diffusion model (A1), together with some central source.

As a first step we consider a circular fixed level or fixed strength source at the equilibrium between inflow over the source boundary and decay away from the source. We have rotational symmetry and at infinity the morphogen concentration goes to zero. So both (A4) and (A5) apply, but with a different boundary condition at $r = r_s$, the radius of the source. This means that the stationary profile is again given by (A9), though with a different value of c.

Next, consider a spatially extended fixed strength source of finite extent and arbitrary form. The morphogen molecules originating at different locations in the source area move and decay independently. Therefore, we can calculate the solution for any form of the source by just adding the contributions of all the minute point sources filling the source area. This means that at a large distance any sufficiently narrow fixed strength source looks like a point source.

For a non-circular source the previous argument no longer works. We have to embark on a slightly more complicated argument; as long as it does not hit the source boundary, a molecule that has moved away from the source, moves independently from all other molecules. Molecules entering the source area effectively cancel the production of some other molecules through the homeostatic process that keeps the source level constant. By a change of names, in which we let a molecule that has just arrived from the outside stand in for the molecule whose production it suppresses, we may do as if the source area becomes an effective sink for molecules once they have left that area, while the production of molecules is not affected by the arrivals from outside. From now on we shall keep to this picture. At equilibrium we have a steady net outward flow of molecules over the source boundary. These molecules start wondering around in the plane, and decaying. But in a plane which has an effective hole. However, for molecules that have come a sufficiently long distance from the hole, the effect of that hole on their future becomes negligible. So we may draw a large circle around the source, and start noticing molecules for the first time when

they cross that circle. This replaces the original fixed level source with an equivalent circular fixed strength source surrounding it at a large distance. We should keep in mind, though, that the plane still has that tiny hole at its centre. However, if we consider a sufficiently large circle, and consider the morphogen concentration at an even larger distance, we get a concentration profile which is effectively indistinguishable from that of a point source at the origin. Conversely, if we consider a very narrow fixed level source, it will at some distance be effectively indistinguishable from a circular fixed level or fixed strength source.

If we have more than one fixed strength source we can just add the solutions for the separate sources, due to the independence of the movement and decay of the morphogen molecules.

Now consider two narrow fixed level sources at some distance away from each other. The molecules coming from those two sources do not move independently. If the molecule from source 1 hits source 2, it is effectively absorbed by the same argument that we used before. It is clear that if the sources are very narrow and far away from each other, the probability of such a hit is negligible.

If we combine the last argument with the previous ones we find that two narrow fixed level sources at a good distance away from each other are effectively indistinguishable from two narrow fixed strength sources.

CHAPTER 6

Gap Junctions

ABTRACT

I report on the existence of open gap-junction channels between cells of the pupal wing epidermis of a Nymphalid butterfly, during the critical time of pattern determination. The presence of these channels is a basic assumption in the developmental models of pattern formation in butterfly wings but their existence and open state had previously not been demonstrated. I also show that these channels can be easily and reversibly blocked with a solution of Ringer containing heptanol in low concentration (5 mM).

INTRODUCTION

The developmental mechanism of butterfly wing pattern formation is not yet fully understood. However, Nijhout (1978, 1991) and French and Brakefield (1992) have developed a model that can account for most of the results of grafting or damage experiments performed on pupal wings. Computer simulations (Nijhout 1990) are able to reproduce most butterfly wing patterns. The model and simulations are based on the existence of specific groups of epidermal cells, that make up a small proportion of the whole wing area, that act as sources or sinks for the generation or uptake of a diffusible chemical substance, a morphogen. This morphogen is thought to diffuse from the sources (or into the sinks) through intracellular gap-junctions channels to form a concentration gradient across the epidermis. At the time of pattern determination the cells over the whole wing, depending on their position relative to

the sources or sinks, will be exposed to different concentrations of this substance. This degree of exposure is believed to determine the developmental fate of the wing cells in terms of the type of pigment they will later produce.

This short communication reports on preliminary experimental evidence for the existence of active gap-junction channels at the time of pattern determination (up to 24 hours after pupation) in the pupal wing of the nymphalid butterfly, *Bicyclus anynana*. Although these channels are present between cells of most embryonic and adult tissues (see Spray, 1994), including larval imaginal disks and epidermal tissues of other insects (e.g. Fraser and Bryant, 1985; Blennerhassett and Caveney, 1994), their presence and active state has not previously been investigated in butterfly wing epidermis.

MATERIALS AND METHODS AND RESULTS

B. anynana was reared at 28° C, high relative humidity and 12L:12D light cycle. A square piece of wing epidermis, attached to the overlying cuticle, was cut from a 3 hour old pupa, around the site of source cells responsible for the induction of an eyespot pattern (Fig.1). The piece of tissue was attached, on the cuticle side, to a glass dish with the help of some glycerine. Drosophila Ringer solution was then added to the dish before placing it on the stage of an inverted microscope (Nikon diaphot). The fluorescent dye Lucifer Yellow (5% wt/vol in distilled water) was intophoresed into a single cell in the epidermis from a glass microelectrode (~20 MOhm if filled with 3 M KCl) attached to a hydraulic micromanipulator (Narashige), and the intercellular spread of the dye observed using xenon epi-illumination with FITC excitation and emission filters.

Under control conditions, 3 injections revealed that within 1-3 min dye diffused to an average of 5 neighbouring cells. An illustration of such an injection is shown in Figure 2a. This spread occurred directly from the cytoplasm of the injected cell to the neighbouring cells, since the fluorescence pattern followed the cell contours. In order to demonstrate that this dye transfer occurred through gap-junctions, the Ringer solution was substituted with a solution of Ringer and heptanol

(5 mM); heptanol in these small concentrations has been demonstrated to block gap-junction channels in several systems including cultured cells from larvae of the insect *Aedes albopictus* (Bukauskas *et al* 1992), and is generally useful as a non-toxic uncoupling agent (see Spray, 1994). Intracellular injection of Lucifer Yellow into heptanol treated cells led to no spread of dye (n=3). An example of this uncoupling is illustrated in Figure 2b. Dye injections 15-30 min after rinsing the heptanol treated preparation with Ringer solution demonstrated recovery toward pretreatment levels of uncoupling (n=2; fig. 2c), demonstrating that the block of coupling by heptanol was not due to irreversible drug toxicity.

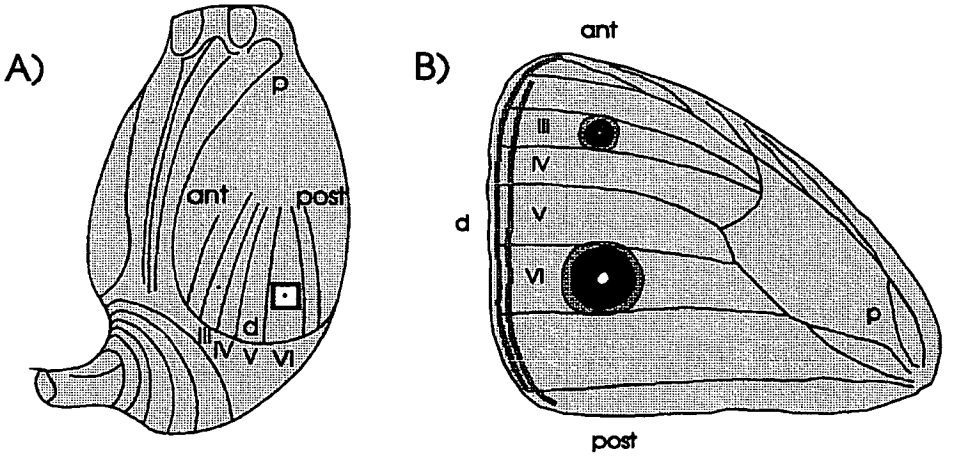

Figure 1. a) Schematic drawing of a pupa of *B. anynana*, showing the venation on the dorsal surface of the forewing, and b) the adult wing pattern from the corresponding surface. The square indicates the area of tissue removed from the pupa for the experiment and the equivalent area in the adult wing. The dots situated between the pupal veins represent areas of raised surface on the cuticle, overlying (but not necessarily congruent with) the source cells in the epidermis responsible for the determination of the eyespots.

The experiments described above demonstrate not only that gap-junctions exist between butterfly wing cells during the critical period of pattern induction, but also that these junctional channels are in their open state. Moreover, these channels can be easily and reversibly blocked by bathing in a Ringer solution containing heptanol (5 mM). This information is useful in confirming one of the assumptions of the developmental model of butterfly wing pattern formation and also in providing

the potential for manipulating cell communication around sources (or sinks) in live pupae to examine the effects on the specification of adult wing pattern.

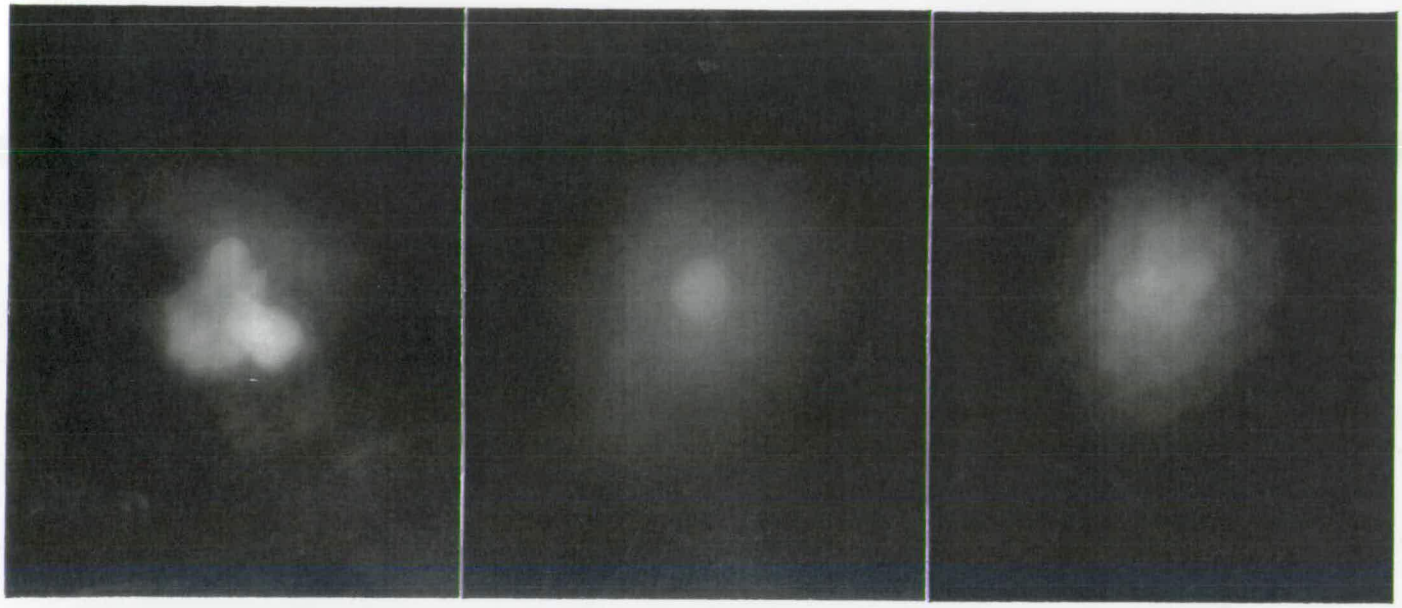

Figure 2. Fluorescence patterns observed after the injection of single cells in the pupal wing epidermis of the butterfly *Bicyclus anynana* with the dye Lucifer Yellow. a) The dye spreads to surrounding cells when tissue is bathed in Ringer solution; b) Uncoupling of cells occurs due to substitution of Ringer with a solution of Ringer and heptanol (5 mM); c) Recovery of coupling between cells after heptanol treated preparation is rinsed with Ringer. The glow present around the fluorescent cells reflects some extracellular leakage during the injection procedure.

CHAPTER 7

Conclusions and Future Work

CONCLUSIONS

The selection experiments for eyespot size (Monteiro et al. 1994), colour ring composition and shape of the large dorsal eyespot on the forewing of *Bicyclus anynana* have shown that:

- There is considerable additive genetic variance for the mechanisms controlling these features.
- The heritabilities are different for each feature. Heritability for size > heritability colour composition > heritability for shape.
- The alleles of the genes affected by each selection regime were controlling different levels of eyespot development. The alleles of genes affecting eyespot size were mainly influencing focal cells. The alleles of genes affecting colour composition altered the response to the focal signal. Alleles affecting eyespot shape were indirectly affecting the shape of the matrix of cells around the eyespot focus.
- All eyespots are developmental homologues to a larger or smaller degree. Selection applied to one eyespot led to correlated changes in other eyespots. Correlated responses included selection for eyespot shape where the changes were at the level of the spacing of the epidermal cells.

These experiments also lead to the identification of some potential genetic or developmental constraints. These were:

- No variability for shape of a signalling focus.
- No change in colour composition when selection was performed on eyespot size (Monteiro et al. 1994).

- No change in size when selection was performed on colour composition.
- No variability in aspects of the signal affecting colour composition
- Limited deformation of the shape of eyespots probably due to a limit in the spacing of epidermal cells.

Only by studying the developmental mechanisms can we attempt to understand the paths available for morphological change. From this study onwards it will be possible to compare the same developmental mechanisms across species, starting with those in the same genus, and find out how easy it is for these mechanisms to evolve. In particular, it will be interesting to find out which of the above mentioned constraints are absolute (and spread across all species) and which are only due to lack of genetic variability. Evolution of an eyespot pattern has depended and will depend on the way variants of genes are expressed through development.

What we now know about the developmental mechanism and its variation across the wing:

Chapters 5 and 6 provided evidence that a concentration gradient of a morphogen diffusing through gap-junctions is consistent with the observed properties of real eyespots and is a plausible mechanism for focal signalling. It is still unclear, however, whether the morphogen gradient model tested in Chapter 5 acts as a source or a sink. Both models, being symmetric versions of each other, can be made to fit the data equally well (e.g. if focal cells act as a sink of morphogen, areas at intermediate distances from two such sinks will suffer additive depletion effects, leading to the appearance of areas of extra pattern).

From the grafting experiments of Chapters 2 and 5 it is clear that the response of cells to the focal signal, the thresholds, are not constant throughout the wing. The two thresholds controlling the extent of the inner black circle and outer gold ring vary across the wing. When thinking of a sink model, the "black" threshold is higher (producing "blacker" eyespots) both distally from the body and more posteriorly on the wing. The outer "gold" threshold is higher distally, leading to both larger eyespots, as well as to asymmetric eyespots with larger distal halves. This threshold

is also higher posteriorly on the wing. Since the responses where studied at only two discrete positions (along each axis) it remains to be elucidated whereas there is a *gradient* for these responses running along the A-P and P-D axes of the wing. The results for the asymmetry of the eyespots along the P-D axes, however, argues in favour of such a gradient.

FUTURE WORK

Developmental biology

As was mentioned in chapter 5, techniques of modern molecular biology potentially provide the means to investigate what is controlling *Distal-less* expression in the focal cells and also to investigate weather expression of other homeobox genes, homologous to those already known for *Drosophila,* can map additional centres responsible for organising bands and chevron patterns. The signal produced by the focal cells will most likely be in the form of a diffusible gene product and it may prove possible to identify this by investigating homologues of *Drosophila* signalling molecules.

Manipulative experiments

The damaging and grafting of epidermal cells constitutes a very powerful tool to explore the position and function of organising centres. Cautery or wing damage can be performed throughout development of the pupa (and perhaps even earlier in the imaginal disc). Wing damage has been applied extensively on the pupal forewing of *Bicyclus anynana* (V. French, pers. commun.), in order to map presumptive centres organising the banding pattern on its ventral surface. These efforts, however, never produced significant alterations to the pattern. It may be the case that bands are determined earlier in development, in the imaginal discs of the larvae. Future work in *Bicyclus anynana* could explore this possibility by operating on larvae, evaginating the imaginal discs without separating them from the body, piercing them at presumptive band organising centres, and reintroducing them into the larvae. Nijhout

and Grunert (1988) applied a similar technique to cut pieces of imaginal discs in *Precis coenia* and had 60% of the operated individuals surviving into adult stage. As well as mapping positions of important organising centres of the colour pattern, surgical damage to these centres, at several time points, can help determine their period of activity. Damage performed after signalling will not affect the final pattern, whereas damage during signalling will. Damage and cautery techniques could further be applied during both the imaginal disc and pupal wing stages of other species with similar patterns to *Bicyclus anynana*, in order to compare variability in timing of the signalling centres.

The grafting of epidermal tissue has only been possible, so far, during a limited number of hours after pupation (when the cuticle is still attached to the epidermis) and only on the accessible dorsal surface of the forewing. To study development of a pattern by means of this technique it is, thus, necessary to choose a species carrying the pattern on this wing surface.

So far, very little experimental attention has been given to the wing veins. These structures have probably the most important role in early organisation of the whole wing pattern. Small cuts, for instance, made to the veins (or lacunae) during imaginal disc development could have serious effects on the establishment of organising centres. Also, later in development, and in species where these structures are likely sources or sinks of morphogen, disturbances of the process by grafting of vein tissue could finally help establish their role as pattern organisers.

Quantitative genetics

Following selection applied to a feature of a single eyespot, it was striking that there were very strong correlated responses in that same feature across most other eyespots. The eyespot pattern elements, sometimes called serial homologues, appear to be, at least in *B. anynana*, under common genetic control. Since response to selection, however, was always stronger in the selected eyespot relative to the others, there is additional independent genetic variation affecting subsets of the eyespots. The extent of this independent genetic variability as well as the strength of the

genetic correlations between serial homologues can be tested by means of artificial selection experiments.

The application of antagonistic selection pressure to some feature of a pair of eyespots, for instance, is a means of quantifying the degree of coupling between the two eyespots. If there are strong genetic correlations between the two, it might prove impossible to increase a feature in one eyespot while decreasing it in the other. Weaker correlations may give an intermediate result. In some instances, high genetic correlations may not indicate a common developmental mechanism but originate due to linkage disequilibrium. This is the case when there are different genes, clustered together on the chromosome, that control features of different eyespots. This clustering can either correspond to a primitive arrangement of genes controlling the serially homologous elements or be produced by the action of natural selection (if butterflies with homogeneous eyespots have a higher fitness). Whatever the origin of the linkage disequilibrium, it may be difficult or even impossible to tease out this situation from a true developmental constraint involving common developmental and genetic determinants. Maybe the only means of identifying the primitive from the derived state of developmental organisation of wing patterns, is via the comparative method.

Phylogenetics

By comparing the developmental mechanisms and genetic correlations present in different species of known ancestry, it may be possible to identify primitive from derived states of developmental organisation. The characters used to produce the phylogenetic grouping of the different species should be independent from the characters whose development we are trying to study. A molecular phylogeny is probably the most appropriate. Other specific predictions that can be tested via a phylogenetic approach are:

(1) That most evolution will be quantitative, but there will be occasional instances of correlation-breaking and/or *de novo* rearrangement evolution.

(2) That important sub-groups will be distinguished from their sister taxa by instances of non-quantitative evolution. In other words, a particular sub-genus might

be characterised by having, for example, new spots not present amongst its sister taxa, whereas evolution within that subgenus will consist merely of quantitative variation on pre-existing themes.

Computer modelling

The diffusion model proposed by Nijhout (1978, 1991) and tested in chapter 5 fitted the experimental data surprisingly well. It is possible, though, that other models could be made to fit the data equally well, in particular, a mixed model of a cascade and a morphogen gradient. In this scenario, a signal, part of a cascade of different signals, would induce the next signal down in the cascade only after diffusing some distance away from its source cells. Only cells perceiving low levels of the first signal could, via a switch mechanism, start producing the next signal down in the cascade and so on. This is a complicated mechanism that looses the simplicity of both the simple cascade and the long range, single morphogen gradient mechanisms. It would, nevertheless, be straightforward to produce a a computer model with these characteristics and compare the results of the simulations with the ones performed in chapter 5.

Gap junctions

The experiments mentioned in chapter 6 were later repeated in a different lab and gave slightly different results. Although the spread of the fluorescent dye, Lucifer yellow, was still observed from a single injected cell, indicating the presence of gap junctions, the effect of heptanol in blocking the junctions, was not consistent with the first experiments. Heptanol did not block the spread of Lucifer Yellow. Recently, however, a promising advance in insect gap junction research has been made, and there is now an antibody available developed against the gap-junction protein, ductin, of the arthropod *Nephrops* (Malcolm Finbow, pers. commun.). Since antibodies have high binding specificity, they are much more appropriate to disturb gap junctional communication than long chain alcohols, like heptanol, with unknown side effects. Injections or this antibody during butterfly pupal wing development could illuminate the means by which positional information is given from foci to surrounding cells.

Mass spectroscopy

If eyespot differentiation occurs via a morphogen concentration gradient, we expect to find different morphogen concentrations around focal cells than elsewhere on the wing. If foci are sources, the concentration of morphogen around them will be higher than at other places in the wing. If foci are sinks, local morphogen concentration will be lower. By taking samples of epidermal tissue at increasing distances from focal cells, we expect to find varying levels of morphogen in our samples. If a sample of tissue is taken sufficiently far away from a focus, and if this acts as a source of morphogen, we expect this sample to contain little or no morphogen molecules.

A recent mass spectroscopy technique named MALDI (Matrix Assisted Laser Desorption / Ionisation; Karas and Hillenkamp 1988) enables the mass analysis of non-volatile biomolecules with molecular weight up to 10^5 Dalton. This technique creates intact gas-phase molecular ions, after light is absorbed by a surrounding matrix on which a sample is embedded. The molecules of the matrix, present in large quantities, receive most of the light and provide a gentle ionisation method to the large sample molecules. These pass onto the gas phase without fragmentation and are detected by a mass spectrometer. The exact mass of all molecules present in the sample can be determined as well as the molecules' relative quantity.

Using this method it is possible to compare cell contents, after hydrolysis of the cell membranes, from different tissue samples. The molecular mass of a substance only present in a subset of the sample could, in this manner, be known. Further biochemical analysis can then attempt to extract and purify such a substance.

LITERATURE CITED

Abramowitz, M. and I. Stegun, 1965. Handbook of Mathematical Fuctions. Dover, New York.

Bard, J. B. L. and V. French, 1984. Butterfly wing patterns: how good a determining mechanism is the simple diffusion of a single morphogen? J. Embryol. exp. Morpho. 84: 225-274.

Blair S. S., 1995. Compartments and appendage development in Drosophila. BioEssays 17: 299-309.

Blennerhassett, M.G., and S. Caveney, 1984. Separation of developmental compartments by a cell type with reduced junctional permeability. Nature 309:361-364.

Bookstein F., B. Chernoff, R. Elder, J. Humphries, G. Smith and R. Strauss, 1985. Morphometrics in Evolutionary Biology. Academy of Natural Sciences of Philadelphia.

Brakefield, P. M., 1984. The ecological genetics of quantitative characters in Maniola jurtina and other butterflies. pp 167-190. In R. I. Vane-Wright and P. R. Ackeryn (Eds.). The Biology of Butterflies. Academic Press. London.

Brakefield, P. M. and V. French, 1993. Butterfly wing patterns: Developmental Mechanisms and Evolutionary Change. Acta Biotheoretica 41: 447-468.

Brakefield, P. M. and V. French,1995. Eyespot Development on Butterfly Wings: The Epidermal Response to Damage. Developmental Biology 168: 98-111

Bukauskas, F., C. Kempf and R. Weingart, 1992. Electrical coupling between cells of the insect *Aedes Albopictus.* J.Physiol. 448:321-337.

Carroll, S. B., J. Gates, D. N. Keys, S. W. Paddock, G. E. F. Panganiban, J. E. Selegue and J. A. Williams, 1994. Pattern Formation and Eyespot Determination in Butterfly Wings. Science 265: 109-113.

Cheverud, J M., 1984. Quantitative genetics and developmental constraints on evolution by selection. Journal of Theoretical Biology 110: 155-171.

Collier, A. E., 1956. A new aberration of *Aphantopus hyperantus* Linn. ab. *lanceolata* Shipp. Entomologist's Rec. J. Var. 68: 1-2.

Condamin, M., 1973. Monographie du genre Bicyclus (Lepidoptera Satyridae). Mem. Inst. Fond. Afr. Noire 88: 1-324.

Crank, J., 1975. The Mathematics of Diffusion (2nd. ed.). Claredon Press, Oxford.

Driever, W. and C. Nusslein-Volhard, 1988. A gradient of *bicoid* protein in Drosophila embryos. Cell 54: 83-93.

Dudley R. and R. B. Srygley, 1994. Flight physiology of neotropical butterflies: allometry or airspees during natural free flight. J. Exp. Biol. 191: 125-139.

Falconer, D.S. 1989. Introduction to quantitative genetics (3rd ed.) Longman, London.

Ford, E. B., 1945. Butterflies. Collins. London.

Fraser, S.E., and P.J. Bryant, 1985. Patterns of dye coupling in the imaginal wing disc of *Drosophila melanogaster*. Nature 317:533-536.

Fry, J. C. 1993. One-way analysis of variance, pp. 3-39 in Biological Data Analysis. A Practical Approach, edited by J. C. Fry. Oxford University Press, Oxford.

French, V. and P. M. Brakefield, 1992. The development of eyespot patterns on butterfly wings: morphogen sources or sinks? Development 116: 103-109.

French, V. and P. M. Brakefield, 1995. Eyespot development on butterfly wings: the focal signal. Developmental Biology 168: 112-123.

Gurdon, J. B., P. Harger, A. Mitchell and P. Lemaire, 1994. Activin signalling and response to a morphogen gradient. Nature 371: 487-492.

Gurdon J. B., A. Mitchell and D. Mahony, 1995. Direct and continuous assessment by cells of their position in a morphogen gradient. Nature 376: 520-521.

Heemskerk, J. and S. DiNardo, 1994. Drosophila *hedgehog* acts as a morphogen in cellular patterning. Cell 76: 449-460.

Holloway, G. J. and P. M. Brakefield, 1995. Artificial selection of reaction norms of wing pattern elements in *Bicyclus anynana*. Heredity 74: 91-99.

Holloway, G. J., P. M. Brakefied and S. Kofman. 1993. The genetics of wing pattern elements in the polyphenic butterfly, *Bicyclus anynana*. Heredity 70: 1179-186.

Johnson, J. W. and E. Walter, 1978. Similarities and differences in forewing shape of six California *Catocala* species (Noctuidae). J. Res. Lepid. 17: 231-239.

Karas, M. and F. Hillenkamp, 1988. Laser desorptio ionization of proteins with molecular masses exceeding 10 000 daltons. Anal. Chem. 60: 2299-2301

Katz, W. S., R. J. Hill, T. R. Clandinin and P. W. Sternberg, 1995. Different levels of the C. elegans growth factor LIN-3 promote distinct vulval precursor fates. Cell 82: 297-307.

Kingsolver, J. G. and M. A. R. Koehl, 1994. Selective factors in the evolution of insect wings. Annu. Rev. Entomol. 39: 425-451.

Kingsolver, J. G. and D. C. Wiernasz, 1987. Dissecting correlated characters: adaptive aspects of phenotypic covariation in melanization pattern of *Pieris* butterflies. Evolution 41: 491-503.

Kühn, A. and M. von Englehardt, 1933. Über die determination des symmetriesystems auf dem vorderflügel von *Ephestia kühniella*. Willem Roux' arch. EntwMech. Org. 130: 660-703.

Kuntze, H., 1935. Die Flügelentwicklung bei Philosamia cynthia Drury, mit besonderer Berücksichtigung des Geäders der Lakunen und der Tracheensysteme. Zeitschrift für Morphologie und Ökologie de Tiere 30: 544-572.

Lecuit, T., W. J. Brook, M. Ng, M. Calleja, H. Sun and S. M. Cohen, 1996. Two distinct mechanisms for long-range patterning by Decapentaplegic in the *Drosophila* wing. Nature 381: 387-393.

Lewis, J., J. M. W. Slack and L. Wolpert, 1977. Thresholds in development. Journal of Theoretical Biology 65: 579-590.

Manly, B. F. J., 1994. Multivariate Statistical Methods: A Primer. 2nd ed. Chapman and Hall, London.

Maynard-Smith, J., R. Burian, S. Kauffman, P. Alberch, J. Campbell, B. Goodwin, R. Lande, D. Raup and L. Wolpert, 1985. Developmental constraints and evolution. Quarterly Review of Biology 60: 265-287.

Meinhardt, H., 1982 Models of biological pattern formation. Academic Press, New York.

Monteiro, A. F., P. M. Brakefield and V. French, 1994. The evolutionary genetics and developmental basis of wing pattern variation in the butterfly *Bicyclus anynana*. Evolution 48: 1147-1157.

Monteiro, A. F., P. M. Brakefield and V. French, 1997a. The genetics and development of an eyespot pattern in the butterfly *Bicyclus anynana*: response to selection for eyespot shape. Genetics (in press).

Monteiro, A. F., P. M. Brakefield and V. French, 1997b. Butterfly eyespots: the genetics and development of the color rings. Evolution (in press).

Monteiro, A. F., P. M. Brakefield and V. French, 1997c. The relationship between eyespot shape and wing shape in the butterfly *Bicyclus anynana*: a genetic and morphometrical approach. J. Evol. Biol. (in press).

Murray, J. D., 1981. On pattern formation mechanisms for lepidopteran wing patterns and mammalian coat markings. Phil. Trans. R. Soc. Lond. B 295: 473-496.

Nijhout, H.F. 1978. Wing pattern formation in Lepidoptera: A model. Journal of Experimental Zoology 206: 119-136.

Nijhout, H. F., 1980a. Pattern formation on lepidopteran wings: Determination of an eyespot. Dev. Biol. 80: 267-274.

Nijhout, H. F., 1980b. Ontogeny of the color pattern on the wings of *Precis coenia* (Lepidoptera: Nymphalidae). Dev. Biol. 80: 275-288.

Nijhout, H. F., 1985. Cautery-induced colour patterns in *Precis coenia* (Lepidoptera: Nymphalidae). Journal of Embryology and Experimental Morphology 86: 191-203.

Nijhout, H. F., 1990. A comprehensive model for color pattern formation in butterflies. Proceedings of the Royal Society of London, Series B: 239: 81-113.

Nijhout, H. F., 1991. The Development and Evolution of Butterfly Wing Patterns. Smithsonian Institution Press. Washington.

Nijhout, H. F., 1994 Genes on the Wing. Science **265:** 44-45.

Nijhout, H. F. and L. Grunert, 1988. Colour pattern regulation after surgery on the wing disks of *Precis coenia* (Lepidoptera: Nymphalidae). Development 102: 377-385.

Nijhout, H. F., G. Wray and L. E. Gilbert, 1990. An analysis of the phenotypic effects of certain color pattern genes in *Heliconius* (Lepidoptera: Nymphalidae). Biol. J. Linn. Soc. 40: 357-372.

Nijhout, H. F., G. A. Wray, C. Kremen and C. K. Teragawa, 1986. Ontogeny, phylogeny and evolution of form: an algorithmic approach. Syst. Zool. 35: 445-457.

Nellen, D., R. Brke, G. Struhl and K. Basler, 1996. Direct and long-range action of a DPP morphogen gradient. Cell 85: 357-368.

Norusis, M. J., 1985. SPSS Advanced Statistics Guide. McGraw-Hill. New York.

Paulsen, S. M. 1994. Quantitative Genetics of Butterfly Wing Color Patterns. Developmental Genetics 15: 79-91.

Paulsen, S. M. and H. F. Nijhout. 1993. Phenotypic correlation structure among elements of the color pattern in *Precis coenia* (Lepidoptera: Nymphalidae). Evolution 47: 593-618.

Perrimon, N., 1995. Hedgehog and Behond. Cell 80: 517-520.

Revels, R., 1975. Notes on breeding the ringlet: *Aphantopus hyperantus* ab. *pallens* and ab. *lanceolata*. Ent. Rec. 87: 283-285.

Ricklefs, R. E. and K. O'Rourke, 1975. Aspect diversity in moths: a temperate-tropical comparison. Evolution 29: 313-324.

Schwartz, V., 1962. Neue versuce zur determination des zentralen symmetriesystems bei *Plodia interpunctella*. Biol. Zbl. 81: 19-44.

Sheppard, P. M., J. R. G. Turner, K. S. Brown, W. R. Benson and M. C. Singer, 1985. Genetics and the evolution of Mullerian mimicry in *Heliconius* butterflies. Philos. T. Roy. Soc. B 308: 33-613.

Simon, C., 1983. Morphological differentiation in wing venation among broods of 13- and 17-year periodical cicadas. Evolution 37: 104-115.

Sokal, R.R. and Rohlf, F.J. 1995. Biometry (3rd ed.). Freeman, San Francisco.

Spray, D.C. (1994) Physiological and pharmacological regulation of gap junction channels. In: S. Citi, ed. Molecular Mechanisms of Epithelial Cell Junctions: From development to Disease. Medical Intelligence Unit, R.G. Landes Co., Biomedical Publishers, in press.

Strauss, R. E., 1987. Allometry and relative growth in evolutionary studies. Syst. Zool. 36: 72-75.

Strauss, R. E., 1990. Patterns of quantitative variation in Lepidopteran wing morphology: the convergent groups Heliconinae and Ithomiinae (Papilionoidea: Nymphalidae). Evolution 44: 86-103.

Strauss, R. E., 1992. Lepidopteran wing morphology: The multivariate analysis of size, shape, and allometric scaling. pp 157-178. In J. T. Sorensen and R. Foottit (Eds.). Ordination in the Study of Morphology, Evolution and Systematics of Insects. Elsevier. Amsterdam.

Tussaint N. and V. French, 1988. The formation of pattern on the wing of the moth, *Ephestia kühniella*. Development 103: 707-718.

Whalley, P., 1986. A review of the current fossil evidence of Lepidoptera in the Mesozoic. Biological Journal of the Linnean Society 28: 253-271.

Weber, K. E., 1990a. Increased selection response in larger populations. I. Selection for wing-tip height in *Drosophila melanogster* at three population sizes. Genetics 125: 579-584.

Weber, K. E., 1990b. Selection on Wing Allometry in *Drosophila melanogaster*. Genetics 126: 975-989.

Weber, K. E., 1992. How Small Are the Smallest Selectable Domains of Form? Genetics 130: 345-353.

Wehrmaker, A., 1959. Modifikabilität und morphogenese des Zeichnungsmusters von *Plodia interpunctella* (Lepidoptera: Pyralidae). Zool. Jahrb. Abt. Zool. Physiol. 68: 425-496.

Wiernasz, D. C. 1989. Female choice and sexual selection of male wing melanin pattern in *Pieris occidentalis* (Lepidoptera). Evolution 43: 1672-1682.

Wiley, E. O., 1981. Phylogenetics: The theory and practice of phylogenetic systematics. Wiley, New York.

Wilnecker L., 1980, Waves and gradients in the wings of *Ephestia kühniella* and *Plodia interpunctella*. D. Phil. Thesis, University of Sussex.

Windig, J. J., 1991. Quantification of Lepidoptera wing patterns using an image analyzer. J. Res. Lepid. 30: 82-94.

Zecca, M., K. Basler and G. Struhl, 1995. Sequential organizing activities of engrailled, hedgehog and decapentaplegic in the *Drosophila* wing. Development 121: 2265-2278.